UNIVERSITÄT KOBLENZ · LANDAU

Mathematisches Institut

Ph. D. Thesis

Reduced basis methods for quasilinear PDEs and applications to electrical machines

von

Denis Korolev
aus Krasnodar

Angenommene Dissertation zur Erlangung des akademischen Grades eines
Doktors der Naturwissenschaften
Fachbereich 3: Mathematik/Naturwissenschaften
Universität Koblenz-Landau

Gutachter:
Prof. Dr. Michael Hinze
Prof. Dr. Stefan Volkwein

Prüfungskommission:
Prof. Dr. Bernhard Köppen
Prof. Dr. Michael Hinze
Prof. Dr. Thomas Götz

Tag der mündlichen Prüfung: 25. Juni, 2021

Abstract

This thesis addresses the reduced basis methods for parametrized quasilinear elliptic and parabolic partial differential equations with strongly monotone differential operator. It presents all of the ingredients of the reduced basis method: basis generation for reduced basis approximation, certification of the approximation error by suitable a-posteriori error control and an Offline-Online decomposition. The methodology is further applied to the magnetostatic and magnetoquasistatic approximations of Maxwell's equations and its validity is confirmed by numerical examples.

Zusammenfassung

Diese Arbeit befasst sich mit den reduzierten Basismethoden für parametrisierte quasilineare elliptische und parabolische partielle Differentialgleichungen mit stark monotonem Differentialoperator. Es werden alle Bestandteile der Methode mit reduzierter Basis vorgestellt: Basisgenerierung für reduzierte Approximation, Zertifizierung des Approximationsfehlers durch geeignete a-posteriori Fehlerkontrolle und Offline-Online-Zerlegung. Die Methodik wird ferner auf die magnetostatischen und magnetoquasistatischen Näherungen der Maxwellschen Gleichungen angewendet und ihre Gültigkeit wird durch numerische Beispiele bestätigt.

Publications

Some of the results of this thesis have already been published or submitted.

- The reduced basis method for linear parabolic problems in section 3.3 in **Chapter 3** is the improved version of author's master thesis [36] with the title "Reduced basis concepts for linear parabolic equations". We note that this master thesis was not published before and it contains unique results, obtained by the author and his scientific supervisor Prof. Dr. Michael Hinze and presented now in this thesis. Compared to [36], we corrected errors and improved the overall style.

- **Chapter 4** is an extended version of

  [27] Michael Hinze, Denis Korolev: Reduced basis methods for quasilinear elliptic PDEs with applications to permanent magnet synchronous motors. arXiv:2002.04288 (2020), which has been accepted for publication in *International Series of Numerical Mathematics* book, Springer.

  For this thesis, we changed notation and organisation of the text in [27] to improve the overall style and added more details to section 4.2.1 on the computational procedure and figures (see e.g. figure 4.3(e) and figure 4.3 (f)) to section 4.3, compared to [27].

- **Chapter 5** is an extended version of

  [26] Michael Hinze and Denis Korolev. "A space-time certified reduced basis method for quasilinear parabolic partial differential equations". In:Advances in Computational mathematics 47.3 (2021).

  In particular, we added more details to section 5.2.2 on the computational procedure, compared to [26].

These collaborations are an essential part of the research that led to this thesis.

Acknowledgement

I would like to thank my PhD supervisor Prof. Dr. Michael Hinze for introducing me to the field of computational and applied mathematics through a series of his inspiring lectures at the University of Hamburg and for his trust and the opportunity to work in his research group. I am grateful for his support, mathematical, scientific and life advice that I received from him over these years of working together. I would also like to acknowledge the financial support of the collaborative research project PASIROM funded by the German Federal Ministry of Education and Research.

I would like to warmly thank my colleagues Christian for his expert advice and Evelyn for her support, substantial help with a variety of issues and for being a nice friend, with whom I could share many moments together. Besides, I heartily thank my friends Yan, Yanush and Max for their understanding and shoulder.

I am deeply grateful to my whole family for their unconditional love and greatest support throughout my life. Thank you Mama for your inspiring example of curiosity, honesty and independence.

Contents

Nomenclature

$|v|$ Euclidean norm of a vector $v \in \mathbb{R}^d$ - p. 8

$\bigoplus$ direct sum operation - p. 25

χ_Ω characteristic function of a set Ω, i.e., $\chi_\Omega(x) = \begin{cases} 1; & x \in \Omega; \\ 0; & x < \Omega: \end{cases}$ - p. 17

δ_{ij} Kronecker delta symbol, i.e., $\delta_{ij} = \begin{cases} 1; & i = j; \\ 0; & i \neq j: \end{cases}$ - p. 30

$\det A$ determinant of a matrix A - p. 39

$\dot{u}$ (generalized) time derivative of u. We use $\dot{u}; \frac{\partial u}{\partial t}; \frac{du}{dt}$ interchangeably - p. 12

$;$ empty set - p. 8

$\langle \cdot ; \cdot \rangle_H$ inner product in some Hilbert space H - p. 12

$\langle \cdot ; \cdot \rangle_{V' V}$ duality pairing between V and V' in some Banach space V - p. 12

$\| \cdot \|_V$ norm on some Banach space V - p. 12

$\mathbb{R}$ field of real numbers - p. 12

$\mathbb{R}^n$ n-dimensional real space - p. 8

$\mathbb{R}_0^+$ non-negative real numbers - p. 10

$O(\ )$ Landau “big-O" asymptotic notation - p. 25

$P_k(I; V)$ space of polynomials $p : I \to V$ of degree k - p. 32

∇ gradient, $\nabla v = \operatorname{grad} v = \left\{ \frac{\partial v}{\partial x_i} \right\}_{i=1}^d$, for $v : \mathbb{R}^d \to \mathbb{R}$ - p. 9

$\nabla \cdot$ divergence operator, $\nabla \cdot v = \operatorname{div} v = \sum_{i=1}^d \frac{\partial v_i}{\partial x_i}$, for $v : \mathbb{R}^d \to \mathbb{R}^d$ - p. 7

$\nabla \times$ curl operator, $\nabla \times v = \operatorname{curl} v = \begin{pmatrix} \frac{\partial v_3}{\partial x_2} - \frac{\partial v_2}{\partial x_3} \\ \frac{\partial v_1}{\partial x_3} - \frac{\partial v_3}{\partial x_1} \\ \frac{\partial v_2}{\partial x_1} - \frac{\partial v_1}{\partial x_2} \end{pmatrix}$, for $v : \mathbb{R}^3 \to \mathbb{R}^3$ - p. 7

ν_1 nonlinear reluctivity function - p. 10

$\otimes$ tensor product - p. 30

$\partial\Omega$ boundary of a set Ω - p. 8

$f|_A$ restriction of a function f to a set A - p. 38

a.e. almost everywhere - p. 13

diam (Ω) diameter of a set Ω - p. 9

span$\{v_1, \ldots, v_n\}$ span of a set of vectors $\{v_1, \ldots, v_n\}$ - p. 25

supp f support of a function $f : \Omega \to \mathbb{R}$, i.e. $\overline{\{x \in \Omega : f(x) \neq 0\}}$ - p. 13

$A \times B$ Cartesian product of two sets A and B - p. 8

A^T transpose of a matrix A - p. 39

$C^k(\Omega)$ space of k-times continuously differentiable functions on Ω. - p. 10

$C_c^1(\Omega)$ space of smooth functions with compact support on Ω - p. 13

f_{BH} B H curve - p. 10

$o(\ )$ Landau "small-o" asymptotic notation - p. 21

$v \cdot w$ dot product in $\mathbb{R}^d$ between two vectors v and w - p. 8

V' dual space of some Banach space V - p. 12

$v \times w$ cross product in $\mathbb{R}^3$ between two vectors v and w - p. 8

Chapter 1

Introduction

1.1 Motivation

A crucial task in the design of electric motors is the creation of proper magnetic circuits [30]. In permanent magnet electric motors, the latter is created by electromagnets and permanent magnets. The corresponding mathematical model is governed by a quasilinear elliptic partial differential equation (PDE), i.e. the so-called magnetostatic approximation of Maxwell equations, which describes the magnetic field generated by the sources in the electrical machine. The mathematical modelling and design of electrical machines, governed by the magnetostatic equation is the subject of broad research (see, e.g. [2, 7, 33, 37, 16, 15, 14, 39]). One of the engineering design goals consists in improving the performance of the motor through modifying the size and/or location of the permanent magnets. This problem can be viewed as a parameter optimization problem [2, 7, 33, 37], where the parameters determine the geometry of the computational domain. The underlying optimization problem then requires repeated solutions of the nonlinear elliptic problem on the parametrized domain. Therefore, there is an increasing demand for the fast and reliable reduced models as surrogates in the optimization problem. To achieve this goal, in this thesis we develop the reduced basis method for quasilinear elliptic PDEs with strongly monotone differential operator and apply it to the nonlinear magnetostatics problem in the modelling framework of the permanent magnet synchronous machine.

The second motivation of this thesis is the development of reduced basis models for the magnetoquasistatic approximation of Maxwell's equations, which is also known as the eddy-current equation. This equation finds its place in important applications, such as the computation of magnetic fields in the presence of eddy currents in electrical machines [46, 32]. The development of fast and accurate simulation methods for such problems is of great importance in the optimization and design of electrical machines and other devices [7, 44]. Therefore there is a demand for reduced order models of this quasilinear PDE, which can be further used as surrogates in the optimization procedure. To achieve this goal, in this thesis we develop the reduced basis method for quasilinear parabolic PDEs with strongly monotone differential operator and apply it to the 2-D nonlinear eddy current equation.

1.2 State of the art and novelty of this work

The certified reduced basis method is known as an efficient method for model order reduction (MOR) of parametrized PDEs [21, 43, 25]. The efficiency comes from the use of the Greedy search algorithm in the basis construction for the numerical approximation of the problem and a-posteriori control of the

approximation error. The later serves not only for rigorous certification of the method, but also as the selection criterion in the Greedy selection process. This process provides incrementally better bases for the approximation and further significant speed-up in multi-query numerical simulations - relevant, for example, in the design, optimization and control contexts, through the use of RB surrogate models.

The extension of reduced basis techniques to nonlinear problems is a non-trivial task and the crucial ingredients of the method then highly depend on the underlying problem. Efficient implementation of the Greedy procedure requires a-posteriori error bounds or estimates, which, to the best of our knowledge, are not yet available for the nonlinear magnetostatics and magnetoquasistatics problems we consider. In [1] the reduced-basis method is applied to approximate the micro-problems in a homogenization procedure for quasilinear elliptic PDEs with non-monotone nonlinearity. However, we note that this is different from the approach in this thesis, where we use the reduced basis method for the approximation of the solution of a quasilinear PDE. In our case, the monotonicity of the problem allows the a-posteriori control of the global reduced-basis approximation error. We provide the corresponding error bound for quasilinear elliptic equations, which is based on a monotonicity argument and can be viewed as a generalisation of the classical error bound for linear elliptic problems [45], where the coercivity constant is now substituted by the monotonicity constant of the spatial differential operator. The computational efficiency of our reduced-basis method is based on the so-called offline-online decomposition. The offline phase corresponds to the construction of the surrogate model and depends on high-dimensional simulations, and thus is expensive. The online phase, where the surrogate model is operated, is usually decoupled from high-dimensional simulations and thus in general is inexpensive. This splitting is feasible if all the quantities in the problem are parameter separable and hence the problem admits an affine decomposition, which essentially means that all parameter dependencies can be separated from the spatial variables. The recovery of the affine decomposition in the presence of nonlinearities represents an additional challenge and it is usually treated with the Empirical Interpolation method (EIM)[5, 20, 38].

The reduced basis method was also successfully applied to linear [19, 48, 49] and nonlinear parabolic problems with polynomial [53, 52] and non-polynomial nonlinearities [18]. In general, there are two approaches for the reduced basis methods applied to unsteady problems: (1) first discretize, then estimate and reduce, (2) first estimate, then discretize and reduce. The approach (1) [19, 22, 18] is based on a time-marching problem in the offline phase and the error bounds or indicators are then stem from the structure of the discrete problem. The POD-Greedy procedure [22] is commonly used to construct the reduced-basis spaces and the EIM is used to treat non-affine and nonlinear problems [18]. In particular, the approach (1) is applied in [18] to semilinear parabolic problems with monotone non-polynomial nonlinearities. However, we note that the error bound, proposed in [18], is not applicable to our quasilinear problem. The approach (2) starts from a weak space-time variational formulation (see, e.g. [48, 49, 53, 52]). The error bounds are then derived in the appropriate Bochner spaces with respect to the natural space-time norms. In this approach, time is treated as a variable and thus it resembles the reduced-basis setting for elliptic problems [45]. The reduced-basis space is consequently constructed in the offline phase out of the space-time snapshots, obtained, for example, with the related Petrov-Galerkin discrete scheme. However, the appropriate choice of the discrete spaces in the Petrov-Galerkin scheme results in a time-marching interpretation (see, e.g. [49, 53]) of the discrete problem. In this way, the time-marching procedure allows to use the standard POD-Greedy approximation and to treat time as the parameter, which leads to the reduced-basis time-marching problem, but the error certification is accomplished with the natural space-time norm error bound. We refer to [17] for the detailed overview and comparison of

these two approaches in the context of linear parabolic equations.

In this thesis we treat quasilinear parabolic problems with the approach (2). We propose an $L^2(0;T;V)$ a-posteriori error estimate, based on the space-time variational formulation of quasilinear parabolic PDEs with strongly monotone differential operators. We introduce a Petrov-Galerkin projection to approximate the continuous variational problem and provide its reduced-basis counterpart. The Petrov-Galerkin problem with its solution u serves as our reference in a-posteriori error control. For computational purposes, we approximate the solution u by the solution of the Crank-Nicolson time-marching scheme and consequently use the POD-Greedy procedure to construct the reduced-basis spaces of small dimension. The right-hand side in our error estimate is approximated with a computable bound, which is used in the computational procedure. The time-marching Crank-Nicolson approximation of the Petrov-Galerkin problem also allows to treat the nonlinearity with the EIM in order to have offline-online decomposition for our problem available. Moreover, the parameter separability in time, achieved with the EIM, leads to a significant speed-up factor in the computational procedure. For the efficient numerical solution of both the quasilinear elliptic and parabolic reduced-basis problems with Newton's method we extend the computational machinery, proposed in [20, 18] for semilinear PDEs. It leads to a reduced numerical scheme with full affine decomposition and thus to a considerable acceleration in the online phase, compared to the original finite element simulations.

The MOR methods for the magnetoquastatic problem, to the best of our knowledge, are only developed in the Proper Orthogonal Decomposition (POD) setting [51], see e.g. [35, 23, 40], and the analogues of the proposed reduced basis methodology are not yet available in the literature for the class of problems we consider. We mention the recent work [29], where the a-posteriori error estimates for quasilinear parabolic PDEs in the presense of non-monotone nonlinearities were obtained. However, we think that the strong monotonicity assumption on the differential operator allows to better capture the structure of the magnetoquasistatic problem in our a-posteriori error estimate, compared to [29].

1.3 Outline of the thesis

This thesis is organized as follows:

- In Chapter 2 we introduce the physical model, derived as a 3-D magnetoquasistatic approximation of Maxwell's equations. We further impose additional assumptions on the domain of the problem and formulate its simplified 2-D version as the problem of our interest. We describe the nonlinear behaviour of ferromagnetic materials by introducing the B H curves and their main properties. We then outline a theoretical background, which is required for weak formulations of our PDEs and then we proceed with a detailed discussion on existence and uniqueness of weak solutions. Finally, we introduce the Newton operator, which will be further used in the numerical schemes for our problems.

- In Chapter 3 we introduce the main ingredients of the reduced basis method for parametrized elliptic and parabolic problems with linear, coercive differential operator. In particular, we address the questions of constructing good approximating spaces with the Greedy algorithms, the parameter-separability assumption and the corresponding affine decomposition of the problem, as well as the question of quantifying the error of the reduced basis approximation and derivations of the corresponding error bounds.

- In Chapter 4 we propose the certified reduced basis method for quasilinear elliptic problems together with its application to nonlinear magnetostatics equation, where the later models the permanent magnet synchronous motor. The parametrization enters through the geometry of the domain and combined with the nonlinearity, drives our reduction problem. We provide the corresponding reduced basis approximation of our problem. Next we prove the residual-based a-posteriori error bound and present the numerical results.

- In Chapter 5 we propose the cerified reduced basis method for quasilinear parabolic problems with strongly monotone spatial differential operator. We prove the residual-based a-posteriori error estimate for a space-time formulation and the provide a corresponding efficiently computable bound for the certification of the method. We introduce a Petrov-Galerkin finite element discretization of the continuous space-time problem and use it as our reference in a-posteriori error control. The Petrov-Galerkin discretization is further approximated by the Crank-Nicolson time-marching problem. Then we present the POD-Greedy approach to construct the reduced-basis spaces of small dimensions and apply the EIM to guarantee the efficient offline-online computational procedure. Finally, we apply our method to the 1-D and the 2-D nonlinear magnetoquasistatic problems and present the corresponding numerical results.

Chapter 2

Magnetoquasistatic approximation of Maxwell's equations

2.1 Physical model

In this section the 3-D magnetoquasistatic approximation of Maxwell's equations is derived together with its 2-D approximation. We also discuss the modelling of material relations in our computational problems.

2.1.1 Model problem

The laws of electromagnetism are given by a set of coupled partial differential equations, known as Maxwell's equations, which describe the relation between electric and magnetic fields [34]:

$$\frac{@\mathbf{B}}{@t} = \mathrm{r} \quad \mathbf{E} \qquad \text{Faraday's law;} \tag{2.1a}$$

$$\frac{@\mathbf{D}}{@t} + \mathbf{J} = \mathrm{r} \quad \mathbf{H} \qquad \text{Maxwell - Ampere's law;} \tag{2.1b}$$

$$\mathrm{r} \quad \mathbf{B} = 0 \qquad \text{Gauss' magnetic law;} \tag{2.1c}$$

$$\mathrm{r} \quad \mathbf{D} = \qquad \text{Gauss' electric law:} \tag{2.1d}$$

Quantities, involved in the equations, together with their units, are defined as follows:

B magnetic flux (or magnetic induction) [tesla]

H magnetic field [ampere/meter]

D electric flux density [coulomb/meter^2]

E electric field [volt/meter]

J current density [ampere/meter^2]

electric charge density [coulomb/meter^2]

All the quantities depend on position in space $x = (x_1; x_2; x_3)$ and on time t. Additionally, the following constitutive laws (material relations) between fields will be considered [32]:

$$\mathbf{B} = \quad \mathbf{H} + \mathbf{M}; \quad \mathbf{D} = \quad \mathbf{E} + \mathbf{P}; \quad \mathbf{J} = \quad \mathbf{E} + \mathbf{J}_s; \tag{2.2}$$

where $\mathbf{M}$ denotes the permanent magnet magnetization, $\mathbf{P}$ denotes an electric polarization and $\mathbf{J}_s$ an impressed current density. Furthermore, denotes the magnetic permeability, the electric permittivity and denotes the electric conductivity, which is strictly positive in conductors, but vanishes in dielectrics. In general, these material coefficients are tensors of rank 2, but in this thesis we assume that materials are isotropic, therefore they become scalar quantities. We also neglect the hysteresis effect in ferromagnetics, which makes the modelling of the materials complicated. We introduce the reciprocal of the magnetic permeability, the magnetic reluctivity , with the relation

$$\mathbf{H} = \quad (\mathbf{B} \quad \mathbf{M}): \tag{2.3}$$

Here we note that $\mathbf{H}_{pm} = \ _{mag}\mathbf{M}$, where $\mathbf{H}_{pm}$ is called the magnetic field such that the magnetic flux density $\mathbf{B}$ vanishes and $_{mag}$ denotes the constant magnetic reluctivity for the permanent magnet [24]. In our applications we will consider ferromagnetic materials, where the magnetic reluctivity is a nonlinear function of the magnitude of the magnetic flux density $(|\mathbf{B}|)$. We provide more details on the magnetic reluctivity function in the next section.

The quasistatic approximation is obtained from Maxwell's equations by neglecting the displacement current $\frac{@\mathbf{D}}{@t}$. Gauss' law, i.e. divergence-free nature of $\mathbf{B}$, implies that there exists a magnetic vector potential $\mathbf{A}$, which is unique up to a gradient field, such that

$$\mathbf{B} = \ r \quad \mathbf{A}: \tag{2.4}$$

The material laws (2.2), the quasistatic approximation to Maxwell-Ampere's law and (2.4) result in the *magnetoquasistatic approximation of Maxwell's equations*:

$$\frac{@\mathbf{A}}{@t} + r \quad (\ (|r \quad \mathbf{A}|) \ r \quad \mathbf{A}) = \mathbf{J}_s + r \quad \mathbf{H}_{pm}: \tag{2.5}$$

In some contexts, the eddy-current term $\frac{@\mathbf{A}}{@t}$ can be neglected and the equation turns into the *magnetostatic* approximation.

For computational purposes, we define a time interval $I = (0; T]$ with $T > 0$ and restrict the equation to a bounded domain $D \quad \mathbb{R}^3$ with a sufficiently smooth boundary $\Gamma := @D$, such that $\Gamma = \bar{\Gamma}_B \ [\ \bar{\Gamma}_H$ and $\Gamma_B \setminus \Gamma_H = \ ;$, and let $\nu(x) = \nu(x_1; x_2; x_3)$ be the outer normal vector to Γ. On Γ_B we impose the normal component of $\mathbf{B}$ to vanish and on Γ_H we impose the tangential component of $\mathbf{H}$ to vanish. It can be shown [4] that it translates into the following boundary conditions in terms of $\mathbf{A}$:

$$\mathbf{H} \quad \nu = 0 \quad , \quad \mathbf{A} \quad \nu = 0; \quad \text{on} \quad \Gamma_H \quad I; \tag{2.6a}$$

$$\mathbf{B} \quad \nu = 0 \quad , \quad [\ (|r \quad \mathbf{A}|) \ r \quad A] \quad \nu = 0; \quad \text{on} \quad \Gamma_B \quad I: \tag{2.6b}$$

We consider the initial-boundary value problem:

$$\frac{\partial \mathbf{A}}{\partial t} + \nabla \times \left((\mu \nabla \times \mathbf{A}) \nabla \times \mathbf{A} \right) = \mathbf{J}_s + \nabla \times \mathbf{H}_{pm}, \quad \text{in} \quad D \times I; \tag{2.7a}$$

$$\mathbf{A} \times \nu = 0; \quad \text{on} \quad \Gamma_H \times I; \tag{2.7b}$$

$$[(\mu \nabla \times \mathbf{A}) \nabla \times \mathbf{A}] \times \nu = 0; \quad \text{on} \quad \Gamma_B \times I; \tag{2.7c}$$

$$\mathbf{A} = \mathbf{A}_0; \quad \text{on} \quad D \times \{0\}; \tag{2.7d}$$

where $\mathbf{A}_0$ denotes the initial condition. The use of Coulomb gauging condition $\nabla \cdot \mathbf{A} = 0$ imposes the selection of solenoidal solutions to the problem and guarantees the existence of a unique solution in a weak sense [4].

Certain assumptions on the geometry of the computational domain D, that is,

- $D = \Omega \times (-\varepsilon_D, \varepsilon_D)$ and $\varepsilon_D > 0$ is small,
- $D = \Omega \times (-l, l)$, $l \sim \operatorname{diam}(\Omega)$ with a symmetric behaviour of the solution,

allow to reduce 3-D problem to 2-D problem, defined on the cross-section of D (see, e.g. [42]) . Therefore, let $\Omega \subset \mathbb{R}^2$ be a bounded domain with a sufficiently smooth boundary $\Gamma := \partial\Omega$, such that $\Gamma = \bar{\Gamma}_B \cup \bar{\Gamma}_H$ and $\Gamma_B \setminus \Gamma_H = \emptyset$, and let $\nu = \nu(x_1, x_2)$ denote the outer normal vector to Γ. We assume that geometrical and physical properties are translation-invariant in the x_3-direction, hence vector fields in the model do not depend on x_3. The magnetic fields $\mathbf{H}$, $\mathbf{H}_{pm}$ lie in the $x_1 \times x_2$ plane and we require that the current density $\mathbf{J}_s$ is perpendicular to the cross-section. Hence, for the fixed time $t > 0$ the vector fields are represented as follows:

$$\mathbf{H} = \begin{pmatrix} H_1(x_1, x_2, t) \\ H_2(x_1, x_2, t) \\ 0 \end{pmatrix}; \quad \mathbf{H}_{pm} = \begin{pmatrix} H_{pm,1}(x_1, x_2, t) \\ H_{pm,2}(x_1, x_2, t) \\ 0 \end{pmatrix}; \quad \mathbf{J}_s = \begin{pmatrix} 0 \\ 0 \\ J_3(x_1, x_2, t) \end{pmatrix}. \tag{2.8}$$

We also have

$$\mathbf{B} = \begin{pmatrix} B_1(x_1, x_2, t) \\ B_2(x_1, x_2, t) \\ 0 \end{pmatrix}; \quad \mathbf{A} = \begin{pmatrix} 0 \\ 0 \\ A_3(x_1, x_2, t) \end{pmatrix}; \tag{2.9}$$

where the form of $\mathbf{B}$ follows from the material relation (2.3) and the ansatz for $\mathbf{A}$ is chosen to satisfy (2.4). We introduce notation $u := A_3$ with $u : \Omega \to \mathbb{R}$. Then it follows that

$$\nabla \times \mathbf{A} = \begin{pmatrix} \frac{\partial u}{\partial x_2} \\ -\frac{\partial u}{\partial x_1} \\ 0 \end{pmatrix}; \quad \nabla \times \mathbf{H}_{pm} = \begin{pmatrix} 0 \\ 0 \\ \frac{\partial H_{pm,1}}{\partial x_2} + \frac{\partial H_{pm,2}}{\partial x_1} \end{pmatrix}; \tag{2.10}$$

and we have $|\nabla \times \mathbf{A}| = |\nabla u|$ and $\nabla \cdot \mathbf{A} = 0$. The following expression is then obtained:

$$\begin{aligned} [\nabla \times ((\mu \nabla \times \mathbf{A}) \nabla \times \mathbf{A})]_3 &= \frac{\partial}{\partial x_1} \left((\mu \nabla u) \frac{\partial u}{\partial x_1} \right) - \frac{\partial}{\partial x_2} \left((\mu \nabla u) \frac{\partial u}{\partial x_2} \right) \\ &= \nabla \cdot ((\mu \nabla u) \nabla u). \end{aligned} \tag{2.11}$$

Set $f := J_3 - \frac{\partial H_{pm,1}}{\partial x_2} + \frac{\partial H_{pm,2}}{\partial x_1}$ with $f : \Omega \to \mathbb{R}$. After transforming our boundary conditions, we obtain the

2-D magnetoquasistatics equation:

$$\begin{aligned} \frac{\partial u}{\partial t} \quad & \mathrm{r}\,(\,(\mathrm{j}\,\mathrm{r}\,u\mathrm{j})\,\mathrm{r}\,u) = f \quad \text{in } \Omega \quad I \\ & u = 0 \quad \text{in } \Gamma_B \quad I; \\ & [\,(\mathrm{j}\,\mathrm{r}\,u\mathrm{j})\,\mathrm{r}\,u]\,\sim = 0 \quad \text{on } \Gamma_H \quad I; \\ & u = u_o \quad \text{on } \Omega \quad \mathrm{f0g}: \end{aligned} \tag{2.12}$$

In the next sections we discuss a weak formulation of (2.12) and the question of unique solvability.

2.1.2 The *B*-*H* curve and its properties

According to (2.1), there exists a magnetic field **H** around any conductor of electric current. The magnetic field **H** is also called the magnetizing force, because materials, placed near such a force may acquire the magnetic properties. The amount of magnetism induced in a body is then described by a magnetic flux density **B**. The magnitude of the magnetic flux $B := \mathrm{j}\mathbf{B}\mathrm{j}$ depends on the magnitude of the magnetizing force $H := \mathrm{j}\mathbf{H}\mathrm{j}$ and on the material properties. The relation between B and H is linear in a variety of materials, i.e. we have $B = \quad H$, where $\quad$ is a constant magnetic permeability. Materials with a strong response to the magnetic field are called ferromagnetics. The $B \quad H$ relation in ferromagnetic materials is described by a nonlinear $B \quad H$ curve:

$$f_{BH} : \mathrm{R}_0^+ \;!\; \mathrm{R}_0^+ : H \,7!\, B = f_{BH}(H): \tag{2.13}$$

The magnetic permeability $\quad_1$ and the magnetic reluctivity $\quad_1$ in ferromagnetics are then defined as

$$\quad_1(s) := \frac{f_{BH}(s)}{s}; \quad \text{and} \quad \quad_1(s) := \frac{f_{BH}^{1}(s)}{s}; \tag{2.14}$$

such that we have

$$\mathbf{B} = \quad_1(\mathrm{j}\mathbf{H}\mathrm{j})\mathbf{H}; \quad \text{and} \quad \mathbf{H} = \quad_1(\mathrm{j}\mathbf{B}\mathrm{j})\mathbf{B}: \tag{2.15}$$

A physical nature of the function f_{BH} imposes the following natural assumptions on it (see, e.g. [42, 24]):

Assumption 1. *Let $f_{BH} : \mathrm{R}_0^+ \;!\; \mathrm{R}_0^+$ be a $B \quad H$ curve. Then the following holds:*

1. $f_{BH}\ 2\ C^1(\mathrm{R}_0^+)$,
2. $f_{BH}(0) = 0$,
3. $f_{BH}^0(s) \quad _0 > 0;\ 8s \quad 0$,
4. $\lim_{s\,!\,1} f_{BH}^0(s) = \quad _0$;

where $\quad_0 = 4 \quad 10^{\ 7}$ denotes the permeability of vacuum.

The following properties of the function $\quad_1$ easily follow from Assumption 1:

Corollary 2.1.1. *Let Assumption 1 hold. Let $\quad_0 := 1= \quad_0$ be the reluctivity of vacuum. Then the reluctivity function for ferromagnetic materials $\quad_1$ satisfies the following conditions:*

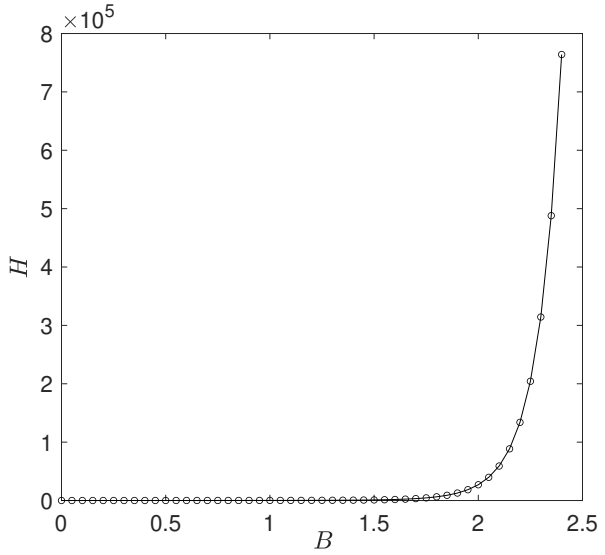

Figure 2.1: An example of f_{HB} used in our simulations (the measurements are denoted by dots).

1. $_1 \in C^1(\mathrm{R}_0^+)$ *and is bounded, that is, there exists* $_{LB} > 0$ *such that, for all* $s \in \mathrm{R}_0^+$ *it satisfies*

$$_{LB} \quad _1(s) \quad _0 \tag{2.16}$$

together with

$$\lim_{s \to 1} \ _1(s) = \ _0; \quad \textit{and} \quad \lim_{s \to 1} \ ^0_1(s) = 0:$$

2. *The mapping* $s \mapsto \ _1(s)s = f_{BH}^{1}(s),\ s \in \mathrm{R}_0^+$ *satisfies*

$$_{LB} \quad (\ _1(s)s)' \quad _0; \tag{2.17}$$

is strongly monotone with monotonicity constant $_{LB}$ *and Lipschitz continuous with Lipschitz constant* $_0$*, that is, for all* $s, t \in \mathrm{R}_0^+$ *it satisfies*

$$(\ _1(s)s \quad _1(t)t)(s \quad t) \quad _{LB}\,(s \quad t)^2; \tag{2.18a}$$

$$|\ _1(s)s \quad _1(t)t| \quad _0\,|s \quad t|: \tag{2.18b}$$

Proof. See [42].

In practice, the analytical form of $B \quad H$ curves is generally not known. Instead, the inverse of the $B \quad H$ curve $f_{HB}(s) := f_{BH}^{1}(s)$ is reconstructed from a finite number of discrete points

$$(H_k; B_k),\ k = 1; :::; K \in \mathrm{N}; \tag{2.19}$$

which are obtained from the real life measurements. For monotone data, as we have in our case, i.e., H_i H_j for $i < j$, the monotonicity-preserving cubic spline interpolation technique, proposed in [13], can be used for reconstruction (see Fig.2.1). Precisely, on each interval $[B_i; B_{i+1}]$ of length $4B_i = B_{i+1} \quad B_i$, f_{HB}

is represented as a cubic polynomial

$$f_{HB}(B) = H_i h_1(B) + H_{i+1} h_2(B) + d_i h_3(B) + d_i h_4(B); \tag{2.20}$$

where $d_j := f'_{HB}(B_j)$; $j = i; i+1$ and $h_p(B)$; $p = 1;:::;4$ are the usual Hermite basis functions on the interval $[B_i; B_{i+1}]$: $h_1(B) = z((B_{i+1} \quad B)=4B_i)$, $h_2(B) = z((B \quad B_i)=4B_i)$, $h_3(B) = \quad 4B_i s((B_{i+1} \quad B)=4B_i)$, $h_4(B) = 4B_i s((B \quad B_i)=4B_i)$, where $z(t) = 3t^2 \quad 2t^3$ and $s(t) = t^3 \quad t^2$. We note that suitable extrapolation techniques can be employed for the points beyond the data range (2.19) (see, e.g. [24]). The nonlinear reluctivity $_1$ is then obtained according to (2.14).

2.2 Analytical background

In this section we define notation and important notions from functional analysis, required for weak formulations of our magnetostatics and magnetoquasistatics PDEs. Afterwards, we prove that the corresponding weak problems are well-posed.

2.2.1 Some facts from functional analysis

We consider a real Banach space V with the norm $\|\cdot\|_V : V \to \mathbb{R}_0^+$. The space V is called *separable*, if there exists a countable dense subset $K := \{u_i \in V;\ i \in \mathbb{N}\} \subset V$ such that

$$\forall u \in V \quad \forall \varepsilon > 0 \quad \exists y \in K : \quad \|u \quad y\|_V < \varepsilon :$$

Let Y be a Banach space with the norm $\|\cdot\|_Y$. A linear operator $T : V \to Y$ is called *bounded* if

$$\exists C > 0 : \ \|Tu\|_Y \quad C\|u\|_V \quad \forall u \in V:$$

The space of linear bounded operators from V to Y is denoted by $\mathcal{L}(V;Y)$ and equipped with the norm

$$\|T\|_{\mathcal{L}(V;Y)} := \sup_{\|u\|_V = 1} \|Tu\|_Y:$$

We recall that $\mathcal{L}(V;Y)$ is Banach if Y is a Banach space. We also note that bounded linear operators between Banach spaces are continuous, therefore for them we use the notion of continuity and boundedness interchangeably.

Besides, we define a continuous *embedding* of V into the space Y as a continuous, linear, injective mapping $i : V \to Y$. If such an i exists, we say that V is continuously embedded in Y and write $V \hookrightarrow Y$.

Definition 2 (Linear functionals, duals spaces)**.**

- Let V be a Banach space. A bounded linear operator $f : V \to \mathbb{R}$, i.e., $f \in \mathcal{L}(V;\mathbb{R})$ is called a *bounded linear functional* on V.
- The space $V' := \mathcal{L}(V;\mathbb{R})$ is called the *dual space* of V and is a Banach space with the operator norm

$$\|f\|_{V'} := \sup_{\|u\|_V = 1} |f(u)|:$$

ˆ We use the notation

$$\langle f, u \rangle_{V' V} := f(u).$$

$\langle \cdot, \cdot \rangle_{V' V}$ is called the *duality pairing* of V and V'.

Let H be a real Hilbert space with the inner product $(\cdot, \cdot)_H : H \times H \to \mathbb{R}_0^+$ and the induced norm $\|\cdot\|_H := (\cdot, \cdot)_H^{1/2}$. We need the following

Theorem 3 (Riesz representation theorem)**.** *Let H be a Hilbert space. For any $f \in H'$ there exists a unique $v_f \in H$ such that*

$$\langle f, u \rangle_{H' H} = (v_f, u)_H \quad \forall u \in H, \tag{2.21}$$

and the mapping $f \mapsto v_f$ is isometric, i.e., $\|f\|_{H'} = \|v_f\|_H$. We say that v_f is the Riesz representer of f.

We denote by $V'' = (V')' = \mathcal{L}(V'; \mathbb{R})$ the *bidual* space of V. We define the evaluation functional $ev_u : V' \to \mathbb{R}$ as

$$ev_u(f) := \langle f, u \rangle_{V' V} \quad \forall f \in V'. \tag{2.22}$$

If all functionals in V'' are of the form (2.22), i.e., the mapping

$$V \ni u \mapsto ev_u \in V''$$

is surjective, then we say that V is *reflexive*. In that case V'' is isometrically isomorphic to V and one can identify V with V''.

We commonly define $L^p(\Omega)$ as the space of equivalence classes of a.e. identical Lebesque measurable functions on $\Omega \subset \mathbb{R}^d$, equipped with the norm

$$\|u\|_{L^p(\Omega)} := \begin{cases} \left(\int_\Omega |u(x)|^p \, dx \right)^{1/p} & \text{for } 1 \le p < \infty; \\ \operatorname{ess\,sup}_{x \in \Omega} |u(x)| & \text{for } p = \infty. \end{cases} \tag{2.23}$$

We also define the Lebesque space $L^1_{\mathrm{loc}}(\Omega)$ of locally integrable functions on Ω, i.e.,

$$L^1_{\mathrm{loc}}(\Omega) := \{ f : \Omega \to \mathbb{R};\ f|_K \in L^1(K);\ \forall K \subset\subset \Omega; K \text{ compact} \}.$$

Let $\Omega \subset \mathbb{R}^d$ be open and let $u \in L^1_{\mathrm{loc}}(\Omega)$. Consider the space of smooth functions $C_c^\infty(\Omega)$ with compact support $\operatorname{supp} f$, $f \in C_c^\infty(\Omega)$. If there exists a function $w \in L^1_{\mathrm{loc}}(\Omega)$ such that

$$\int_\Omega w \varphi \, dx = (-1)^{|\alpha|} \int_\Omega u D^\alpha \varphi \, dx, \quad \forall \varphi \in C_c^\infty(\Omega); \tag{2.24}$$

then $D^\alpha u := w$ is called the α-th weak partial derivative of u. We then commonly introduce Sobolev spaces $W^{k,p}(\Omega)$ as subspaces of functions $u \in L^p(\Omega)$, for which the weak derivatives $D^\alpha u$, $|\alpha| \le k$, are in

$L^p(\Omega)$. The norm on $W^{k,p}(\Omega)$ is given by

$$\|u\|_{W^{k,p}(\Omega)} := \begin{cases} \left(\sum_{|a| \le k} \|D^a u\|^p_{L^p(\Omega)} \right)^{1/p} & \text{for } 1 \le p < \infty; \\ \sum_{|a| \le k} \|D^a u\|_{L^1(\Omega)} & \text{for } p = \infty: \end{cases} \tag{2.25}$$

We note that for $p = 2$ we have a Hilbert space $H^k(\Omega) := W^{k,p}(\Omega)$. We refer the reader to [8] for more details on functional analysis and Sobolev spaces.

2.2.2 Brief on Bochner spaces

In this subsection we briefly introduce the necessary functional analytic tools to study abstract parabolic equations and their weak solutions. Solutions to parabolic PDEs are functions of time and space, therefore the regularity in space and time may be different. We introduce some important spaces, called Bochner spaces (see, e.g. [54, 11]), which formalize the later regularity issues of weak solutions to parabolic PDEs and are suitable for our problems.

Following [54], we first introduce the concept of a function with values in a Banach space, or a vector-valued function. Let $[0;T] \subset \mathbb{R}$ and V be a Banach space and consider a vector-valued function $u : [0;T] \to V$, that is, for any fixed $t \in [0;T]$, the function $x \mapsto u(x;t)$ belongs to V. For a Banach space V and $1 \le p \le \infty$, the linear space $L^p(0;T;V)$ consists of all measurable vector-valued functions $u : [0;T] \to V$, such that

$$\|u\|_{L^p(0;T;V)} := \begin{cases} \left(\int_0^T \|u(t)\|^p_V \, dt \right)^{1/p} < \infty \text{ for } 1 \le p < \infty; \\ \operatorname{ess\,sup}_{t \in [0;T]} \|u(t)\|_V < \infty \text{ for } p = \infty: \end{cases} \tag{2.26}$$

We also denote by $C(0;T;V)$ a space of vector-valued functions with values in V, which are continuous on $[0;T]$, with the norm

$$\|u\|_{C(0;T;V)} := \max_{t \in [0;T]} \|u(t)\|_V: \tag{2.27}$$

It is known (see, e.g. [11]) that this choice of norms makes the corresponding spaces complete. Moreover, if H is a Hilbert space, then $L^2(0;T;H)$ is also a Hilbert space with the inner product

$$(u, v)_{L^2(0;T;H)} := \int_0^T (u(t), v(t))_H dt; \quad u, v \in L^2(0;T;H): \tag{2.28}$$

Furthermore, let V be a reflexive Banach space, $1 \le p < \infty$ and $1/p + 1/q = 1$. We have the identification

$$[L^p(0;T;V)]' = L^q(0;T;V'):$$

The duality pairing of the spaces $L^q(0;T;V')$ and $L^p(0;T;V)$ is given by

$$(u(t), v(t))_{L^q(0;T;V') \, L^p(0;T;V)} := \int_0^T \langle u(t), v(t) \rangle_{V' V} dt; \quad u \in L^q(0;T;V'), v \in L^p(0;T;V):$$

The treatment of parabolic equations requires the simultaneous use of two appropriately coupled spaces H and V. This coupling is formalized with the notion of a Gelfand triple.

Definition 4 (Gelfand triple, see [54]). *The chain of embeddings $V \hookrightarrow H \hookrightarrow V^0$ is called a Gelfand triple if*

- *V - real separable reflexive Banach space;*
- *H - real separable Hilbert space;*
- *V is dense in H and embedding $V \hookrightarrow H$ is continuous, that is,*

$$\exists C > 0 : \|v\|_H \leq C\|v\|_V \quad \forall v \in V.$$

In the Gelfand triple, we identify H with its dual space H^0 via the following linear, continuous, injective mapping

$$H \ni h \mapsto \langle h, \cdot\rangle_H \in H^0, \tag{2.29}$$

which is also surjective, according to the Riesz representation theorem. Then the embedding $H^0 \hookrightarrow V^0$ is simply the restriction of $\langle h, \cdot\rangle_H \in H^0$ to V, which means that for $h \in H, v \in V$ it holds $\langle h, v\rangle_{V^0 V} = \langle h, v\rangle_H$.

We define a weak (or generalized) derivative of a vector-valued function: for $u \in L^1(0;T;V)$, a function $y \in L^1(0;T;V)$ satisfying

$$\int_0^T u(t)\,\varphi'(t)dt = -\int_0^T y(t)\,\varphi(t)dt, \quad \forall \varphi \in C_c^1((0;T)); \tag{2.30}$$

is called the weak derivative of u on $(0;T)$ and one writes $\dot{u} := y$.

Consider a Gelfand triple $V \hookrightarrow H \hookrightarrow V^0$ and let $u \in L^p(0;T;V)$. If there exists $w \in L^q(0;T;V^0)$, such that

$$\int_0^T \langle u(t), v\rangle_H\,\varphi'(t)dt = -\int_0^T \langle w(t), v\rangle_{V^0 V}\,\varphi(t)dt \quad \forall v \in V, \quad \forall \varphi \in C_c^1((0;T)); \tag{2.31}$$

then $\dot{u} := w$ is the generalized derivative of u and

$$\frac{d}{dt}\langle u(t), v\rangle_H = \langle \dot{u}(t), v\rangle_{V^0 V} \quad \forall v \quad \text{a.e. } t \in (0;T). \tag{2.32}$$

We define the space, which is going to be the solution (or trial) space for weak parabolic PDEs

$$W(0;T) := \{u \in L^2(0;T;V);\ \dot{u} \in L^2(0;T;V^0)\}; \tag{2.33}$$

and state some of its important properties.

Proposition 2.2.1. *Let $V \hookrightarrow H \hookrightarrow V^0$ be a Gelfand triple. Then the following hold:*

- *The space $W(0;T)$ is a Hilbert space with the inner product*

$$\langle u, v\rangle_{W(0;T)} := \int_0^T [\langle u(t), v(t)\rangle_V + \langle \dot{u}(t), \dot{v}(t)\rangle_{V^0}]\,dt, \quad u, v \in W(0;T); \tag{2.34}$$

where $\langle u, v\rangle_{V^0} := \langle J u, J v\rangle_V$, and $J : V^0 \to V$ is the duality mapping from the Riesz representation theorem.

- *There is a continuous embedding*

$$W(0;T) \hookrightarrow C(0;T;H): \tag{2.35}$$

More precisely, for $u \in W(0;T)$ there exists a unique continuous function $\bar{u} : [0;T] \to H$, such that $\bar{u} = u$ a.e. in $[0;T]$ and we have

$$\exists C > 0 : \max_{t \in [0;T]} \|u(t)\|_H \leq C\|u\|_{W(0;T)}: \tag{2.36}$$

- *For $u, v \in W(0;T)$ and $t_1, t_2 \in [0;T]$, $t_1 \leq t_2$, the generalized integration by parts formula holds:*

$$\langle u(t_2), v(t_2)\rangle_H - \langle u(t_1), v(t_1)\rangle_H = \int_{t_1}^{t_2} [\langle \dot{u}(s), v(s)\rangle_{V^0 V} + \langle \dot{v}(s), u(s)\rangle_{V^0 V}]\, ds: \tag{2.37}$$

Proof. See [54].

2.2.3 Existence and uniqueness of weak solutions

In this subsection we present the mathematical analysis of magnetostatic and magnetoquasistatic problems. In the following definition we list some important properties of an operator, which will be essential in this analysis.

Definition 5 (see [55])**.** *Let V be a Banach space and $A : V \to V^0$ be an operator. Then*

- *A is called monotone if*

$$\langle A(u) - A(v), u - v\rangle_{V^0 V} \geq 0, \quad \forall u, v \in V;$$

- *A is called strongly monotone if $\exists C > 0$ such that:*

$$\langle A(u) - A(v), u - v\rangle_{V^0 V} \geq C\|u - v\|_V^2, \quad \forall u, v \in V;$$

- *A is called coercive if*

$$\frac{\langle A(u), u\rangle_{V^0 V}}{\|u\|_V} \to \infty, \text{ as } \|u\|_V \to \infty;$$

- *A is called Lipschitz continuous if $\exists C > 0$ such that:*

$$\langle A(u) - A(w), v\rangle_{V^0 V} \leq L\|u - w\|_V\|v\|_V, \quad \forall u, w, v \in V;$$

- *A is called hemicontinuous if the mapping*

$$s \mapsto \langle A(u + sw), v\rangle_{V^0 V}$$

is continuous on $[0;1]$, $\forall u, v, w \in V$.

Firstly, we discuss a domain structure and a structure of the nonlinearity, which is common for both stationary and non-stationary problems. We recall that $\Omega \subset \mathbb{R}^2$ is a bounded domain with a sufficiently

smooth boundary $\Gamma =: \partial\Omega$, such that $\Gamma = \bar{\Gamma}_B \cup \bar{\Gamma}_H$ and $\Gamma_B \cap \Gamma_H = \emptyset$, and $\nu = \nu(x_1, x_2)$ denotes the outer normal vector to Γ. Let Ω_f denote the subdomain, which consists of ferromagnetic material. Let $\Omega_{air} = \Omega \setminus \bar{\Omega}_f$ be the subdomain, which consists of all other materials, i.e. the magnet areas Ω_{mag}, the coil areas Ω_c and the air gap regions Ω_g. We assume that the interface lines between the materials are piecewise C^2 and Lipschitz continuous. We now define the magnetic reluctivity function for our problem:

$$\nu(x, |\nabla u|) = \begin{cases} \nu_1(|\nabla u|), & \text{for } x \in \Omega_f; \\ \nu_0, & \text{for } x \in \Omega_{air} \cup \Omega_{mag}; \\ \nu_{mag}, & \text{for } x \in \Omega_{mag}; \end{cases} \tag{2.38}$$

where ν_1 is a nonlinear function that is defined via $B - H$ curve (2.14), $\nu_0 = 4\pi \cdot 10^7$ is the reluctivity of vacuum (which is also a feasible value for the reluctivity of air) and ν_{mag} is the reluctivity of the permanent magnet material. For simplicity of presentation, we set $\nu_{mag} = \nu_0$ and use the value $\nu_{mag} = \nu_0 = 1.086$ for numerical examples in this thesis. Then we have

$$\nu(x, |\nabla u|) = \chi_{\Omega_f}(x)\, \nu_1(|\nabla u|) + \chi_{\Omega_{air}}(x)\, \nu_0. \tag{2.39}$$

The magnetic reluctivity $\nu : \Omega \times \mathbb{R}_0^+ \to \mathbb{R}_0^+$ satisfies the *Carathéodory condition* [12]; i.e., for every $s \in \mathbb{R}_0^+$ the function $\nu(\cdot, s)$ is measurable, and ν is continuous in s for almost every $x \in \Omega$. Furthermore, due to (2.16), we have that

$$\nu_{LB} \le |\nu(x, s)| \le \nu_0 < \infty \quad \text{a.e. in } \Omega, \ \forall s \in \mathbb{R}_0^+; \tag{2.40}$$

which implies that $\nu(\cdot, |\nabla u(\cdot)|) \in L^\infty(\Omega)$ for each $u \in H^1(\Omega)$.

Remark 6. *We note that $\nu(x, s)$ satisfies* (2.18a) *and* (2.18b) *for all $x \in \Omega$. It follows from the Corollary 2.1.1 that the mapping $\mathbb{R}_0^+ \ni s \mapsto \nu(x, s)s \in \mathbb{R}_0^+$ is strongly monotone with monotonicity constant ν_{LB} and Lipschitz continuous with Lipschitz constant ν_0.*

We consider a two-dimensional nonlinear magnetostatic field problem, that is, a stationary case of problem (2.12):

$$\begin{aligned} -\nabla \cdot (\nu(|\nabla u|)\nabla u) &= f \quad \text{in } \Omega \\ u &= 0 \quad \text{in } \Gamma_B \\ [\nu(|\nabla u|)\nabla u] \cdot \nu &= 0 \quad \text{on } \Gamma_H \end{aligned} \tag{2.41}$$

We proceed with an abstract formulation of problem (2.41). Let Γ_B be a Dirichlet boundary with $\text{meas}(\Gamma_B) > 0$. The function space V is such that

$$V := \{v : \ v \in H^1(\Omega), \ v|_{\Gamma_B} = 0\}. \tag{2.42}$$

The inner product on V is defined by $\langle w, v \rangle_V = \int_\Omega \nabla w \cdot \nabla v \, dx$ and the induced norm is given by $\|v\|_V = \langle v, v \rangle_V^{1/2}$, which is indeed a norm due to Poincare-Friedrichs inequality [11]. We introduce the nonlinear operator $A : V \to V^0$, which stems from the integration by parts of the left-hand side of equation (2.41),

defined by

$$\langle A(u), v\rangle_{V^0 V} := a[u](u,v) = \int_\Omega (x, |\nabla u|)\nabla u \cdot \nabla v \, dx, \quad \forall u, v \in V, \tag{2.43}$$

where $a[u](u,v)$ is the induced *quasilinear* form. The weak form of the right-hand side of equation (2.41) reads:

$$\langle f, v\rangle_{V^0 V} = \int_\Omega (J_e v - H_{pm;2}\frac{\partial v}{\partial x_1} + H_{pm;1}\frac{\partial v}{\partial x_2})dx, \tag{2.44}$$

where $J_e \in L^2(\Omega)$ represents the current density and $H_{pm;1}, H_{pm;2} \in L^2(\Omega)$ are the components of the permanent magnet magnetic field. We note that the integrals, appearing in (2.43) and (2.44), are well-defined. Then the abstract formulation of problem (2.41) reads as follows: find $u \in V$ such that

$$\langle A(u), v\rangle_{V^0 V} = \langle f, v\rangle_{V^0 V}, \quad \forall v \in V. \tag{2.45}$$

The governing weak PDE (2.45) is then of a quasilinear elliptic type. For existence and uniqueness of solutions of problem (2.45), we use a theorem, provided by Zarantonello.

Theorem 7. *([55, Theorem 25.B]) Let V be a Hilbert space, $f \in V^0$ and $A : V \to V^0$ an operator, which is strongly monotone and Lipschitz continuous. Then the operator equation $A(u) = f$ has a unique solution $u \in V$.*

Proof. See [55].

In order to apply Theorem 7 to our problem (2.45), we need the following Lemma 8. Due to its overall importance not only for the current analysis, but also for the upcoming error bounds in the next sections, we provide the proof of this lemma.

Lemma 8 (see [24])**.** *If $\nu(x,\cdot) : \mathbb{R}_0^+ \to \mathbb{R}_0^+$ is strongly monotone with monotonicity constant ν_{LB} and Lipschitz continuous with Lipschitz constant ν_0. Then the nonlinear operator A is strongly monotone with monotonicity constant $m_a := \nu_{LB}$ and Lipschitz continuous with Lipschitz constant $L_a := 2\nu_{LB} + \nu_0$.*

Proof. First we show that the mapping $\nu(x,|\cdot|) : \mathbb{R}^2 \to \mathbb{R}^2$ is strongly monotone with monotonicity constant ν_{LB}. By assumption, it holds that

$$\nu(x,|\mathbf{p}|)|\mathbf{p}| \quad \nu(x,|\mathbf{q}|)|\mathbf{q}| \quad |\mathbf{p}| \quad |\mathbf{q}| \quad \nu_{LB} \quad |\mathbf{p}| \quad |\mathbf{q}|^2;$$

which implies that

$$\nu(x,|\mathbf{p}|)|\mathbf{p}|^2 \quad \nu_{LB} \quad |\mathbf{p}| \quad |\mathbf{q}|^2 + \quad \nu(x,|\mathbf{p}|) + \nu(x,|\mathbf{q}|)\,|\mathbf{p}||\mathbf{q}| \quad \nu(x,|\mathbf{q}|)|\mathbf{q}|^2.$$

It follows from the above inequality that

$$\begin{aligned}\nu(x,|\mathbf{p}|)\mathbf{p} \quad \nu(x,|\mathbf{q}|)\mathbf{q} \quad \mathbf{p} \quad \mathbf{q} &= \nu(x,|\mathbf{p}|)|\mathbf{p}|^2 + \nu(x,|\mathbf{q}|)|\mathbf{q}|^2 \quad \nu(x,|\mathbf{p}|) + \nu(x,|\mathbf{q}|)\ \mathbf{p} \quad \mathbf{q} \\ &\nu_{LB} \quad |\mathbf{p}| \quad |\mathbf{q}|^2 + \quad \nu(x,|\mathbf{p}|) + \nu(x,|\mathbf{q}|)\ |\mathbf{p}||\mathbf{q}| \quad \mathbf{p} \quad \mathbf{q} \\ &\nu_{LB} \quad |\mathbf{p}| \quad |\mathbf{q}|^2 + 2\ \nu_{LB}\ |\mathbf{p}||\mathbf{q}| \quad \mathbf{p} \quad \mathbf{q} = \nu_{LB}|\mathbf{p} \quad \mathbf{q}|^2.\end{aligned}$$

We now set $\mathbf{p} = \nabla u; \mathbf{q} = \nabla v$ and apply the estimate above to establish the strong monotonicity of A:

$$\begin{aligned}\langle A(u) - A(v), u - v\rangle_{V^0 V} &= \int_\Omega [a[u](u, u - v) - a[v](v, u - v)] \\ &= \int_\Omega \left(\nu(x, |\nabla u|)\nabla u - \nu(x, |\nabla v|)\nabla v \right) \cdot (\nabla u - \nabla v) dx \\ &\geq \alpha_{LB} \int_\Omega |\nabla u - \nabla v|^2 dx = m_a \|u - v\|_V^2.\end{aligned}$$

We now prove Lipschitz continuity of the mapping $\nu(x, |\cdot|)\cdot$. We have the following estimate

$$\begin{aligned}\nu(x, |\mathbf{p}|)\mathbf{p} - \nu(x, |\mathbf{q}|)\mathbf{q} &= \nu(x, |\mathbf{p}|)(\mathbf{p} - \mathbf{q}) + [\nu(x, |\mathbf{p}|) - \nu(x, |\mathbf{q}|)]\,\mathbf{q} \\ &\quad [\nu(x, |\mathbf{p}|) - \nu(x, |\mathbf{q}|)]\mathbf{p} - \mathbf{q}| + [\nu(x, |\mathbf{p}|) - \nu(x, |\mathbf{q}|)]\,|\mathbf{q}| \\ &= \nu(x, |\mathbf{p}|)|\mathbf{p} - \mathbf{q}| + [\nu(x, |\mathbf{p}|) - \nu(x, |\mathbf{q}|)](|\mathbf{p}| - |\mathbf{q}|) + [\nu(x, |\mathbf{p}|) - \nu(x, |\mathbf{q}|)]|\mathbf{p}| - |\mathbf{q}| \\ &\quad 2\,[\nu(x, |\mathbf{p}|) - \nu(x, |\mathbf{q}|)]|\mathbf{p} - \mathbf{q}| + [\nu(x, |\mathbf{p}|) - \nu(x, |\mathbf{q}|)]|\mathbf{p}| - |\mathbf{q}|\end{aligned}$$

By the assumption on Lipschitz continuity of $\nu(x, \cdot)$, it holds that

$$|\nu(x, |\mathbf{p}|)\mathbf{p} - \nu(x, |\mathbf{q}|)\mathbf{q}| \leq (2\,[\nu(x, |\mathbf{p}|) + \alpha_{UB}])|\mathbf{p} - \mathbf{q}| \leq (2\,\alpha_{LB} + \alpha_0)|\mathbf{p} - \mathbf{q}| = L_a|\mathbf{p} - \mathbf{q}|.$$

We now apply the estimate above to establish the Lipschitz continuity of A:

$$\begin{aligned}\langle A(u) - A(v), w\rangle_{V^0 V} &= \int_\Omega [a[u](u, w) - a[v](v, w)] \\ &= \int_\Omega [\nu(x, |\nabla u|)\nabla u - \nu(x, |\nabla v|)\nabla v] \cdot \nabla w\, dx \\ &\quad \int_\Omega \nu(x, |\nabla u|)\nabla u - \nu(x, |\nabla v|)\nabla v |\nabla w| dx \\ &\leq L_a \int_\Omega |\nabla u - \nabla v||\nabla w| dx \leq L_a \|u - v\|_V \|w\|_V.\end{aligned}$$

All together, the well-posedness of problem (2.45) follows, so that (2.45) admits a unique solution $u \in V$.

Further we present the analysis of magnetoquasistatic problem (2.12). We set V as in (2.42) and $H := L^2(\Omega)$ and consider a corresponding Gelfand triple $V \hookrightarrow H \hookrightarrow V^0$. We multiply equation (2.12) by an arbitrary function $v \in V$ and integrate over the domain Ω to obtain the following weak formulation of problem: find $u \in W(0; T)$ such that

$$\begin{aligned}\langle \dot{u}(t), v\rangle_{V^0 V} + \langle A(u(t)), v\rangle_{V^0 V} &= \langle f(t), v\rangle_{V^0 V} \quad \text{a.e. } t \in (0; T) \\ u(0) &= u_o \in H.\end{aligned} \tag{2.46}$$

Here the operator $A : V \to V^0$ is given by and $f \in L^2(0; T; V^0)$. Derivative $\dot{u}$ is understood in the generalized sense, specified in (2.32). Moreover, the initial condition is well-defined in H due to the continuous embedding $W(0; T) \hookrightarrow C(0; T; H)$ (see Proposition 2.2.1).

We can write a weak formulation of (2.12) in a way, which would let us treat the space and time variable similarly. Precisely, we multiply equation by an arbitrary function $v \in L^2(0; T; V)$ and integrate over both the domain Ω and the time interval $(0; T)$. In addition, we incorporate an initial condition in a

weak manner. Then a space-time variational formulation reads: find $u \in W(0;T)$ such that

$$B[u](u;v) = F(v); \quad \forall v := (v^{(1)}; v^{(2)}) \in L^2(0;T;V) \quad H; \tag{2.47}$$

where

$$B[u](u;v) := \int_0^T \langle \dot{u}; v^{(1)} \rangle_{V'V} + a[u](u; v^{(1)}) dt + \langle u(0); v^{(2)} \rangle_H; \text{ and} \tag{2.48}$$

$$F(v) := \int_I \langle f; v^{(1)} \rangle_{V'V} dt + \langle u_o; v^{(2)} \rangle_H: \tag{2.49}$$

We note that the space-time variational formulation (2.47) is equivalent to the weak formulation (2.46) (see, e.g. [28]). For existence and uniqueness of solutions to problem (2.47), we need the following theorem.

Theorem 9. *([55, Theorem 30.A]) Let $V \hookrightarrow H \hookrightarrow V'$ be a Gelfand triple and let $u_o \in H$ and $f \in L^2(0;T;V')$. If*

1. *operator $A : V \to V'$ is monotone, hemicontinuous, coercive and bounded;*
2. *the mapping $t \mapsto \langle A(u(t)); v \rangle_{V'V}$ is measurable on $(0;T)$, $\forall u; v \in V$,*

then the problem has a unique solution $u \in W(0;T)$.

Proof. See, e.g. [55]

The strong monotonicity of the operator A implies its monotonicity. Lipschitz continuity of A implies its hemicontinuity and boundedness. We are left to show that the operator A is coercive: it easily follows from the fact that is bounded from below by $_{LB}$. Therefore, the first point of the Theorem 9 is satisfied. The magnetic reluctivity satisfies the Carathéodory condition, therefore the second point of the Theorem 9 is satisfied. All together, it implies that problem (2.47) admits a unique solution.

Remark 10. *We note that hemicontinuity easily follows from the continuity of on $\mathbb{R}_0^+$ and* (2.40) *easily implies boundedness of A.*

2.2.4 The Newton operator

Application of Newton's method requires knowledge of the Frechét derivative $A'(u) : V \to V'$ of the operator A. In the context of our problem, we have the following definitions of various derivatives in Banach space.

Definition 11 (see [28])**.** *Let V be a Banach space and $A : U \quad V \to V'$ be an operator, U , ; open. Then*

ˆ *A is called directionally di erentiable at $u \in U$ if the limit*

$$dA(u;h) = \lim_{\to 0} \frac{A(u + h) \quad A(u)}{} = \frac{d}{d} \Big|_{=0} A(u + h) \in V'$$

exists for all $h \in V$. In this case, $dA(u;h)$ is called directional derivative of A in the direction h.

- *A is called Gateaux differentiable (or G-differentiable) at $u \in U$ if A is directionally differentiable at u and the directional derivative $A'(u) : V \ni h \mapsto dA(u;h) \in V'$ is bounded and linear, i.e., $A'(u) \in L(V;V')$.*

- *A is called Fréchet differentiable (or F-differentiable) at $u \in U$ if A is Gateaux differentiable at u and the following condition holds:*

$$\langle A(u+h) - A(u) - A'(u)(h), v\rangle_{V'V} \leq o(\|h\|_V)\|v\|_V;$$

where $o(\cdot)$ denotes the Landau "small o" notation.

We split the operator A into two parts, which correspond to ferromagnetic and linear materials

$$\langle A(u), v\rangle_{V'V} = \int_{\Omega_f} \nu_1(|\nabla u|)\nabla u \cdot \nabla v\,dx + \int_{\Omega_{air}} \nu_0 \nabla u \cdot \nabla v\,dx. \tag{2.50}$$

For $\nabla u \neq 0$, we form the directional derivative $dA(u;h)$ and test it with an arbitrary $v \in V$ to obtain

$$\begin{aligned}\langle dA(u;h), v\rangle_{V'V} &= \frac{d}{d\tau}\Big|_{\tau=0}\left[\int_{\Omega_f} \nu_1(|\nabla(u+\tau h)|)\nabla(u+\tau h)\cdot\nabla v\,dx + \int_{\Omega_{air}} \nu_0 \nabla(u+\tau h)\cdot\nabla v\,dx\right] \\ &= \int_{\Omega_f} \frac{\nu_1'(|\nabla u|)}{|\nabla u|}(\nabla u\cdot\nabla h)(\nabla u\cdot\nabla v) + \nu_1(|\nabla u|)\nabla h\cdot\nabla v\,dx + \int_{\Omega_{air}} \nu_0 \nabla h\cdot\nabla v\,dx.\end{aligned} \tag{2.51}$$

In general, for $p = 0$ the mapping $\mathbb{R}^2 \ni p \mapsto \nu_1(|p|)$ is not differentiable, but the mapping $\mathbb{R}^2 \ni p \mapsto \nu_1(|p|)p$ is. Indeed, let $p \in \mathbb{R}^2$, $|p| > 0$, then

$$\lim_{\tau\to 0}\frac{\nu_1(|\tau p|)\,\tau p - \nu_1(0)0}{\tau} = \lim_{\tau\to 0}\nu_1(|\tau p|)p = \nu_1(0)p. \tag{2.52}$$

Therefore, for $\nabla u = 0$ we have

$$\begin{aligned}\langle dA(u;h), v\rangle_{V'V} &= \frac{d}{d\tau}\Big|_{\tau=0}\left[\int_{\Omega_f} \nu_1(|\tau\nabla h|)\,\tau\nabla h\cdot\nabla v\,dx + \int_{\Omega_{air}} \nu_0 \nabla(u+\tau h)\cdot\nabla v\,dx\right] \\ &= \int_{\Omega_f} \nu_1(0)\nabla h\cdot\nabla v\,dx + \int_{\Omega_{air}} \nu_0 \nabla h\cdot\nabla v\,dx.\end{aligned} \tag{2.53}$$

Linearity of the mapping $h \mapsto dA(u;h)$ is obvious, therefore we write $dA(u;h) = A'(u)h$. We define the differential reluctivity tensor $\hat{\nu}_{\mathbf{df}} : \mathbb{R}^2 \to \mathbb{R}^{2\times 2}$:

$$\hat{\nu}_{\mathbf{df}}(q) = \begin{cases} \nu_1(|q|)I + \frac{\nu_1'(|q|)}{|q|}qq^T; & \text{for } q \neq 0; \\ \nu_1(|q|)I; & \text{for } q = 0; \end{cases} \tag{2.54}$$

where $I \in \mathbb{R}^{2\times 2}$ denotes the identity matrix. Moreover, for a fixed $\mathbb{R}^2 \ni q \neq 0$, we can compute the eigenvalues and eigenvectors of $\hat{\nu}_{\mathbf{df}}(q)$ (see, e.g. [42]):

$$\begin{aligned}\lambda_1(q) &= q^\perp \cdot \nu_1(|q|); & v_1 &= (-q_2;q_1)^T; \\ \lambda_2(q) &= q \cdot \nu_1(|q|) + \nu_1'(|q|)|q|; & v_2 &= (q_1;q_2)^T.\end{aligned} \tag{2.55}$$

Then we introduce the general differential reluctivity tensor $_{\mathbf{df}} : \Omega \quad R^2 \ ! \ R^{2 \ 2}$, given by

$$_{\mathbf{df}}(x;q) := \ _{\Omega_f}(x)\hat{}_{\mathbf{df}}(q) + \ _{\Omega_{air}}(x) \ _0 q: \tag{2.56}$$

Then the derivative of the operator A can be written as

$$\hbar A^0(u)w; v\mathrm{i}_{V^0V} = \int_\Omega \ _{\mathbf{df}}(x; \ r\,u) \, r\,w \quad r\,v dx: \tag{2.57}$$

We now prove the following lemma.

Lemma 12. *Let $u \ 2 \ V$, and define the bilinear form $\hbar A^0(u)w; v\mathrm{i}_{V^0V} := da[u](w;v)$. Then $da[u](\ ;\ )$ is coercive and continuous, i.e.,*

$$\begin{aligned} da[u](v;v) \quad & _{LB}\mathrm{k}v\mathrm{k}_V^2; \ 8v \ 2 \ V; \\ da[u](w;v) \quad & _0\mathrm{k}w\mathrm{k}_V\mathrm{k}v\mathrm{k}_V; \ 8v;w \ 2 \ V: \end{aligned}$$

Proof. We use the computed eigenvalues (2.55) and bound (2.18a) to prove coercivity

$$da[u](w;w) \quad \int_\Omega \min\{ \ _1(\ r\,u); \ _2(\ r\,u)\} \, r\,w \quad r\,w dx \quad _{LB}\mathrm{k}w\mathrm{k}_V^2;$$

and similarly with bound (2.17) we prove continuity

$$da[u](w;v) \quad \int_\Omega \max\{ \ _1(\ r\,u); \ _2(\ r\,u)\} \, r\,w \quad r\,v dx \quad _0\mathrm{k}w\mathrm{k}_V\mathrm{k}v\mathrm{k}_V:$$

From Lemma 12, we conclude that $A^0(u) \ 2 \ L(V;V^0)$ and hence the operator A is G-differentiable. Moreover, for $p;q \ 2 \ R^2$, $p \ , \ 0$, it holds

$$_1(\mathrm{j}p + \ q\mathrm{j})(p + \ q) \quad _1(\mathrm{j}p\mathrm{j})p = \ _1(\mathrm{j}p\mathrm{j})q + \ \frac{^0_1(\mathrm{j}p\mathrm{j})}{\mathrm{j}p\mathrm{j}}(p \ \ q)p + o(\ \mathrm{j}q\mathrm{j}); \tag{2.58}$$

and implies that

$$\hbar A(u + \ h) \quad A(u) \quad A^0(u)(\ h); v\mathrm{i}_{V^0V} \quad \int_\Omega o(\ \mathrm{j}\,r\,h\mathrm{j})\mathrm{j}\,r\,v\mathrm{j}dx \quad o(\ )\mathrm{k}h\mathrm{k}_V\mathrm{k}v\mathrm{k}_V: \tag{2.59}$$

Therefore, we established that the operator A is F-differentiable with continuously invertible F-derivative $A^0(u)$, which will be subsequently used to solve arising nonlinear equations with Newton's method.

Chapter 3

The Reduced Basis Method

3.1 Overview

Consider an *exact* solution map $\Phi : \mathsf{D} \to V$ for some parametric partial differential equation, where $\mathsf{D} \subset \mathsf{R}^p$ is a compact parameter set, V is an appropriate Hilbert space and $\Phi(\mu) \in V$ is the certain solution of our PDE. Its image induces the solution manifold

$$\mathsf{M} := \Phi(\mathsf{D}) = \{u(\mu) \in V : \mu \in \mathsf{D}\} \subset V. \tag{3.1}$$

The main idea of the reduced basis method is the realization that, in many instances, the solution manifold (3.1) can be approximated sufficiently well by its projection on a low-dimensional linear subspace V_N, spanned by appropriately chosen *snapshots* $\Phi(\bar{\mu}_1), \ldots, \Phi(\bar{\mu}_N)$; $\bar{\mu}_1 \in \mathsf{D}, \ldots, \bar{\mu}_N \in \mathsf{D}$. The good approximation space V_N attempts to minimize the Kolmogorov N-widths

$$d_N(\mathsf{M}; V_N) := \inf_{\substack{V_N \subset V \\ \dim(V_N)=N}} \varepsilon(\mathsf{M}; V_N), \tag{3.2}$$

where by

$$\varepsilon(\mathsf{M}; V_N) := \sup_{\mu \in \mathsf{D}} \inf_{v_N \in V_N} \|u(\mu) - v_N\|_V \tag{3.3}$$

we denote the deviation of V_N from M. The optimization problem (3.2) is difficult to solve, therefore the heuristic Greedy procedure, based on the linear search in the parameter set D, was proposed [50]. The Greedy algorithm iteratively picks up the snapshots from M and constructs the approximation space V_N. Convergence results for the Greedy procedure are achieved by applying the convergence rates of the Kolmogorov N-widths, see e.g. [9] and [6] for respective exponential and algebraic convergence rates.

In actual practice, we do not have an access to the exact solution of the problem and thus to the solution manifold M, therefore we replace Φ with its *truth approximation* Φ_h, obtained, e.g. by a Galerkin projection on a suitable finite element approximation space $V_h \subset V$ of very large dimension N. We assume that the induced M_h can be made as close to M as desired by choosing an appropriate discretization.

The efficient implementation of the Greedy procedure requires *a-posteriori error estimates* or *bounds* and also certain structural assumptions on the problems of interest, such as the *parameter-separability*, which leads to the *offline-online decomposition*. In this chapter we sketch the main ingredients of the

reduced basis modelling for linear elliptic and parabolic PDEs. We refer the reader to [21, 43, 25] for the comprehensive introduction into reduced-basis methods and to [41] for the brief overview of the field.

3.2 Reduced basis method for linear elliptic PDEs

In this section we briefly outline the reduced basis method for linear elliptic problems with coercive differential operator (see e.g. [22] for the detailed treatment).

3.2.1 Abstract formulation

Let $\Omega \subset \mathbb{R}^d$ be the spatial domain and $\mu \in \mathcal{D} \subset \mathbb{R}^p$, where $\mathcal{D}$ is a compact parameter set. Let $V \subset H^1(\Omega)$ be a separable Hilbert space. We denote by $(\cdot,\cdot)_V$ and $\|\cdot\|_V$ the inner product and induced norm on V. For given $\mu \in \mathcal{D}$ we consider a linear, bounded, coercive differential operator $A(\mu) : V \to V'$ with induced bilinear form $a(\cdot,\cdot;\mu) : V \times V \to \mathbb{R}$:

$$a(u, v; \mu) := (A(\mu)u, v)_{V' V}. \tag{3.4}$$

For given $f(\cdot;\mu) \in V'$, we consider the weak form of parametrized elliptic PDE or *truth* problem: given $\mu \in \mathcal{D}$, find $u(\mu) \in V$ such that

$$a(u(\mu), v; \mu) = f(v; \mu), \quad \forall v \in V. \tag{3.5}$$

We assume that bilinear forms (3.4) are coercive on V with coercivity constants $\alpha(\mu) > 0$, i.e.

$$a(v, v; \mu) \geq \alpha(\mu)\|v\|_V^2 \quad \forall v \in V, \tag{3.6}$$

and continuous on V with continuity constants $\gamma(\mu) > 0$, i.e.

$$|a(w, v; \mu)| \leq \gamma(\mu)\|w\|_V\|v\|_V \quad \forall w, v \in V. \tag{3.7}$$

In addition, we assume that these conditions hold uniformly:

$$\alpha_0 := \inf_{\mu \in \mathcal{D}} \alpha(\mu) > 0, \qquad \gamma_0 := \sup_{\mu \in \mathcal{D}} \gamma(\mu) < \infty. \tag{3.8}$$

Lax-Milgram lemma [54] implies that problem (3.5) admits a unique solution $u(\mu) \in V$.

Besides, we assume that problem is *parameter separable* or *affinely decomposed*, i.e., there are continuous mappings $\theta_{a,q}, \theta_{f,q} : \mathcal{D} \to \mathbb{R}$ and continuous forms $a_q : V \times V \to \mathbb{R}$ $(1 \leq q \leq Q_a)$, $f_q : V \to \mathbb{R}$ $(1 \leq q \leq Q_f)$ such that

$$a(w, v; \mu) = \sum_{q=1}^{Q_a} \theta_{a,q}(\mu) a_q(w, v), \quad f(v; \mu) = \sum_{q=1}^{Q_f} \theta_{f,q}(\mu) f_q(v). \tag{3.9}$$

3.2.2 Finite Element Truth Approximation

We introduce a high dimensional finite element discretization (or *truth approximation*) of problem (3.5) in the space $V_{\mathcal{N}} = \text{span}\{\zeta_1, \ldots, \zeta_{\mathcal{N}}\} \subset V$ of piecewise linear and continuous finite element functions.

The finite element approximation of problem (3.5) is obtained by a standard Galerkin projection: given $\in D$, find $u_N(\ ) \in V_N$ such that

$$a(u_N(\ ); v_N; \ ) = f(v_N; \ ); \quad \forall v_N \in V_N: \tag{3.10}$$

Given the ansatz $u_N(\ ) = \sum_{j=1}^{N} \mathbf{u}_{N\ j}(\ )\ _j$ for the discrete solution and testing against the basis elements in V_N leads to the system

$$\mathbf{A}_N(\ )\mathbf{u}_N(\ ) = \mathbf{F}_N(\ ); \tag{3.11}$$

of linear algebraic equations, where $\mathbf{F}_N(\ ) := f f(\ _j; \ )g_{j=1}^N \in R^N$ and $\mathbf{A}_N(\ ) := fa(\ _j; \ _i; \ )g_{i;j=1}^N \in R^{N\ N}$. We assume that a single solution of (3.11) requires $O(N^2)$ operations, resulting from N steps of an iterative solver at cost $O(N)$ for each matrix-vector multiplication.

3.2.3 Reduced basis approximation with the Greedy method

To perform the reduced basis approximation, we first introduce a subset D_{train} D from which a sample $D_N = f^-_1 \in D; :::; ^-_N \in D g$ with associated reduced-basis space $V_N = \text{span} f\ _n := u_N(^-_n); \ 1 \quad n \quad N g$ of dimension N, which is built with the help of a weak greedy algorithm. This algorithm constructs iteratively nested spaces $V_n; \ 1 \quad n \quad N$ using an a-posteriori error estimator $4(Y; \ )$, which predicts the expected approximation error for a given parameter in the space $V_n = Y$. We want the expected approximation error to be less than the prescribed tolerance $"_{RB}$. We initiate the algorithm with an arbitrary chosen parameter $^-_1$ with the corresponding snapshot $u_N(^-_1)$ for the basis enrichment. Next we proceed as stated in the following Algorithm 1. We note that the basis functions $_n$ are also

Algorithm 1: RB-Greedy algorithm

1 **Input:** Tolerance $"_{RB}$, max. number of iterations $N_{\max}$, $V_1 = \text{span} f u_N(^-_1) g$, parameter set D_{train} D

2 **Output:** RB spaces $f V_n g_{n=1}^N$

1: **while** n $N_{\max}$ and $"_n := \max_{2D_{train}} 4(V_n; \ ) > "_{RB}$ **do**
2: ^-_n $\arg\max_{2D_{train}} 4(V_{n\ 1}; \ )$
3: D_n $D_{n\ 1} [f^-_n g$
4: V_n $V_{n\ 1}$ $\text{span} f\ _n$ $u_N(^-_n) g$
5: n $n + 1$
6: **end while**

orthonormalized relative to the $h \ ; \ i_V$ inner product with a Gram-Schmidt procedure to generate a well-conditioned system of equations.

Remark 13. *We note that the error sequence $f"_n g_{n=1}^N$ is only a training error in statistical learning terminology. The quality of the reduced basis model is then typically tested on D_{test} D to prevent overfitting, i.e. $\max_{2D_{test}} 4(V_N; \ ) >> "_{RB}$, where D_{test} is chosen such that $D_{test} \setminus D_{train} = \emptyset$.*

The reduced basis approximation of problem (3.10) is then obtained by a Galerkin projection: given $\in D$, find $u_N(\ ) \in V_h$ such that

$$a(u_N(\ ); v_N; \ ) = f(v_N; \ ); \quad \forall v_N \in V_N: \tag{3.12}$$

Given the ansatz $u_N(\ ) = \sum_{j=1}^{N} \mathbf{u}_{N\ j}(\ )\ _j$ for the discrete solution and testing against the basis elements in V_N leads to the system

$$\mathbf{A}_N(\ )\mathbf{u}_N(\ ) = \mathbf{F}_N(\ ); \tag{3.13}$$

of linear algebraic equations, where $\mathbf{F}_N(\ ) := \mathrm{f}f(\ _j;\ )\mathrm{g}_{j=1}^{N} \in \mathrm{R}^N$ and $\mathbf{A}_N(\ ) := \mathrm{f}a(\ _j;\ _i;\ )\mathrm{g}_{i;j=1}^{N} \in \mathrm{R}^{N\ N}$.

Remark 14. *We note that the RB sti ness matrix $\mathbf{A}_N(\ )$ is small, but dense, compared to $\mathbf{A}_{\mathrm{N}}(\ )$, which is typically large, but sparse. We assume that a single solution of* (3.13) *requires $\mathrm{O}(N^3)$ operations, resulting from N steps of an iterative solver, where we perform dense matrix-vector multiplications or direct inversions at cost $\mathrm{O}(N^2)$. We also note that the Gramm-Schmidt orthonormalization procedure guarantees that the condition number of $\mathbf{A}_N(\ )$ is upper bounded by $\frac{(\ )}{(\ )}$.*

It follows from the affine decomposition (3.9) of problem (3.5) that

$$\mathbf{A}_N(\ ) = \sum_{q=1}^{Q_a} {}_{a;q}(\ )\mathbf{A}_{N;q}; \quad \mathbf{F}_N(\ ) = \sum_{q=1}^{Q_f} {}_{f;q}(\ )\mathbf{F}_{N;q}(v); \tag{3.14}$$

where $\mathbf{F}_{N;q} := \mathrm{f}f_q(\ _j)\mathrm{g}_{j=1}^{N} \in \mathrm{R}^N$ $(1 \quad q \quad Q_f)$, and $\mathbf{A}_{N;q} := \mathrm{f}a_q(\ _j;\ _i)\mathrm{g}_{i;j=1}^{N} \in \mathrm{R}^{N\ N}$ $(1 \quad q \quad Q_a)$. It implies the so-called *o ine-online decomposition*: the computations in the offline phase depend on the dimension N of the finite element space and are expensive, but should be performed only once. The computations in the online phase are usually independent of N and thus are inexpensive. Precisely, we assemble the matrix $\mathbf{A}_N(\ )$ and the right-hand side $\mathbf{F}_N(\ )$ at cost $\mathrm{O}(Q_a N^2)$ and $\mathrm{O}(Q_f N)$ respectively, and then we invert $\mathbf{A}_N(\ )$ at cost $\mathrm{O}(N^3)$.

3.2.4 Error estimation

An important ingredient of the reduced basis methodology is the verification of the error (certification of the reduced basis method). It is based on an a-posteriori error bound, which allows quick evaluation and only requires the knowledge of reduced-basis solution. We denote by $r(\ ;\ ) \in V_{\mathrm{N}}^{0}$ the residual of the problem, defined naturally as:

$$r(v_{\mathrm{N}};\ ) = f(v_{\mathrm{N}};\ ) \quad a(u_N; v_{\mathrm{N}};\ ); \quad v_{\mathrm{N}} \in V_{\mathrm{N}}: \tag{3.15}$$

The residual-error relation $r(v_{\mathrm{N}};\ ) = a(u_{\mathrm{N}} \quad u_N; v_{\mathrm{N}};\ )$ yields together with the coercivity condition:

$$\mathrm{k}u_{\mathrm{N}}(\ ) \quad u_N(\ )\mathrm{k}_V \quad \frac{\mathrm{k}r(\ ;\ )\mathrm{k}_{V_{\mathrm{N}}^{0}}}{(\ )} =: 4(\ ): \tag{3.16}$$

If $(\ )$ is not avaiable analytically, the SCM (successive constraint method) approximation can be applied to obtain $_{LB}(\ )$ with $_{LB}(\ ) \quad (\ )$ [31]. We choose $4(\mathrm{M}; V_N) := \sup_{2\mathrm{D}} 4(\ )$ to measure the deviation $(\mathrm{M}; V_N)$ in (3.3), where $(\mathrm{M}; V_N) \quad 4(\mathrm{M}; V_N)$.

The computation of $\mathrm{k}r(\ ;\ )\mathrm{k}_{V_{\mathrm{N}}^{0}}$ requires the knowledge of its Riesz representer $v_r(\ ) \in V_{\mathrm{N}}$. Thanks to the Riesz representation theorem, it can be obtained from the equation

$$(v_r(\ ); v_{\mathrm{N}})_V = r(v_{\mathrm{N}};\ ) \quad 8v_{\mathrm{N}} \in V_{\mathrm{N}}: \tag{3.17}$$

The parameter separability structure of the residual

$$r(v_N;\ ) = \sum_{q=1}^{Q_r} {}_{r;q}(\ )r_q(v_N)$$

is transferred by the linearity of the Riesz isomorphism to the parameter separability of its Riesz representer $v_r(\ )$ together with the parameter dependent functions ${}_{r;q} : D \to R$. Therefore, for $1 \quad q \quad Q_r$ we have

$$v_r(\ ) = \sum_{q=1}^{Q_r} {}_{r;q}(\ )v_{r;q} \text{ with } (v_{r;q}; v_N)_V = r_q(v_N) \quad 8v_N \ 2 \ V_N: \tag{3.18}$$

Since the dual norm of the residual is equal to the norm of its Riesz representer, we have

$$kr(\ ;\ )k_{V_N'} = kv_r(\ )k_V = (\ {}^r(\ )^T \mathbf{G}_r \ {}^r(\ ))^{1=2}; \tag{3.19}$$

where ${}^r(\ ) = f\Phi_q^r(\ )g_{q=1}^{Q_r} \ 2 \ R^{Q_r}$ and $\mathbf{G}_r \ 2 \ R^{Q_r \ Q_r}$ with $(\mathbf{G}_r)_{q;q'} = (v_{r\ q}; v_{r\ q'})_V$ and the dual norm is then computed at cost $O(Q_r^2)$.

3.3 Reduced basis method for linear parabolic PDEs

In this section we consider a space-time variational formulation of linear parabolic partial differential equations, which we denote as the *exact problem*. The corresponding discrete Petrov-Galerkin approximation is called the *truth* problem, as it is common in the RB setting. We assume that the solution to the exact problem can be approximated arbitrarily well by the discrete solution of the truth problem. We then neglect the corresponding approximation error. This section and the proposed concept is based on the author's master thesis [36].

3.3.1 Space-Time formulation

Let $\Omega \quad R^d$ be the spatial domain and $\ 2 \ D \quad R^p$, where D is a compact parameter set. Let $V \quad H^1(\Omega)$ be a separable Hilbert space and $H := L^2(\Omega)$. We denote by $h\ ;\ i_V$, $h\ ;\ i_H$ and $k\ k_V$, $k\ k_H$ corresponding inner products and induced norms, respectively. To V and H we associate the Gelfand triple $V\ ,! \ H\ ,! \ V'$ with duality pairing $h\ ;\ i_{V'V}$. The norm of $l \ 2 \ V'$ is defined by $klk_{V'} := \sup_{2V;k\ k_V\ ,0} hl;\ i_{V'V}=k\ k_V$. For given $\ 2 \ D$ we consider a linear, bounded differential operator $A(\ ) : V \to V'$ with induced bilinear form

$$hA(\ )u; vi_{V'V} := a(u; v;\ ): \tag{3.20}$$

We assume that the forms (3.20) are coercive on V with coercivity constants $(\ ) > 0$, i.e.

$$a(v; v;\ ) \quad (\ )kvk_V^2 \quad 8v \ 2 \ V; \tag{3.21}$$

and continuous on V with continuity constants $(\ ) > 0$, i.e.

$$ja(w; v;\ )j \quad (\ )kwk_V kvk_V \quad 8\, w; v \ 2 \ V: \tag{3.22}$$

In addition, we assume that these conditions hold uniformly:

$$:= \inf_{2D} \quad (\ ) > 0; \qquad := \sup_{2D} \quad (\ ) < 1: \tag{3.23}$$

For given $(g(\ ; \ ); u_o)$ 2 $L^2(I; V^0)$ H we consider the linear parabolic initial value problem of finding $u(t) := u(t; \ )$ 2 $V; t$ 2 I a.e. on the time interval $I = (0; T]$, such that

$$\dot{u}(t) + A(\ )u(t) = g(t) \text{ in } V^0; \ u(0) = u_o \text{ in } H; \tag{3.24}$$

where $\dot{u} := \frac{@u}{@t}$ is understood in the generalized sense. We now define a space-time variational formulation of (3.24). We use the trial space

$$X := W(0; T) = L^2(I; V) \setminus H^1(I; V^0) = \{v \text{ 2 } L^2(I; V) : v; \dot{v} \text{ 2 } L^2(I; V^0)\}$$

with the norm $\|w\|_X^2 := \|w\|^2_{L^2(I;V^0)} + \|w\|^2_{L^2(I;V)}$, and the test space $Y := L^2(I; V)$ H with the norm $\|v\|_Y^2 := \|v^{(1)}\|^2_{L^2(I;V)} + \|v^{(2)}\|^2_H$ for $v := (v^{(1)}; v^{(2)})$. The weak formulation of problem (3.24) reads: find $u := u(\ )$ 2 X such that

$$B(u; v; \ ) = F(v; \ ); \quad 8 v \text{ 2 } Y; \tag{3.25}$$

where

$$B(u; v; \ ) := \int_I \langle \dot{u}; v^{(1)} \rangle_{V^0 V} + a(u; v^{(1)}; \ )dt + \langle u(0); v^{(2)} \rangle_H; \text{ and} \tag{3.26}$$

$$F(v; \ ) := \int_I \langle g(\ ); v^{(1)} \rangle_{V^0 V} dt + \langle u_o; v^{(2)} \rangle_H: \tag{3.27}$$

Since X , ! $C(I; H)$, the initial value $u(0)$ is well-defined in H (see Proposition 2.2.1). The well-posedness of problem (3.25) follows from (3.23), so that (3.25) admits a unique solution $u(\ )$ 2 X for all 2 D, see e.g. [54, Proposition 23.30].

3.3.2 Petrov-Galerkin Truth Approximation

From here onwards we omit the dependence on wherever appropriate. For the temporal discretization of (3.25) we use the time grid $0 = t^0 < t^1 < ::: < t^K = T$ and set $I^k = (t^{k-1}; t^k]$ for $k = 1; :::; K$. We set $4t^k = t^k - t^{k-1}$ and define $4t := \max_{1 \le k \le K} 4t^k$. For the spatial discretization we set $V_h = \text{span}\{ _1; :::; _{N_h}\}$ V as our finite-element space, where $\dim V_h = N_h$ and h denotes the spatial discretization parameter. With := $(4t; h)$ we introduce the discrete trial space

$$X \ := \{u \text{ 2 } C^0(I; V); \ u|_{I^k} \text{ 2 } P_1(I^k; V_h); \ k = 1; :::; K\} \quad X$$

and the discrete test space

$$Y \ := \{v \text{ 2 } L^2(I; V); \ v|_{I^k} \text{ 2 } P_0(I^k; V_h); \ k = 1; :::; K\} \quad V_h \quad Y:$$

With these choices of spaces the fully discrete truth approximation problem reads: find $u := u(\,) \in X$, such that $u^0 := u(0) = P_H^h u_o$ and

$$B(u; v; \,) = F(v; \,) \quad \forall v \in Y; \tag{3.28}$$

where $P_H^h : H \to V_h$ denotes the H-orthogonal projection onto V_h. It follows as for (3.25) that problem (3.28) admits a unique solution $u \in X$.

The Petrov-Galerkin space-time discrete formulation (3.28) can be interpreted as the Crank-Nicolson time-stepping scheme. Indeed, since the test space Y consists of piecewise constant polynomials in time, the problem can be solved via the following procedure for $k = 1; :::; K$:

$$\int_{I^k} \langle \dot{u}; v_h \rangle_{V^0 V} + a(u; v_h; \,) dt = \int_{I^k} \langle g(\,); v_h \rangle_{V^0 V} dt \quad \forall v_h \in V_h. \tag{3.29}$$

Since the trial space X consists of piecewise linear and continuous polynomials in time with the values $u^k := u(t^k)$ and $u^{k-1} := u(t^{k-1})$, we can represent u on I^k as the linear function

$$u(t) = \frac{1}{\Delta t^k}\{(t^k - t)u^{k-1} + (t - t^{k-1})u^k\}; \; t \in I^k. \tag{3.30}$$

We use the representation (3.30) in (3.29), test (3.29) against the basis functions $\varphi_i \in V_h$ $(i = 1; :::; N_h)$ and use the trapezoidal quadrature rule for the approximation of the appearing integrals. We introduce the following notation

$$g^{k-1/2}(v; \,) := \frac{1}{2}\langle g(t^k; \,) + g(t^{k-1}; \,); v \rangle_{V^0 V}.$$

From now on, time index $k - 1/2$ means the average of the quantitiy at time k and $k - 1$. In this way we obtain the Crank-Nicolson time-stepping scheme, which for $k = 1; :::; K$ reads

$$(u^k - u^{k-1}; \varphi_i)_H + \Delta t^k a(u^{k-1/2}; \varphi_i; \,) = \Delta t^k g^{k-1/2}(\varphi_i; \,), \quad 1 \le i \le N_h. \tag{3.31}$$

Here we recall that the initial condition u^0 is obtained as an H-orthogonal projection of u_o onto V_h. Given the ansatz $u^k = \sum_{i=1}^{N_h} \mathbf{u}_i^k \varphi_i$ and defining $\mathbf{u}^k := \{\mathbf{u}_i^k\}_{i=1}^{N_h} \in \mathbb{R}^{N_h}$, the resulting linear algebraic equations are then given by

$$\frac{1}{\Delta t^k}\mathbf{M}_h(\mathbf{u}^k - \mathbf{u}^{k-1}) + \mathbf{A}_h(\,)\mathbf{u}^{k-1/2} = \mathbf{g}_h^{k-1/2}(\,) \tag{3.32}$$

where $\mathbf{M}_h := \{(\varphi_i; \varphi_j)_H\}_{i;j=1}^{N_h}$; $\mathbf{A}_h(\,) := \{a(\varphi_i; \varphi_j; \,)\}_{i;j=1}^{N_h} \in \mathbb{R}^{N_h \times N_h}$ and the right-hand side $\mathbf{g}_h^{k-1/2}(\,) := \{g^{k-1/2}(\varphi_i; \,)\}_{i=1}^{N_h} \in \mathbb{R}^{N_h}$. The initial condition for the time-stepping scheme (3.32) is given by $\mathbf{u}^0 := \{(u_o; \varphi_i)_H\}_{i=1}^{N_h} \in \mathbb{R}^{N_h}$.

Remark 15. *The space-time variational problem* (3.25) *can be discretized using finite-dimensional discrete trial and test spaces* $X_{\Delta t} \subset X$ *and* $Y_{\Delta t} \subset Y$ *build up from finite-dimensional temporal subspaces of the form*

$$S_{\Delta t}^p := \{v_{\Delta t} \in L^2(I); \, v_{\Delta t}|_{I^k} \in \mathbb{P}_p(I^k); \; k = 1; :::; K\}$$

and spatial subspaces $V_h \subset V$. Then we have the space-time tensor product representation

$$X := S^p_{4t} \otimes V_h, \quad Y := (S^q_{4t} \setminus \{0\}) \otimes V_h.$$

Let $p = 1$ and $q = 0$, i.e., $S^1_{4t} := \mathrm{span}\{\varphi^1, \ldots, \varphi^K\} \subset H^1(I)$ and $S^0_{4t} := \mathrm{span}\{\psi^1, \ldots, \psi^K\} \subset L^2(I)$ are piecewise linear and piecewise constant finite element spaces in time. Discretizing the bilinear form $B(\cdot;\cdot)$ using the bases for the corresponding tensor product spaces leads to the following matrix with Kronecker product structure

$$\mathbf{B}(\mu) := \begin{pmatrix} \mathbf{N}_{Mt} \otimes \mathbf{M}_h + \mathbf{M}_{Mt} \otimes \mathbf{A}_h(\mu) \\ \mathbf{M}_h \end{pmatrix},$$

where $\mathbf{M}_{Mt} = (\varphi^k, \varphi^l)_{L^2(I)})_{k,l=1}^K$, $\mathbf{N}_{Mt} = (\varphi^k{}', \varphi^l)_{L^2(I)})_{k,l=1}^K$ are temporal finite-element matrices. This choice of bases and additional approximation of the right-hand side by the trapezoidal quadrature rule leads to the Crank-Nicolson interpretation [49]. However, in the space-time discretization setting we can obtain the discrete solution by solving a single linear system without appealing to time-marching schemes (see, e.g. [3]). We refer the reader to [49, 17] for details on the space-time reduced-basis method for linear parabolic problems.

3.3.3 Proper Orthogonal Decomposition (POD)

The aim of the POD method is to describe the solution trajectiory space $\mathcal{V} = \mathrm{span}\{u(t); t \in [0,T]\}$ by means of few orthonormal functions $\{\psi_i\}_{i=1}^{\ell} \subset V$, with $\ell \leq d := \dim \mathcal{V}$, such that the error of the trajectory projection onto the POD subspace $V_\ell = \mathrm{span}\{\psi_1, \ldots, \psi_\ell\} \subset V$ is minimized in the following sense:

$$\begin{aligned} &\min_{\psi_1,\ldots,\psi_\ell \in V} \int_0^T \left\| u(t) - \sum_{i=1}^{\ell} \langle u(t), \psi_i \rangle_V \psi_i \right\|_V^2 dt \\ &\text{s.t. } \langle \psi_i, \psi_j \rangle_V = \delta_{ij}, \text{ for } 1 \leq i, j \leq \ell, \end{aligned} \tag{3.33}$$

where δ_{ij} denotes the Kronecker symbol. The problem (3.33) is known as the continuous version of the POD method [51]. In practice, we do not have the PDE solution $u : [0,T] \to V$, but rather a discrete set of snapshots, stored in the snapshot matrix

$$\mathbf{U} := \begin{pmatrix} | & | & & | \\ \mathbf{u}^0 & \mathbf{u}^1 & \cdots & \mathbf{u}^K \\ | & | & & | \end{pmatrix} \in \mathbb{R}^{N_h \times (K+1)}, \tag{3.34}$$

which is obtained, e.g., by the Crank-Nicolson scheme. The integral in (3.33) is approximated by the quadrature rule, where the quadrature points are chosen according to the specified time grid $\{t^k\}_{k=0}^K$ in our PDE discretization. Given the ansats $\psi_i = \sum_{j=1}^{N_h} \psi_i^j \varphi_j$ and the isomorphic correspondence $\psi_i \cong \Psi_i := (\psi_i^j)_{j=1}^{N_h} \in \mathbb{R}^{N_h}$, the fully discrete counterpart of problem (3.33) reads:

$$\begin{aligned} &\min_{\Psi_1,\ldots,\Psi_\ell \in \mathbb{R}^{N_h}} \sum_{k=0}^{K} \rho_k \left\| \mathbf{u}^k - \sum_{i=1}^{\ell} \langle \mathbf{u}^k, \Psi_i \rangle_{\mathbf{W}} \Psi_i \right\|_{\mathbf{W}}^2 \\ &\text{s.t. } \langle \Psi_i, \Psi_j \rangle_{\mathbf{W}} = \delta_{ij}, \text{ for } 1 \leq i, j \leq \ell, \end{aligned} \tag{3.35}$$

where $\mathbf{W} = \{\langle \varphi_i, \varphi_j \rangle_V\}_{i,j=1}^{N_h} \in \mathbb{R}^{N_h \times N_h}$ is a symmetric positive definite inner product matrix with $\langle \mathbf{u}, \mathbf{v} \rangle_{\mathbf{W}} = \mathbf{u}^T \mathbf{W} \mathbf{v}$ and $\{\alpha_k\}_{k=0}^{K}$ are non-negative quadrature weights for $\int_0^T dt$. For the chosen trapezoidal quadrature rule we have

$$\alpha_0 = \frac{\Delta t^1}{2}, \quad \alpha_k = \frac{\Delta t^k + \Delta t^{k+1}}{2} \text{ for } k = 1, \ldots, K-1 \text{ and } \alpha_K = \frac{\Delta t^K}{2}. \tag{3.36}$$

The problem (3.35) admits a unique solution $\{\Psi_1, \ldots, \Psi_\ell\}$, which corresponds to the first ℓ eigenvectors, corresponding to ℓ largest eigenvalues of the self-adjoint, non-negative, linear and bounded operator $R : \mathbb{R}^{N_h} \to \mathbb{R}^{N_h}$, i.e., $R\Psi_i = \lambda_i \Psi_i$, where R is defined as follows

$$R\Psi = \sum_{k=0}^{K} \alpha_k \langle \mathbf{u}^k, \Psi \rangle_{\mathbf{W}} \mathbf{u}^k, \quad \Psi \in \mathbb{R}^{N_h}. \tag{3.37}$$

The POD projection error then satisfies

$$\sum_{k=0}^{K} \alpha_k \left\| \mathbf{u}^k - \sum_{i=1}^{\ell} \langle \mathbf{u}^k, \Psi_i \rangle_{\mathbf{W}} \Psi_i \right\|_{\mathbf{W}}^2 = \sum_{i=\ell+1}^{K+1} \lambda_i. \tag{3.38}$$

Hence, the fast decay of eigenvalues $\{\lambda_i\}_{i=1}^{K+1}$ is important for an application of the POD method.

The eigenvalue problem (3.37) can be transformed to a generalized eigenvalue problem in a matrix form. Let $\mathbf{D} \in \mathbb{R}^{(K+1)\times(K+1)}$ be a diagonal matrix with quadrature weights (3.36) on the diagonal. Set $\tilde{\Psi}_i = W^{1/2} \Psi_i$, hence $\langle \Psi_i, \Psi_j \rangle_{\mathbb{R}^{N_h}} = \langle \varphi_i, \varphi_j \rangle_V = \delta_{ij}$ and consider

$$\mathbf{W}^{1/2} \mathbf{U} \mathbf{D} \mathbf{U}^T \mathbf{W}^{1/2} \tilde{\Psi}_i = \lambda_i \tilde{\Psi}_i, \ 1 \le i \le K+1; \tag{3.39}$$

$$\text{s.t. } \langle \tilde{\Psi}_i, \tilde{\Psi}_j \rangle_{\mathbb{R}^{N_h}} = \delta_{ij} \tag{3.40}$$

Set $\tilde{\mathbf{U}} = \mathbf{W}^{1/2} \mathbf{U} \mathbf{D}^{1/2}$ and consider the symmetric eigenvalue problem

$$\tilde{\mathbf{U}}^T \tilde{\mathbf{U}} \tilde{\Psi}_i = \lambda_i \tilde{\Psi}_i, \ 1 \le i \le K+1 \tag{3.41}$$

After finding the eigenvalues and eigenvectors of problem (3.41), we set

$$\Psi_i = \frac{1}{\sqrt{\lambda_i}} \mathbf{W}^{-1/2} \mathbf{U} \mathbf{D}^{1/2} \tilde{\Psi}_i \tag{3.42}$$

to obtain the POD modes of interest. We note that (3.42) represents a linear combinations of columns of (3.34), i.e., a linear combination of our time snapshots.

For notation purposes, we use $\text{POD}_\ell(\{u^k\}_{k=0}^K)$ to denote the extraction of ℓ dominant modes. For example, we have $\text{POD}_1(\{u^k\}_{k=0}^K) = \{\Psi_1\} = \sum_{j=1}^{N_h} \frac{1}{j} \varphi_j$, where $\Psi_1 := \{\Psi_j^1\}_{j=1}^{N_h}$ is computed as in (3.42). We refer the reader to [51] for more details on the POD method.

3.3.4 Reduced basis approximation with the POD-Greedy method

The idea of the reduced-basis approximation consists in replacing the “truth" (high-dimensional) space V_h in the definition of X and Y by a low-dimensional subspace $V_N \subset V_h$. With V_N available we

introduce the corresponding reduced trial space

$$X_{4t;N} := \{u_N \in C^0(I;V);\ u_N|_{I^k} \in P_1(I^k;V_N);\ k = 1;:::;K\}$$

and the reduced test space

$$Y_{4t;N} := \{v_N \in L^2(I;V);\ v_N|_{I^k} \in P_0(I^k;V_N);\ k = 1;:::;K\} \quad V_N:$$

We construct $V_N := \text{span}\{\ _1;:::;\ _N\} \quad V_h$ by the POD-Greedy procedure in Algorithm 2, compare e.g. [22]. In our setting, the POD-Greedy alogorithm constructs iteratively nested spaces $V_n;\ 1 \quad n \quad N$ using an a-posteriori error estimator $\Delta(Y;\ )$ (see the next section for details on a-posteriori error analysis), which predicts the expected approximation error for a given parameter $\ \in D_{train}$ in the space $Y := Y_{4t;n}$. We want the expected approximation error to be less than the prescribed tolerance $\varepsilon_{RB} > 0$. We initiate the algorithm with the choice of the initial basis vector $\ _1 := u^0/\|u^0\|_V$; this choice is motivated by the assumption in Proposition 3.3.1. The snapshots $u(\ )$ for the procedure are provided by the parametrized "truth" approximation (3.28). Next we proceed as stated in the Algorithm 2. In Algorithm 2, $P_V : V_h \ !$

Algorithm 2: : POD-Greedy algorithm

Input: Tolerance ε_{RB}, max. number of iterations $N_{\max}$, $V_1 = \text{span}\{\ _1\}$, parameter set D_{train}.
Output: RB spatial spaces $\{V_n\}_{n=1}^N$, RB trial spaces $\{X_{4t;n}\}_{n=1}^N$, RB test spaces $\{Y_{4t;n}\}_{n=1}^N$.

1: **while** $2 \quad n \quad N_{\max}$ and $\varepsilon_n := \max_{\in D_{train}} \Delta(Y_{4t;n};\ ) > \varepsilon_{RB}$ **do**
2: $[\varepsilon_n;\ _n] \quad \arg\max_{\in D_{train}} \Delta(Y_{4t;n\ 1};\ )$
3: $e_n^k := u^k(\ _n) \quad P_V u^k(\ _n);\ k = 1;:::;K$
4: $\ _n := \text{POD}_1(\{e_n^k\}_{k=1}^K)$
5: $V_n := V_{n\ 1} \quad \text{span}\{\ _n\}$
6: $X_{4t;n} \quad X_{4t;n\ 1};\quad Y_{4t;n} \quad Y_{4t;n\ 1}$
7: $n \quad n+1$
8: **end while**

V_n denotes the V-orthogonal projection, and the operation $\text{POD}_1(\{e_n^k\}_{k=1}^K)$ denotes the extraction of the dominant mode of the Proper Orthogonal Decomposition (see section 3.3.3). We also note that more modes can be extracted in every step of the algorithm: it reduces the offline computational time, but there is no guarantee that the produced basis will be of the smallest possible dimension.

The reduced-basis approximation of problem (3.28) reads: find $u_N := u_N(\ ) \in X_{4t;N}$, such that $u_N^0 := u_N(0) = P_H^N u_o$ and

$$B(u_N;v_N;\ ) = \tilde{F}(v_N;\ ) \quad \forall v_N \in Y_{4t;N}; \tag{3.43}$$

where

$$B(u_N;v_N;\ ) = \int_I (\dot{u}_N;v_N^{(1)})_{V'V} + a(u_N;v_N^{(1)};\ )dt + (P_H^N u_o;v_N^{(2)})_H;$$
$$\tilde{F}(v_N;\ ) := \int_I (g(\ );v_N^{(1)})_{V'V}dt + (u^0;v_N^{(2)})_H;$$

and $P_H^N : V_h \ ! \ V_N$ denotes the H-orthogonal projection onto V_N. It follows as for (3.25) that the problem

(3.43) admits a unique solution $u_N(\ ) \in X_{4t;N}$ for all $\in D$.

The problem (3.43) can be interpreted as the reduced-basis approximation of the Crank-Nicolson time-marching scheme, i.e.

$$\hbar u_N^k \quad u_N^{k\ 1}; v_N^{(1)}\mathrm{i}_H + \mathrm{M}\ t^k a(u_N^{k\ 1=2}; v_N^{(1)};\ ) = \mathrm{M}\ t^k g^{k\ 1=2}(v_N^{(1)};\ ); \tag{3.44}$$

where the initial condition u_N^0 is obtained as an H-projection of u^0 onto V_N. Given the ansatz $u_N^k = \mathrm{P}_{i=1}^N u_{i;N}^k\ _i$ and defining $\mathbf{u}_N^k := \mathrm{f}u_{i;N}^k\mathrm{g}_{i=1}^N \in \mathrm{R}^N$, the resulting linear algebraic equations are then given by

$$\frac{1}{\mathrm{M}\ t^k}\mathbf{M}_N(\mathbf{u}_N^k \quad \mathbf{u}_N^{k\ 1}) + \mathbf{A}_N(\ )\mathbf{u}_N^{k\ 1=2} = \mathbf{g}_N^{k\ 1=2}(\ ); \tag{3.45}$$

where $\mathbf{M}_N := \mathrm{fh}\ _i;\ _j\mathrm{i}_H\mathrm{g}_{i;j=1}^N; \mathbf{A}_N(\ ) := \mathrm{fa}(\ _i;\ _j;\ )\mathrm{g}_{i;j=1}^N \in \mathrm{R}^{N\ N}$ and $\mathbf{g}_N^{k\ 1=2}(\ ) := \mathrm{fg}^{k\ 1=2}(\ _i;\ )\mathrm{g}_{i=1}^N \in \mathrm{R}^N$. The initial condition is given by $\mathbf{u}_N^0 := \mathrm{fh}u^0;\ _i\mathrm{i}_H\mathrm{g}_{i=1}^N \in \mathrm{R}^N$.

We assume the affine decomposition of problem (3.44):

$$a(w; v;\ ) = \sum_{q=1}^{Q_a} {}_{a;q}(\ )a_q(w; v); \quad g^{k\ 1=2}(v;\ ) = \sum_{q=1}^{Q_g} {}_{g;q}^{k\ 1=2}(\ )g_q(v): \tag{3.46}$$

It transfers to the parameter separability of the stiffness matrix and the load vector

$$\mathbf{A}_N(\ ) = \sum_{q=1}^{Q_a} {}_{a;q}(\ )\mathbf{A}_{N;q}; \quad \mathbf{g}_N^{k\ 1=2}(\ ) = \sum_{q=1}^{Q_g} {}_{g;q}^{k\ 1=2}(\ )\mathbf{g}_{N;q}(v); \tag{3.47}$$

where $\mathbf{g}_{N;q} := \mathrm{fg}_q(\ _j)\mathrm{g}_{j=1}^N \in \mathrm{R}^N$, $1 \quad q \quad Q_g$, and $\mathbf{A}_{N;q} := \mathrm{fa}_q(\ _j;\ _i)\mathrm{g}_{i;j=1}^N \in \mathrm{R}^{N\ N}$, $1 \quad q \quad Q_a$. The proposed reduced numerical scheme contains parameter separable quantities and thus allows offline-online decomposition. The offline phase depends on expensive high-dimensional finite element simulations and thus on N, but should be performed only once. However, the assembling of all the high-dimensional parameter-dependent quantities is computationally simplified due to the affine dependence on the parameters (3.46). In the online phase the computational complexity scales polynomially in N, independently of N and thus is inexpensive. We assemble the matrix $\mathbf{A}_N(\ )$ at cost $\mathrm{O}(Q_a N^2)$ and the right-hand side $\mathbf{g}_N^{k\ 1=2}(\ )$ at cost $\mathrm{O}(Q_g K N)$. The operation count for the reduced Crank-Nicolson scheme (3.45) depends on the number of time steps K and the corresponding inversions of dense reduced-basis matrices at cost $\mathrm{O}(N^3)$, thus it scales as $\mathrm{O}(KN^3)$.

3.3.5 Error estimation

An important ingredient of the reduced basis methodology is the verification of the error (certification of the reduced basis method). In the present work we provide an a-posteriori error bound, based on the residual, which allows quick evaluation. We denote by $R(\ ;\ ) \in \mathrm{Y}^0$ the residual of the problem, defined naturally as:

$$R(v\ ;\ ) := \tilde{F}(v\ ;\ ) \quad B(u_N; v\ ;\ ) = \int_I \hbar r(t;\ );v\ \mathrm{i}_{V^0 V} dt \quad \forall v \in \mathrm{Y}: \tag{3.48}$$

We have the following

Proposition 3.3.1 (A-posteriori Error Bound)**.** *Let* $(\ ) > 0$ *be a coercivity constant from* (3.21) *and*

assume that $u^0 \in V_N$. *Then the error* $e(\mu) = u(\mu) - u_N(\mu)$ *of the reduced basis approximation is bounded by*

$$\|e(\mu)\|_Y \leq \frac{1}{\alpha(\mu)} \|R(\cdot;\mu)\|_{Y'} =: \Delta_N(\mu). \tag{3.49}$$

Proof. Since in the case $e = 0$ there is nothing to show, we assume that $e \neq 0$. We have $u^0 \in V_N$ and $P^N_{H\,V_N} = Id$, therefore $u^0_N := P^N_H u^0 = u^0$. It implies that $\|e(0)\|_H = 0$, $\|e\|_Y = \|e\|_{L^2(I;V)}$ and $\|R(\cdot;\mu)\|_{Y'} = \|R(\cdot;\mu)\|_{L^2(I;V_h')}$. We then use the identity

$$\int_I \langle \dot{e}, e \rangle_{V'V} dt = \frac{1}{2}\|e(T)\|_H^2 - \frac{1}{2}\|e(0)\|_H^2 \tag{3.50}$$

together with the coercivity condition (3.21) to derive the bound:

$$\alpha(\mu)\|e\|_Y^2 \leq \int_I a(e,e;\mu)dt + \frac{1}{2}\|e(T)\|_H^2 = \int_I \langle \dot{e}, e \rangle_{V'V} dt + \int_I a(e,e;\mu)dt + \frac{1}{2}\|e(0)\|_H^2 \leq \|R(\cdot;\mu)\|_{Y'}\|e\|_Y.$$

Dividing both sides by $\|e\|_Y$ yields the result.

Remark 16. *We note that the assumption* $u^0 \in V_N$ *implies that* $\|e(0)\|_H = 0$. *We can guarantee this by choosing* $\zeta_1 := u^0/\|u^0\|_V$ *as the initial basis for* V_N *in the POD-Greedy procedure.*

The error bound in can be improved by a factor $\sqrt{\alpha(\mu)}$ with the choice of a different norm on $L^2(I;V)$. We assume that $a(\cdot;\cdot;\mu)$ is symmetric and define

$$\langle v, w \rangle := a(v,w;\mu). \tag{3.51}$$

The form is positive definite by coercivity of $a(\cdot;\cdot;\mu)$, hence defines an inner product on V and induces parameter-dependent *energy norm*

$$\|v\| := \langle v, w \rangle^{1/2}. \tag{3.52}$$

By continuity and coercivity of $a(\cdot;\cdot;\mu)$ one can easily see that the energy norm is equivalent to the norm $\|\cdot\|_V$ on V, i.e, we have

$$\sqrt{\alpha(\mu)}\|v\|_V \leq \|v\| \leq \sqrt{\gamma(\mu)}\|v\|_V, \quad v \in V. \tag{3.53}$$

We proceed by defining the space-time energy norm on $L^2(I;V)$ as follows

$$\|u\|_{L^2(I;V)} := \left(\int_I \|u(t)\|^2 dt \right)^{1/2}. \tag{3.54}$$

Similarly, one can show that the space-time energy norm is equivalent to the norm $\|\cdot\|_{L^2(I;V)}$ on $L^2(I;V)$, i.e, we have

$$\sqrt{\alpha(\mu)}\|v\|_{L^2(I;V)} \leq \|v\|_{L^2(I;V)} \leq \sqrt{\gamma(\mu)}\|v\|_{L^2(I;V)}, \quad v \in L^2(I;V). \tag{3.55}$$

Proposition 3.3.2 (A-posteriori $L^2(I;V)$ Error Bound)**.** *Let* $\alpha(\mu) > 0$ *be a coercivity constant from* (3.21) *and assume that* $u^0 \in V_N$. *Then the error* $e(\mu) = u(\mu) - u_N(\mu)$ *of the reduced basis approximation*

is bounded by

$$\|e(\cdot)\|_{L^2(I;V)} \leq \sqrt{\frac{1}{\alpha(\mu)}}\|R(\cdot;\cdot)\|_{Y'} =: \Delta_N^{en}(\mu). \tag{3.56}$$

Proof. Since in the case $e = 0$ there is nothing to show, we assume that $e \neq 0$. Then we proceed similarly to the proof to show that $\|e(0)\|_H = 0$, hence $\|e\|_{L^2(I;V)_H} = \|e\|_{L^2(I;V)}$. Then we use the identity and the coercivity condition (3.21) to derive the bound:

$$\|e\|^2_{L^2(I;V)} \leq \int_I a(e,e;\mu)dt + \frac{1}{2}\|e(T)\|^2_H = \int_I \langle \dot{e}, e\rangle_{V',V} dt + \int_I a(e,e;\mu)dt + \frac{1}{2}\|e(0)\|^2_H$$
$$\leq \|R(\cdot;\mu)\|_{Y'}\|e\|_Y \leq \sqrt{\frac{1}{\alpha(\mu)}}\|R(\cdot;\mu)\|_{Y'}\|e\|_{L^2(I;V)}.$$

Dividing both sides by $\|e\|_{L^2(I;V)}$ yields the result.

The computation of $\|R(\cdot;\mu)\|_{Y'}$ requires the knowledge of its Riesz representer $v_{;R}(\mu) \in Y$. Thanks to the Riesz representation theorem, it can be obtained from the equation

$$(v_{;R}(\mu), v)_Y = R(v;\mu) \quad \forall v \in Y. \tag{3.57}$$

Since the test space Y consists of piecewise constant polynomials in time, the problem (3.57) can be solved via the time-marching procedure for $k = 1, \ldots, K$ as follows:

$$\int_{I^k} \langle v_{;R}(t;\mu), v_h\rangle_V dt = \int_{I^k} \langle r(t;\mu), v_h\rangle_{V',V} dt \quad \forall v_h \in V_h. \tag{3.58}$$

We note that $v_R^k(\mu) := v_{;R}(\mu)_{|I^k}$ is constant in time, hence the integration on the left-hand side of (3.58) is exact. For the right-hand side of (3.58) we represent $u_N(\mu) \in X_{\Delta t;N}$ as the linear function (3.30) on I^k and use it as an input for the residual (3.48). We then apply the trapezoidal quadrature rule for the approximate evaluation of the integral. The quadrature rule is chosen such that the quadrature error is of the size of the error of the truth Crank-Nicolson solution. We thus need to solve the following problems:

$$\langle v_R^k(\mu), v_h\rangle_V = R^k(v_h;\mu) \quad \forall v_h \in V_h \ (k = 1, \ldots, K); \tag{3.59}$$

where the right-hand side is given by

$$R^k(v_h;\mu) = \frac{1}{2}[\langle g(t^k;\mu) + g(t^{k-1};\mu), v_h\rangle_{V',V} - \tilde{a}[u_N^k](u_N^k, v_h;\mu) \tag{3.60}$$
$$- \tilde{a}[u_N^{k-1}](u_N^{k-1}, v_h;\mu)] - \frac{1}{\Delta t^k}\langle u_N^k - u_N^{k-1}, v_h\rangle_H.$$

Therefore the computation of the Riesz representer leads to a sequence of K uncoupled spatial problems in V_h. The parameter separability structure of the residual

$$R^k(v_h;\mu) = \sum_{q=1}^{Q_R} \Theta_{R;q}^k(\mu) R_q(v_h)$$

is transferred by the linearity of the Riesz isomorphism to the parameter separability of its Riesz representer $v_R^k(\mu)$ together with the parameter dependent functions $\Theta_{R;q}^k : D \to \mathbb{R}$. Therefore, for $1 \leq q \leq Q_R$

we have

$$v_R^k(\ ) = \sum_{q=1}^{Q_R} {}^k_{R;q}(\ )v_{R;q} \text{ with } (v_{R;q}; v_h)_V = R_q(v_h) \quad \forall v_h \in V_h: \tag{3.61}$$

Finally, we state the formulas for the residual norm as well as the spatio-temporal norm of u_N. Since $v_{;R}(\ )_{I^k}$ is constant in time, the integration on I^k is exact and we can compute the spatio-temporal norm of $v_{;R}(\ )$ as follows:

$$\|v_{;R}(\ )\|_Y^2 = \sum_{k=1}^{K} 4t^k \|v_R^k(\ )\|_V^2 = \sum_{k=1}^{K} 4t^k \Theta_R^k(\ )^T \mathbf{G}_R \Theta_R^k(\ );$$

where $\mathbf{G}_R := \{(v_{R;q}, v_{R;q'})_V\}_{q,q'=1}^{Q_R} \in \mathbb{R}^{Q_R \times Q_R}$ and $\Theta_R^k(\ ) := \{{}^k_{R;q}(\ )\}_{q=1}^{Q_R} \in \mathbb{R}^{Q_R}$. The isometry of the Riesz isomorphism implies that $\|R(\ ;\ )\|_{Y'} = \|v_{;R}(\ )\|_Y$. Since $u_N(\ )|_{I^k}$ is a linear function in time, the trapezoidal quadrature rule on I^k is exact. We then can compute the spatio-temporal norm $\|u_N\|_Y$ of $u_N \in X_{4t;N}$ according to

$$\begin{aligned}\|u_N\|_Y^2 &= \sum_{k=1}^{K} \frac{\Delta t^k}{2}(\|u_N^k\|_V^2 + \|u_N^{k-1}\|_V^2) + \|u_N^0\|_H^2 \\ &= \sum_{k=1}^{K} \frac{\Delta t^k}{2}[\mathbf{u}_N^{k\,T}\mathbf{K}_N\mathbf{u}_N^k + \mathbf{u}_N^{k-1\,T}\mathbf{K}_N\mathbf{u}_N^{k-1}] + \mathbf{u}_N^{0\,T}\mathbf{M}_N\mathbf{u}_N^0;\end{aligned}$$

where $\mathbf{K}_N := \{(\zeta_i, \zeta_j)_V\}_{i,j=1}^N \in \mathbb{R}^{N \times N}$. Since in our case the reduced basis is orthonormal in V, $\mathbf{K}_N$ is the identity matrix. The operation count in the online phase, associated with computation of the residual norm and the spatio-temporal norm on Y is correspondingly $O(Q_R^2 K)$ and $O(NK + N^2)$.

Chapter 4

Reduced basis method for quasilinear elliptic PDEs and applications to magnetostatics equation

In this chapter, we propose a certified reduced basis (RB) method for quasilinear elliptic problems together with its application to nonlinear magnetostatics equations, where the later model permanent magnet synchronous motors (PMSM). The parametrization enters through the geometry of the domain and thus, combined with the nonlinearity, drives our reduction problem. We provide a residual-based a-posteriori error bound which, together with the Greedy approach, allows to construct reduced-basis spaces of small dimensions. We use the empirical interpolation method (EIM) to guarantee the efficient offline-online computational procedure. The reduced-basis solution is then obtained with the surrogate of the Newton's method. The numerical results indicate that the proposed reduced-basis method provides a significant computational gain, compared to a finite element method.

4.1 The quasilinear parametric elliptic PDE

In this section we introduce our parametrised nonlinear magnetostatics equation of quasilinear elliptic type and its corresponding variational formulation together with our finite-element discretization.

4.1.1 Abstract formulation

We start by introducing the model for a permanent magnet synchronous machine. We consider a three-phase 6-pole permanent magnet synchronous machine (PMSM) with one buried permanent magnet per pole. We parametrize the problem through the size of the magnet by introducing a three dimensional parameter $p = (p_1; p_2; p_3)$ which characterizes magnet's width p_1, magnet's height p_2 and the perpendicular distance from the magnet to the rotor p_3 in mm. In Fig. 4.1 the geometry of the problem is shown. PMSM then can be described with sufficient accuracy by the magnetostatic approximation of Maxwell's equations

$$\mathrm{r} \quad (\ (x; \mathrm{j}\, \mathrm{r}\, u(p)\mathrm{j})\, \mathrm{r}\, u(p)) = J_e \quad \frac{@}{@x_2} H_{pm;1}(p) + \frac{@}{@x_1} H_{pm;2}(p) \text{ in } \Omega(p) \tag{4.1}$$

with boundary conditions

$$u|_{BC} = u|_{DA} = 0 \quad \text{and} \quad u|_{AB} = u|_{CD}:$$

Here $AB; BC; CD; DA$ represent parts of the boundary $\partial\Omega$ and marked in Fig. 4.1. We assume that $\Omega(\ )$ represents the cross-section of the electric motor which is located in the x_1 x_2 plane of $\mathbb{R}^3$ and the solution u is the x_3-component of the magnetic vector potential. The x_3-component of the current density is represented by J_e, and $H_{pm;1}(p)$ and $H_{pm;2}(p)$ are components of the permanent magnet magnetic field. The nonlinear magnetic reluctivity function

$$(x; s) = \begin{cases} {}_1(s); \text{ for } x \in \Omega^1(p) \\ {}_2(x); \text{ for } x \in \Omega^2(p); \end{cases} \tag{4.2}$$

represents ferromagnetic properties of the material. Here we split the domain $\Omega(p)$ into two non-overlapping subdomains $\Omega^1(p)$ (ferromagnetic steel) and $\Omega^2(p)$ (air, magnet, coils) such that ${}_1 \in C^1(\Omega^1(p))$ and ${}_2$ is piecewise constant on $\Omega^2(p)$ (i.e. constant for each material). In practice, we reconstruct ${}_1$ from the real B H measurements of PMSM by using cubic spline interpolation, see section 2.1.2. We use physical constants for ${}_2$. Then the reluctivity function satisfies

$$0 < {}_{\text{LB}} \quad (x; s) \quad {}_0; \quad \forall x \in \Omega(p); \ s \in \mathbb{R}_0^+; \tag{4.3}$$

where ${}_{\text{LB}}$ and ${}_0$ can be chosen independently of the parameter p (see section 4.3 for details).

We continue with an abstract formulation of a two-dimensional nonlinear magnetostatic field problem with geometric parametrisation, where the parameter set is given by $\mathcal{D} \subset \mathbb{R}^3$ and describes the geometry of the permanent magnet. The regular, bounded and p-dependent domain $\Omega(p) \subset \mathbb{R}^2$ gives rise to a p-dependent real and separable Hilbert space $V(p) := V(\Omega(p))$ and the corresponding dual space $V^0(p) := V^0(\Omega(p))$. The function space $V(p)$ is such that

$$V(p) := \{v \mid v \in L^2(p); \ \nabla v \in (L^2(p))^2; \ u|_{BC} = u|_{DA} = 0; \ u|_{AB} = u|_{CD}\}$$

with $H_0^1(p) \subset V(p) \subset H^1(p)$, where $H^1(p) := \{v \mid v \in L^2(p); \nabla v \in (L^2(p))^2\}$, $H_0^1(p) := \{v \mid v \in H^1(p); v|_{\partial\Omega} = 0\}$. The inner product on $V(p)$ is defined by $(w; v)_{V(p)} = \int_{\Omega(p)} \nabla w \cdot \nabla v \, dx$ and the induced norm is given by $\|v\|_{V(p)} = (v; v)_{V(p)}^{1/2}$, which is indeed a norm due to Poincare-Friedrichs inequality. Then the abstract problem reads as follows: given $p \in \mathcal{D}$, find $u(p) \in V(p)$ such that

$$a[u(p)](u(p); v; p) = f(v; p); \quad \forall v \in V(p); \tag{4.4}$$

where we have

$$a[u](w; v; p) = \int_{\Omega(p)} (x; |\nabla u|) \nabla w \cdot \nabla v \, dx; \tag{4.5}$$

$$f(v; p) = \int_{\Omega(p)} (J_e v - H_{pm;2} \frac{\partial v}{\partial x_1} + H_{pm;1} \frac{\partial v}{\partial x_2}) dx: \tag{4.6}$$

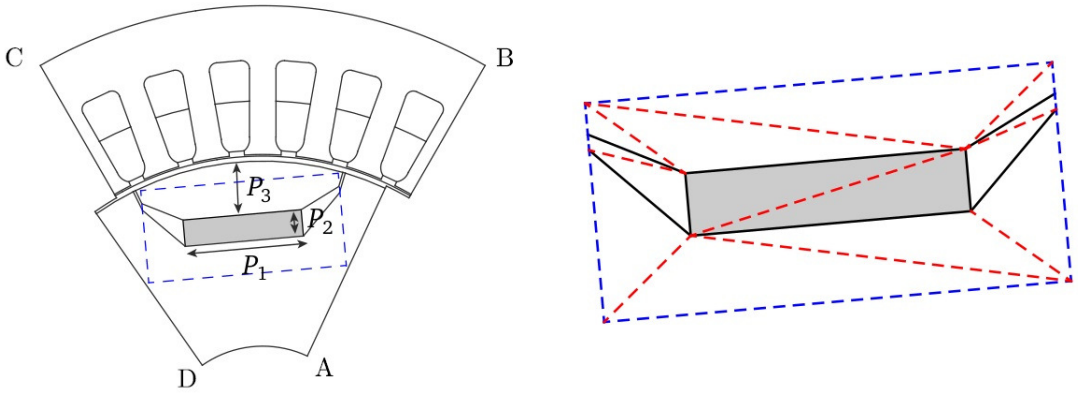

Figure 4.1: The cross-section of one pole of the machine with the magnet depicted in gray and the region of the geometric parametrisation indicated by the dashed box. The dashed lines indicate the triangulation into L triangles. Figure is adapted from [7].

The quasilinear form $a[\,](\,;\,;p)$ is strongly monotone on $V(p)$ with monotonicity constant $_{\mathrm{LB}} > 0$, i.e.

$$a[v](v; v \quad w; p) \quad a[w](w; v \quad w; p) \quad {}_{\mathrm{LB}}\|v \quad w\|^2_{V(p)} \quad 8\, v; w \; 2 \; V(p); \tag{4.7}$$

and Lipschitz continuous on $V(p)$ with Lipschitz constant $L_a := 2 \; {}_{LB} + \; {}_0 > 0$, i.e.

$$|a[u](u; v; p) \quad a[w](w; v; p)| \quad L_a\|u \quad w\|_{V(p)}\|v\|_{V(p)} \quad 8\, u; w; v \; 2 \; V(p): \tag{4.8}$$

The conditions (4.7), (4.8) are established in Lemma 8. Then problem (4.4) admits a unique solution, see section 2.2.3, Theorem 7. Moreover, those properties will be needed for the error estimates.

In order to avoid domain re-meshing caused by the change of the parameters, we transfer the domain $\Omega(p)$ to a fixed domain $\hat{\Omega} := \Omega(\hat{p})$, where $\hat{p}$ is the reference parameter with $\hat{x} := x(\hat{p})$ as a spatial coordinate on $\hat{\Omega}$ (see e.g. [45]). Further we assume that $\hat{\Omega} = \hat{\Omega}^1 \; [\; \hat{\Omega}^2$ and this can be decomposed into $L = L_1 + L_2$ (in our case $L = 12$) non-overlapping triangles (see Fig.4.1) so that $\hat{\Omega} = [_{d=1}^{L}\hat{\Omega}_d$ and in particular $\hat{\Omega}^1 = [_{d=1}^{L_1}\hat{\Omega}^1_d$ and $\hat{\Omega}^2 = [_{d=1}^{L_2}\hat{\Omega}^2_d$. The transformation $\mathsf{T}(p)$ on each triangle is affine, whereas piecewise-affine and continuous over the whole domain according to:

$$\begin{aligned} \mathsf{T}(p)|_{\hat{\Omega}_d} : \hat{\Omega}_d \quad &! \quad \Omega(p) \\ \hat{x} \quad &7! \quad C_d(p)\hat{x} + z_d(p); \end{aligned} \tag{4.9}$$

for $d = 1; ::: ; L$, where $C_d(p) \; 2 \; \mathsf{R}^{2 \; 2}$ and $z_d(p) \; 2 \; \mathsf{R}^2$. According to (4.9), the Jacobian matrix $J_{\mathsf{T}}(p)$ of the transformation $\mathsf{T}(p)$ is constant and non-singular on each region of the given parametrisation, i.e. we have $J_{\mathsf{T}}(p)|_{\hat{\Omega}_d} = C_d(p)$ with $\det C_d(p) \; , \; 0$.

Now we state the problem (4.4) on the reference domain $\hat{\Omega}$ with the corresponding Hilbert space $\hat{V} := V(\hat{p})$ equipped with the inner product $\langle \hat{w}; \hat{v} \rangle_{\hat{V}} = \int_{\hat{\Omega}} r\hat{w} \quad r\hat{v} d\hat{x}$ and the induced norm $\|\hat{v}\|_{\hat{X}} = \langle \hat{v}; \hat{v} \rangle^{1=2}_{\hat{V}}$. It reads as follows: for $p \; 2 \; \mathsf{D}$, find $\hat{u}(p) \; 2 \; \hat{V}$ so that

$$a[\hat{u}(p)](\hat{u}(p); \hat{v}; p) = f(\hat{v}; p); \quad 8\hat{v} \; 2 \; \hat{V}; \tag{4.10}$$

where the quasilinear form in (4.5) is now transformed with the change of variables formula into

$$a[\hat{u}](\hat{w};\hat{v};p) = \int_{\hat{\Omega}} (\hat{x};|J_T^T(p)\nabla\hat{u}|)[J_T^T(p)\nabla\hat{w}]\ [J_T^T(p)\nabla\hat{v}]|\det J_T(p)|\,d\hat{x}: \tag{4.11}$$

Similarly, the linear form in (4.5) is transformed into

$$f(\hat{v};p) = \int_{\hat{\Omega}} [f\ \ T(p)]\hat{v}|\det J_T(p)|\,d\hat{x}: \tag{4.12}$$

Since $\hat{\Omega} = \hat{\Omega}^1\ [\ \hat{\Omega}^2$, we have the decomposition

$$a[\hat{w}](\hat{w};\hat{v};p) := a^{\ 1}[\hat{w}](\hat{w};\hat{v};p) + a^{\ 2}(\hat{w};\hat{v};p); \tag{4.13}$$

where $a^{\ 1}$ is the restriction of (4.11) to $\hat{\Omega}^1$ with nonlinear reluctivity function $_1$, and $a^{\ 2}$ is the restriction of (4.11) to $\hat{\Omega}^1$ with piecewise constant reluctivity function $_2$. Application of Newton's method requires the computation of the derivative of $a^{\ 1}$, which is given by

$$da[u](w;v;p) = \int_{\Omega^1(p)} \frac{^0_1(|\nabla u|)}{|\nabla u|}(\nabla u\ \ \nabla w)(\nabla u\ \ \nabla v)dx + a^{\ 1}(w;v;p) \tag{4.14}$$

and transformed as in (4.11) to the reference domain $\hat{\Omega}^1$ with the change of variables formula, thus we have

$$da^{\ 1}[\hat{u}](\hat{w};\hat{v};p) = \int_{\hat{\Omega}^1} \frac{^0_1(|J_T^T(p)\nabla\hat{u}|)}{|J_T^T(p)\nabla\hat{u}|}(J_T^T(p)\nabla\hat{u}\ \ J_T^T(p)\nabla\hat{w})(J_T^T(p)\nabla\hat{u}\ \ J_T^T(p)\nabla\hat{v})|\det J_T(p)|d\hat{x}:$$

To solve (4.10), we apply Newton's method: starting with $\hat{u}^{(0)}(p)\ 2\ \hat{V}$, for $z = 0; 1; ::$ solve the problem

$$da[\hat{u}^{(z)}](\ \hat{u}^{(z)};\hat{v};p) = R[\hat{u}^{(z)}](\hat{v};p); \quad R[\hat{u}^{(z)}](\hat{v};p) := f(\hat{v};p)\ \ a[\hat{u}^{(z)}](\hat{u}^{(z)};\hat{v};p) \tag{4.15}$$

to obtain $\hat{u}^{(z)}(p)\ 2\ \hat{V}$, and then update the solution $\hat{u}^{(z+1)}(p) := \hat{u}^{(z)}(p) + \hat{u}^{(z)}(p)$. To prove that problem (4.15) is well-posed, we need the following lemma

Lemma 17. *Let* $T(p) : \hat{\Omega}\ !\ \Omega(p)$ *be the geometric transformation from* (4.9)*. Then we have the following equivalence*

$$C_1(p)\|\hat{v}\|^2_{\hat{V}}\ \ \|v\|^2_{V(p)}\ \ C_2(p)\|\hat{v}\|^2_{\hat{V}}; \tag{4.16}$$

with the positive geometric constants

$$C_1(p) := \min_{1\ d\ L}\{\ _{min}(C_d(p)\ ^1C_d(p)\ ^T)|\det C_d(p)|\}; \tag{4.17a}$$

$$C_2(p) := \max_{1\ d\ L}\{\ _{max}(C_d(p)\ ^1C_d(p)\ ^T)|\det C_d(p)|\}: \tag{4.17b}$$

Proof. We inspect the geometric dependence to prove the lower bound

$$\|v\|^2_{V(p)} = \sum_{d=1}^{D}\sum_{i,j=1}^{d} [C_d(p)^{-1} C_d(p)^{-T}]_{ij} |\det C_d(p)| \int_{\hat{\Omega}_d} \frac{\partial \hat{v}}{\partial \hat{x}_i}\frac{\partial \hat{v}}{\partial \hat{x}_j}\, d\hat{x}$$
$$> \min_{1 \le d \le D} \{ \sigma_{min}(C_d(p)^{-1} C_d(p)^{-T}) |\det C_d(p)| \} \|\hat{v}\|^2_{\hat{V}} = C_1(p)\|\hat{v}\|^2_{\hat{V}}.$$

Similarly we prove the upper bound

$$\|v\|^2_{V(p)} \le \max_{1 \le d \le D} \{ \sigma_{max}(C_d(p)^{-1} C_d(p)^{-T}) |\det C_d(p)| \} \|\hat{v}\|^2_{\hat{V}} = C_2(p)\|\hat{v}\|^2_{\hat{V}}.$$

Lemma 12 and Lemma 17 implies that for $\hat{u} \in \hat{V}$ the bilinear form $da[\hat{u}](\cdot\,;\cdot\,;p) : \hat{V} \times \hat{V} \to \mathbb{R}$ is coercive and continuous for all $p \in \mathcal{D}$, i.e., we have

$$da[\hat{u}](\hat{v};\hat{v};p) \ge \alpha_{LB} C_1(p)\|\hat{v}\|^2_{\hat{V}}, \quad \forall \hat{v} \in \hat{V}; \tag{4.18a}$$
$$da[\hat{u}](\hat{w};\hat{v};p) \le \gamma_0 C_2(p)\|\hat{w}\|_{\hat{V}}\|\hat{v}\|_{\hat{V}}, \quad \forall \hat{v}, \hat{w} \in \hat{V}. \tag{4.18b}$$

Thus, the well-posedness of problem (4.15) follows from the lemma of Lax-Milgram (see, e.g. [54]): given a current iterate $\hat{u}^{(z)}(p) \in \hat{V}$, there exists a unique solution $\hat{u}^{(z)}(p) \in \hat{V}$ of problem (4.20).

4.1.2 Finite Element Truth Approximation

We introduce a high dimensional finite element discretization (truth approximation) of our problem in the space $\hat{V}_\mathcal{N} = \text{span}\{\zeta_1, \ldots, \zeta_\mathcal{N}\} \subset \hat{V}$ of piecewise linear and continuous finite element functions. The finite element approximation is obtained by a standard Galerkin projection: given $p \in \mathcal{D}$, find $u_\mathcal{N}(p) \in \hat{V}_\mathcal{N}$ such that

$$a[\hat{u}_\mathcal{N}(p)](\hat{u}_\mathcal{N}(p), \hat{v}_\mathcal{N}; p) = f(\hat{v}_\mathcal{N}; p), \quad \forall \hat{v}_\mathcal{N} \in \hat{V}_\mathcal{N}. \tag{4.19}$$

Given the ansatz $\hat{u}_\mathcal{N}(p) = \sum_{j=1}^{\mathcal{N}} \hat{\mathbf{u}}_{\mathcal{N}\,j}(p)\,\zeta_j$ for the discrete solution and testing against the basis elements in $\hat{V}_\mathcal{N}$ leads to the system of nonlinear algebraic equations

$$\mathbf{A}_\mathcal{N}(\hat{\mathbf{u}}_\mathcal{N}; p)\hat{\mathbf{u}}_\mathcal{N}(p) = \mathbf{F}_\mathcal{N}(p); \tag{4.20}$$

where $\mathbf{F}_\mathcal{N}(p) \in \mathbb{R}^\mathcal{N}$; $\mathbf{F}_{\mathcal{N}\,j}(p) = f(\zeta_j; p)$ and $\mathbf{A}_\mathcal{N}(\hat{\mathbf{u}}_\mathcal{N}; p) \in \mathbb{R}^{\mathcal{N}\times\mathcal{N}}$, $\mathbf{A}_\mathcal{N}(\hat{\mathbf{u}}_\mathcal{N}; p)_{ij} = a[\hat{u}_\mathcal{N}(p)](\zeta_j, \zeta_i; p)$, $1 \le i, j \le \mathcal{N}$. To solve (4.20), we apply a Newton's iterative scheme: starting with $\hat{\mathbf{u}}^{(0)}_\mathcal{N}(p)$, for $z = 0, 1, \ldots$ solve the linear system

$$\mathbf{J}_\mathcal{N}(\hat{\mathbf{u}}^{(z)}_\mathcal{N}; p)\ \hat{\mathbf{u}}^{(z)}_\mathcal{N}(p) = \mathbf{R}_\mathcal{N}(\hat{\mathbf{u}}^{(z)}_\mathcal{N}; p) \tag{4.21}$$

to obtain $\hat{\mathbf{u}}^{(z)}_\mathcal{N}(p)$, and then update the solution $\hat{\mathbf{u}}^{(z+1)}_\mathcal{N}(p) := \hat{\mathbf{u}}^{(z)}_\mathcal{N}(p) + \hat{\mathbf{u}}^{(z)}_\mathcal{N}(p)$. The residual $\mathbf{R}_\mathcal{N}(p) \in \mathbb{R}^\mathcal{N}$ for the Newton's scheme must be calculated at every Newton iteration according to

$$\mathbf{R}_{\mathcal{N}\,i}(\hat{\mathbf{u}}_\mathcal{N}; p) = \mathbf{F}_{\mathcal{N}\,i}(p) - \sum_{j=1}^{\mathcal{N}} \mathbf{A}_\mathcal{N}(\hat{\mathbf{u}}_\mathcal{N}; p)_{ij}\hat{\mathbf{u}}_{\mathcal{N}\,j}(p), \quad 1 \le i \le \mathcal{N}. \tag{4.22}$$

The Jacobian matrix $\mathbf{J}_N(\hat{\mathbf{u}}_N; p) \in \mathbb{R}^{N \times N}$ in (4.21) is given by $\mathbf{J}_N(\hat{\mathbf{u}}_N; p)_{ij} = da[\hat{u}_N](\varphi_j, \varphi_i; p)$ and its invertibility for all $p \in \mathcal{D}$ follows from the coercivity property (4.18a).

4.2 Reduced basis approximation

4.2.1 An EIM-RB method

To perform the reduced basis approximation, we first introduce a subset $\mathcal{D}_{train} \subset \mathcal{D}$ from which a sample $\mathcal{D}_N^u = \{\bar{p}_1 \in \mathcal{D}; \ldots; \bar{p}_N \in \mathcal{D}\}$ with associated reduced-basis space $\hat{W}_N^u = \text{span}\{\zeta_n := \hat{u}_N(\bar{p}_n);\ 1 \le n \le N\}$ of dimension N, which is built with the help of a weak greedy algorithm. This algorithm constructs iteratively nested spaces $\hat{W}_n^u;\ 1 \le n \le N$ using an a-posteriori error estimator $\Delta_u(Y; p)$, which predicts the expected approximation error for a given parameter p in the space $\hat{W}_n^u = Y$. We want the expected approximation error to be less than the prescribed tolerance ε_{RB}. We initiate the algorithm with an arbitrary chosen parameter $\bar{p}_1$ with the corresponding snapshot $\hat{u}(\bar{p}_1)$ for the basis enrichment. Next we proceed as stated in the following Algorithm 3. We note that the basis functions ζ_n are also

Algorithm 3: RB-Greedy algorithm

1 **Input:** Tolerance ε_{RB}, max. number of iterations $N_{\max}$, $\hat{W}_1^u = \text{span}\{\hat{u}(\bar{p}_1)\}$, parameter set $\mathcal{D}_{train} \subset \mathcal{D}$

2 **Output:** RB spaces $\{\hat{W}_n^u\}_{n=2}^N$

1: **while** $2 \le n \le N_{\max}$ and $\varepsilon_n := \max_{p \in \mathcal{D}_{train}} \Delta_u(\hat{W}_n^u; p) > \varepsilon_{RB}$ **do**
2: $\bar{p}_n \leftarrow \arg\max_{p \in \mathcal{D}_{train}} \Delta_u(\hat{W}_{n-1}^u; p)$
3: $\mathcal{D}_n^u \leftarrow \mathcal{D}_{n-1}^u \cup \{\bar{p}_n\}$
4: $\hat{W}_n^u \leftarrow \hat{W}_{n-1}^u \oplus \text{span}\{\zeta_n \leftarrow \hat{u}_N(\bar{p}_n)\}$
5: $n \leftarrow n + 1$
6: **end while**

orthonormalized relative to the $\langle \cdot, \cdot \rangle_V$ inner product with a Gram-Schmidt procedure to generate a well-conditioned system of equations.

The Empirical Interpolation Method (EIM) [5] is used to ensure the availability of offline/online decomposition in the presence of the nonlinearity

$$\gamma_1(\hat{u}_N(\hat{x}; p); p) := \gamma_1(|J_T^T(\hat{x}; p) \cdot \hat{u}_N(\hat{x}; p)|). \tag{4.23}$$

Given an EIM tolerance $\varepsilon_{EIM} > 0$ and a fine sample $\mathcal{D}_{train}^{EIM} \subset \mathcal{D}$ of size n_{train}^{EIM}, we construct with the Algorithm 4 the nested sample sets $\mathcal{D}_M \subset \mathcal{D}_{train}^{EIM}$, where $\mathcal{D}_M = \{p_1 \in \mathcal{D}; \ldots; p_M \in \mathcal{D}\}$ and associated approximation spaces $W_M = \text{span}\{\psi_m := \gamma_1(\hat{u}_N(\hat{x}; p_m); p_m); 1 \le m \le M\} = \text{span}\{q_1; \ldots; q_M\}$ together with a set of interpolation points $T_M = \{\hat{x}_1^M; \ldots; \hat{x}_M^M\}$. Then we build an affine approximation $\gamma_1^M(\hat{u}_N(\hat{x}; p); p)$ of $\gamma_1(\hat{u}_N(\hat{x}; p); p)$ as

$$\begin{aligned} \gamma_1^M(\hat{u}_N(\hat{x}; p); p) &:= \gamma_1^M(|J_T^T(\hat{x}; p) \cdot \hat{u}_N(\hat{x}; p)|) = \sum_{m=1}^M \theta_m(p) q_m(\hat{x}) \\ &= \sum_{m=1}^M (B_M^{-1} \gamma_p)_m q_m(\hat{x}) = \gamma_1(\hat{u}_N(\hat{x}; p); p) + \rho_M(\hat{x}; p), \end{aligned} \tag{4.24}$$

where $_M(\,;p)$ is the EIM approximation error: it holds $_M(p) := \| _M(\,;p)\|_{L^1(\hat\Omega)} <$ $_{EIM}$ for all $p \in D^{EIM}_{train}$. In (4.24) we also have $_p := \{ _1(\hat u_N(\hat x^M_m;p);p)\}_{m=1}^M \in \mathbb{R}^M$ and $B_M \in \mathbb{R}^{M\times M}$ with $(B_M)_{ij} = q_j(\hat x^M_i)$ is the lower triangular interpolation matrix by construction.

Algorithm 4: EIM algorithm

Input: Tolerance $_{EIM}$, max. number of iterations $M_{\max}$, parameter set D^{EIM}_{train} D
Output: Approximation spaces $\{W_m\}_{m=1}^M$, interpolation points $\{T_m\}_{m=1}^M$

$p_1 := \arg\max_{p\in D^{EIM}_{train}} \| _1(\hat u_N(\,;p);p)\|_{L^1(\hat\Omega)}$
$D_1 = \{p_1\}$
$r_1(\hat x) := _1(\hat u_N(\hat x;p_1);p_1)$
$x^M_1 := \arg\max_{\hat x\in\Omega} |r_1(\hat x)|; \quad q_1 := r_1/r_1(\hat x^M_1)$
$T_1 := \{\hat x^M_1\}; \quad Q_1 := \{q_1\}; \quad W_1 := \mathrm{span}(Q_1)$
while $2 \le m \le M_{\max}$ and $^{max}_m >$ $_{EIM}$ **do**
  $^{max}_m = \max_{p\in D^{EIM}_{train}} \| _1(\hat u_N(\,;p);p) - {}^{m-1}_1(\hat u_N(\,;p);p)\|_{L^1(\hat\Omega)}$
  $p_m = \arg\max_{p\in D^{EIM}_{train}} \| _1(\hat u_N(\,;p);p) - {}^{m-1}_1(\hat u_N(\,;p);p)\|_{L^1(\hat\Omega)}$
  $D_m = D_{m-1} \cup \{p_m\}$
  $r_m(\hat x) = _1(\hat u_N(\hat x;p_m);p_m) - {}^{m-1}_1(\hat u_N(\hat x;p_m);p_m)$
  $\hat x^M_m = \arg\max_{\hat x\in\hat\Omega} |r_m(\hat x)|; \quad q_m = r_m/r_m(\hat x^M_m)$
  $T_m := T_{m-1} \cup \{\hat x^M_m\}; \quad Q_m := Q_{m-1} \cup \{q_m\}; \quad W_m := \mathrm{span}(Q_m)$
  $m \leftarrow m+1$
end while

Remark 18. *We note that for any* $_1(\,;p)$*, the interpolation error satisfies*

$$\| _M(p)\| \le (1+\Lambda_M) \inf_{z\in W_M} \| _1(\hat u_N(\,;p);p) - z\|_{L^1(\hat\Omega)}, \quad \forall p \in D,$$

where $\Lambda_M := \sup_{\hat x\in\hat\Omega} \sum_{m=1}^M |\, ^M_m(\hat x)|$ *is the Lebesque interpolation constant and* $^M_m \in W_M$ *are the characteristic functions of* W_M *with* $^M_m(\hat x^M_n) =$ $_{mn}$*. The Lebesque constant can be upper bounded* $\Lambda_M \le 2^M - 1$*, but in practice the actual behaviour of* Λ_M *is much lower. In fact,* Λ_M *depends on the set of interpolation points* T_M*; the interpolation points are selected in the Greedy fashion to minimize the supremum norm of the residual. The optimality with respect to the supremum norm also characterizes the Chebyshev points. In this way the points* T_M *"magically" coincide with the Chebyshev points on the interval* $[-1,1]$ *and sometimes called as "magic points". Therefore the EIM algorithm generalizes the selection of optimal interpolation points to arbitrary-shaped geometries [38].*

The EIM approximation of $_1$ results in the EIM-approximation $a_M[\,](\,;\,;p)$ of the quasilinear form $a[\,](\,;\,;p)$ and then the reduced basis approximation is obtained by a standard Galerkin projection: given $p \in D$, find $\hat u_{N;M}(p) \in \hat W^u_N$ such that

$$a_M[\hat u_{N;M}(p)](\hat u_{N;M}(p);\hat v_N;p) = f(\hat v_N;p), \quad \forall \hat v_N \in \hat W^u_N \tag{4.25}$$

holds. Since $\hat{\Omega} = \hat{\Omega}^1 \cup \hat{\Omega}^2$, we have the decomposition

$$a_M[\hat{w}](\hat{w};\hat{v};p) := a_M^1[\hat{w}](\hat{w};\hat{v};p) + a^2(\hat{w};\hat{v};p); \tag{4.26}$$

where $a_M^1[\,](\,;\,;p)$ is the EIM-approximation of $a^1[\,](\,;\,;p)$ with nonlinear reluctivity $\nu_1(\,;p)$ replaced by its EIM counterpart $\nu_1^M(\,;p)$.

We define $V_N(p) := \{v_N \mid v_N = \hat{v}_N \circ T^{-1};\ \hat{v}_N \in \hat{V}_N\}$ as a push-forward finite-element space over the parametrised domain $\Omega(p)$. For mathematical convenience, we assume that the EIM approximation $a_M[\,](\,;\,;p)$ is sufficiently accurate in the sense that the form $a_M[\,](\,;\,;p)$ is strongly monotone on $V_N(p)$ with monotonicity constant $\tilde{\alpha}_{LB} := \alpha_{LB}^{\alpha_a} > 0$, i.e., for all $v_N, w_N \in V_N(p)$ it holds

$$a_M[v_N](v_N;v_N - w_N;p) - a_M[w_N](w_N;v_N - w_N;p) \geq \tilde{\alpha}_{LB}\|v_N - w_N\|^2_{V(p)}; \tag{4.27}$$

and Lipschitz continuous on $V_N(p)$ with Lipschitz constants $\tilde{L}_a := L_a^{\alpha_a} > 0$, i.e., for all $u_N, w_N, v_N \in V_N(p)$ it holds

$$|a_M[u_N](u_N;v_N;p) - a_M[w_N](w_N;v_N;p)| \leq \tilde{L}_a\|u_N - w_N\|_{V(p)}\|v_N\|_{V(p)}; \tag{4.28}$$

where $\alpha_a \in \mathbb{R}_+$ is small enough and is related to the EIM approximation error. Then problem (4.25) admits a unique solution. However, in the EIM practice we can guarantee that conditions (4.27) and (4.28) hold uniformly together with $\alpha_a < \alpha_{EIM}$ only on $\mathcal{D}_{train}^{EIM}$. It is difficult to check these properties a-priori for $p \in \mathcal{D} \cap \mathcal{D}_{train}^{EIM}$, so that arguing the well-posedness of (4.25) and the upcoming discrete system (4.43) in general is not possible.

Finally, we achieve an affine decomposition of the quasilinear form

$$a_M^1[\hat{u}_{N;M}(p)](\hat{w};\hat{v};p) = \sum_{m=1}^{M}\sum_{d=1}^{\mathcal{L}}\sum_{i,j=1}^{\mathcal{D}} \vartheta_m(p)\Phi_{d;\mathcal{L}_1}^{i;j}(p)a_{m;d}^{i;j}(\hat{w};\hat{v}); \tag{4.29}$$
$$a^2(\hat{w};\hat{v};p) = \sum_{d=1}^{\mathcal{L}}\sum_{i,j=1}^{\mathcal{D}} \Phi_{d;\mathcal{L}_2}^{i;j}(p)a_d^{i;j}(\hat{w};\hat{v});$$

such that $\Phi_{d;\mathcal{L}_1}^{i;j} : \mathcal{D} \to \mathbb{R}$ for $d = 1,\ldots,\mathcal{L}_1$; $i,j = 1,2$ and $\Phi_{d;\mathcal{L}_2}^{i;j} : \mathcal{D} \to \mathbb{R}$ for $d = 1,\ldots,\mathcal{L}_2$; $i,j = 1,2$ are functions depending on p and the parameter independent forms

$$a_{m;d}^{i;j}(\hat{w};\hat{v}) = \int_{\hat{\Omega}_d^1} q_m \frac{\partial\hat{w}}{\partial\hat{x}_i}\frac{\partial\hat{v}}{\partial\hat{x}_j}\,d\hat{x};\quad 1 \leq d \leq \mathcal{L}_1;\ 1 \leq i,j \leq 2;$$
$$a_d^{i;j}(\hat{w};\hat{v}) = \int_{\hat{\Omega}_d^2} \frac{\partial\hat{w}}{\partial\hat{x}_i}\frac{\partial\hat{v}}{\partial\hat{x}_j}\,d\hat{x};\quad 1 \leq d \leq \mathcal{L}_2;\ 1 \leq i,j \leq 2:$$

For notational convenience, we set

$$c_m(\hat{w};\hat{v};p) := \sum_{d=1}^{\mathcal{L}}\sum_{i,j=1}^{\mathcal{D}} \Phi_{d;\mathcal{L}_1}^{i;j}(p)a_{m;d}^{i;j}(\hat{w};\hat{v}); \tag{4.30}$$

so that

$$a_M^1[\hat{u}_{N;M}(p)](\hat{w};\hat{v};p) = \sum_{m=1}^{M} \Theta_m(p) c_m(\hat{w};\hat{v};p).$$

Similarly, the affine decomposition of f has the form

$$f(\hat{v};p) = \int_{\hat{\Omega}} J_e \hat{v}\, d\hat{x} \sum_{d=1}^{D}\sum_{i=1}^{d} |\det C_d(p)| C_d(p)^{-1}_{di} \int_{\hat{\Omega}_d} H_{pm;1} \frac{\partial \hat{v}}{\partial \hat{x}_i} d\hat{x} \tag{4.31}$$
$$+ \sum_{d=1}^{D}\sum_{i=1}^{d} |\det C_d(p)| C_d(p)^{-1}_{di} \int_{\hat{\Omega}_d} H_{pm;2} \frac{\partial \hat{v}}{\partial \hat{x}_i} d\hat{x} = \sum_{q=1}^{Q_f} \Theta_q^f(p) f_q(\hat{v});$$

where $\Theta_q^f : \mathcal{D} \to \mathbb{R}$ for $q = 1,\ldots,Q_f$ are parameter dependent functions and parameter independent forms $f_q(\hat{v})$.

4.2.2 Error estimation

We define $W_N^u(p) := \{w_N \mid w_N = \hat{w}_N \circ \mathcal{T}^{-1};\ \hat{w}_N \in \hat{W}_N^u\}$ as a push-forward reduced-basis space over the parametrised domain $\Omega(p)$ for error estimation purposes, where $\mathcal{T}^{-1}$ is the inverse of the geometric transformation (4.9). First we study the convergence of $\hat{u}_{N;M}(p) \to \hat{u}_N(p)$.

Proposition 4.2.1 (A-priori Error Bound)**.** *Assume that the EIM-approximation error of the nonlinearity satisfies* $\sup_{p\in\mathcal{D}} \|\Theta_1(p) - \Theta_1^M(p)\|_{L^1} \le \varepsilon_{EIM}$. *Assume further that* $a[\,](\cdot;\cdot;p)$ *is Lipschitz continuous on* $V(p)$ *with Lipschitz constant* $L_a = 2\gamma_{LB} + \gamma_0 > 0$ (4.8) *and that the EIM-approximation* $a_M[\,](\cdot;\cdot;p)$ *of* $a[\,](\cdot;\cdot;p)$ *is strongly monotone with monotonicity constant* $\tilde{\gamma}_{LB} := \gamma_{LB} - \varepsilon_a > 0$ (4.27)*. Then we have*

$$\|\hat{u}_N(p) - \hat{u}_{N;M}(p)\|_{\hat{Y}} \le \sqrt{\frac{C_2(p)}{C_1(p)}} \inf_{\hat{w}_N \in \hat{W}_N^u} \left\{ 1 + \frac{L_a}{\tilde{\gamma}_{LB}} \|\hat{u}_N(p) - \hat{w}_N\|_{\hat{Y}} + \frac{\varepsilon_{EIM}}{\tilde{\gamma}_{LB}} \|\hat{w}_N\|_{\hat{Y}} \right\}$$

with the geometric constants

Proof. Set $u_N := u_N(p) \in V(p)$; $u_{N;M} := u_{N;M}(p) \in W_N^u(p)$ and let $w_N \in W_N^u(p)$ be arbitrary. Set $\varepsilon_{N;M} := u_{N;M} - w_N$. First we note that

$$a_M[u_{N;M}](u_{N;M};w_N) - a[u_N](u_N;w_N) = 0,\ \forall w_N \in W_N^u(p) \subset V_N(p). \tag{4.32}$$

Then we use (4.32), the strong monotonicity condition and Lipschitz continuity to obtain the bound

$$\begin{aligned}
\tilde{\gamma}_{LB}\|\varepsilon_{N;M}\|^2_{X(p)} &\le a_M[u_{N;M}](u_{N;M};\varepsilon_{N;M}) - a_M[w_N](w_N;\varepsilon_{N;M}) \\
&= a[u_N](u_N;\varepsilon_{N;M}) - a[w_N](w_N;\varepsilon_{N;M}) \\
&+ a[w_N](w_N;\varepsilon_{N;M}) - a_M[w_N](w_N;\varepsilon_{N;M}) \\
&\le L_a\|u_N - w_N\|_{V(p)}\|\varepsilon_{N;M}\|_{V(p)} \\
&+ \sup_{p\in\mathcal{D}} \|\Theta_1(p) - \Theta_1^M(p)\|_{L^1} \|w_N\|_{V(p)} \|\varepsilon_{N;M}\|_{V(p)}.
\end{aligned}$$

Dividing both sides by $\tilde{}_{\mathrm{LB}}\| \ _{N;M}\|_{V(p)}$ and using the triangle inequality

$$\|u_{\mathrm{N}} \quad u_{N;M}\|_{V(p)} \quad \|u_{\mathrm{N}} \quad w_N\|_{V(p)} + \| \ _{N;M}\|_{V(p)};$$

we obtain the estimate

$$\|u_{\mathrm{N}}(p) \quad u_{N;M}(p)\|_{V(p)} \quad 1 + \frac{L_a}{\tilde{}_{\mathrm{LB}}} \ \|u_{\mathrm{N}}(p) \quad w_N\|_{V(p)} + \frac{EIM}{\tilde{}_{\mathrm{LB}}}\|w_N\|_{V(p)}: \tag{4.33}$$

The desired result follows from the Lemma 17 after a short calculation.

For efficient implementation of the reduced basis methodology and the verification of the error, it is necessary to provide an a-posteriori error bound, which can be quickly evaluated. For this we establish an error bound based on the residual. We denote by $r_M(\ ; p) \ 2 \ \hat{V}_{\mathrm{N}}^0$ the residual (formed on the reference domain) of the problem, defined naturally as

$$r_M(\hat{v}_{\mathrm{N}} ; p) = f(\hat{v}_{\mathrm{N}} ; p) \quad a_M[\hat{u}_{N;M}](\hat{u}_{N;M}; \hat{v}_{\mathrm{N}} ; p) \quad 8\hat{v}_{\mathrm{N}} \ 2 \ \hat{V}_{\mathrm{N}}: \tag{4.34}$$

We have the following

Proposition 4.2.2 (A-posteriori Error Bound)**.** *Let* $_{LB} > 0$ *be the lower bound of the monotonicity constant. Then, the RB-EIM error* $\hat{e}_{N;M}(p) := \hat{u}_{\mathrm{N}}(p) \quad \hat{u}_{N;M}(p)$ *can be bounded by*

$$\|\hat{e}_{N;M}(p)\|_{\hat{Y}} \quad \frac{\|r_M(\ ; p)\|_{\hat{Y}_{\mathrm{N}}^0}}{_{LB} \ C_1(p)} + \frac{C_2(p) \ _M(p)}{_{LB} C_1(p)}\|\hat{u}_{N;M}(p)\|_{\hat{Y}} := 4_{N;M}(p) \tag{4.35}$$

with the geometric constants (4.17a)*,* (4.17b) *and the EIM approximation error*

$$_M(p) = \sup_{\hat{x}2\hat{\Omega}} \mathrm{j} \ _1(\mathrm{j}J_{\mathrm{T}}{}^T(\hat{x}; p) \, \hat{u}_{N;M}(\hat{x}; p)\mathrm{j}) \quad {}^M_1(\mathrm{j}J_{\mathrm{T}}{}^T(\hat{x}; p) \, \hat{u}_{N;M}(\hat{x}; p)\mathrm{j})\mathrm{j} \tag{4.36}$$

of the nonlinearity

Proof. Since in the case $e_{N;M} = 0$ there is nothing to show, we assume that $e_{N;M} \ , \ 0$. We then use strong monotonicity condition (4.7) and the definition of the residual (4.34) to estimate

$$\begin{aligned}
_{\mathrm{LB}}\|e_{N;M}\|^2_{X(p)} \quad a[u_{\mathrm{N}}](u_{\mathrm{N}} ; e_{N;M}) \quad a[u_{N;M}](u_{N;M}; e_{N;M}) \\
= f(e_{N;M}) \quad a_M[u_{N;M}](u_{N;M}; e_{N;M}) \\
+a_M[u_{N;M}](u_{N;M}; e_{N;M}) \quad a[u_{N;M}](u_{N;M}; e_{N;M}) \\
:= r_M(e_{N;M}) + a_M[u_{N;M}](u_{N;M}; e_{N;M}) \quad a[u_{N;M}](u_{N;M}; e_{N;M}) \\
= r_M(\hat{e}_{N;M}) + a_M[u_{N;M}](u_{N;M}; e_{N;M}) \quad a[u_{N;M}](u_{N;M}; e_{N;M}) \\
\|r_M\|_{\hat{Y}_{\mathrm{N}}^0}\|\hat{e}_{N;M}\|_{\hat{Y}} + \ _M(p)\|u_{N;M}\|_{X(p)}\|e_{N;M}\|_{V(p)}
\end{aligned}$$

Now the final result follows from the Lemma 17, applied to $\|e_{N;M}\|^2_{V(p)}$ and the right-hand side of the inequality, correspondingly.

We address the computational realization of the estimator (4.35) in the next section. Next we denote

by $r(\,;p) \in \hat{V}_{\mathrm{N}}^0$ the residual of the original problem (without EIM reduction), defined as

$$r(\hat{v}_{\mathrm{N}};p) = f(\hat{v}_{\mathrm{N}};p) \quad a[\hat{u}_N](\hat{u}_N;\hat{v}_{\mathrm{N}};p) \tag{4.37}$$

and let $\hat{e}_N(p) := \hat{u}_{\mathrm{N}}(p) \quad \hat{u}_N(p)$ be the error of the reduced-basis approximation. Along the lines of proposition 3.2 one can prove the error bound

$$\|\hat{e}_N(p)\|_{\hat{Y}} \quad \frac{\|r(\,;p)\|_{\hat{Y}_{\mathrm{N}}^0}}{\mathrm{LB}\ C_1(p)} := \Delta_N(p). \tag{4.38}$$

We use (4.38) to investigate the factor of overestimation in the reduced-basis approximation.

Proposition 4.2.3 (Effectivity bound for RB-approximation)**.** *Let* $\eta_N(p) = \frac{\Delta_N(p)}{\|\hat{e}_N\|_{\hat{Y}}}$*. Then*

$$\eta_N(p) \quad \frac{L_a}{LB}\sqrt{C_1(p)C_2(p)} \tag{4.39}$$

Proof. Let $\hat{v}_r \in \hat{V}_{\mathrm{N}}$ denote the Riesz-representative of $r(\,;p)$. Then we have

$$\langle \hat{v}_r;\hat{v}_{\mathrm{N}}\rangle_{\hat{Y}} = r(\hat{v};p);\ \hat{v}_{\mathrm{N}} \in \hat{V}_{\mathrm{N}};\quad \|\hat{v}_r\|_{\hat{Y}} = \|r(\,;p)\|_{\hat{Y}_{\mathrm{N}}^0}:$$

Now let $v_r := \hat{v}_r \quad \mathsf{T}^{-1} \in V_{\mathrm{N}}(p)$. Then, using Lipshitz continuity of (4.8), we have

$$\begin{aligned}\|v_r\|^2_{V(p)} = \langle v_r;v_r\rangle_{V(p)} = r(v_r;\ ) = a[u_{\mathrm{N}}](u_{\mathrm{N}};v_r;p) \quad a[u_N](u_N;v_r;p)\\ L_a\|e_N\|_{V(p)}\|v_r\|_{V(p)}:\end{aligned}$$

With the Lemma 17, we obtain

$$\frac{\|\hat{v}_r\|_{\hat{Y}}}{\|\hat{e}_N\|_{\hat{Y}}} \quad L_a\sqrt{\frac{C_2(p)}{C_1(p)}}:$$

With (4.38) we then conclude

$$\eta_N(p) = \frac{\Delta_N(p)}{\|\hat{e}_N\|_{\hat{Y}}} = \frac{\|\hat{v}_r\|_{\hat{Y}}}{\mathrm{LB}\ C_1(p)\|\hat{e}_N\|_{\hat{Y}}} \quad \frac{L_a}{\mathrm{LB}}\sqrt{C_1(p)C_2(p)}:$$

and obtain the effectivity bound.

This bound is further used to explain the gap between the true error and the estimator.

4.2.3 Computational procedure

The computational process in the reduced basis modelling can be split into the offline and the online phase. The computations in the offline phase depend on the dimension N of the finite element space and are expensive, but should be performed only once. The computations in the online phase are independent of N, with computational complexity which depends only on the the dimension N of the reduced-basis approximation space and the dimension M of the EIM approximation space. The key concept utilized here is parameter-separability (or affine decomposition) of all the forms involved in the problem. We now give the details of the numerical scheme for the nonlinear part, defined on the domain $\hat{\Omega}^1$. The

second term in (4.29) is linear and can be treated similarly. We expand our reduced basis solution as $\hat{u}_{N;M}(p) = \sum_{j=1}^{N} \hat{\mathbf{u}}_{N;M\,j}\,\zeta_j$ and test against the basis elements in $\hat{W}_N^u$ to obtain the algebraic equations

$$\sum_{j=1}^{N}\sum_{m=1}^{M} \omega_m(p)\mathbf{C}_{i\,m}^{j(N;M)}(\hat{\mathbf{u}}_{N;M};p)\hat{\mathbf{u}}_{N;M\,j}(p) = \mathbf{F}_{N\,i}(p), \quad 1 \le i \le N; \tag{4.40}$$

where $\mathbf{C}^{j(N;M)}(\hat{\mathbf{u}}_{N;M};p) \in \mathbb{R}^{N\times M}$; $\mathbf{C}_{i\,m}^{j(N;M)}(\hat{\mathbf{u}}_{N;M};p) = c_m(\zeta_j,\zeta_i;p)$; $1 \le i,j \le N$; $1 \le m \le M$, and $\mathbf{F}_{N\,i}(p) = f(\zeta_i;p)$. Let $\omega_M(p) = \{\omega_{M\,k}(p)\}_{k=1}^{M} \in \mathbb{R}^M$, then

$$\begin{aligned}\sum_{k=1}^{M} \mathbf{B}_{m\,k}^{M}\,\omega_{M\,k}(p) &= \psi_1(\hat{u}_{N;M}(\hat{x}_m^M;p);p), \quad 1 \le m \le M \\ &= \psi_1\Big(\sum_{n=1}^{N}\hat{\mathbf{u}}_{N;M\,n}(p)\,\zeta_n(\hat{x}_m^M);p\Big), \quad 1 \le m \le M.\end{aligned} \tag{4.41}$$

We then insert (4.41) into (4.40) to get the following nonlinear algebraic equation system

$$\sum_{j=1}^{N}\sum_{m=1}^{M} \mathbf{D}_{i\,m}^{j(N;M)}(\hat{\mathbf{u}}_{N;M};p)\;\psi_1\Big(\sum_{n=1}^{N}\hat{\mathbf{u}}_{N;M\,n}(p)\,\zeta_n(\hat{x}_m^M);p\Big)\,\hat{\mathbf{u}}_{N;M\,j}(p) = \mathbf{F}_{N\,i}(p); \tag{4.42}$$

where $1 \le i \le N$ and $\mathbf{D}^{j(N;M)}(\hat{\mathbf{u}}_{N;M};p) = \mathbf{C}^{j(N;M)}(\hat{\mathbf{u}}_{N;M};p)(\mathbf{B}^M)^{-1} \in \mathbb{R}^{N\times M}$.

To solve (4.42) for $\hat{\mathbf{u}}_{N;M}(p)$, we apply a Newton's iterative scheme: starting with $\hat{\mathbf{u}}_{N;M}^{(0)}(p)$, for $z = 0,1,\ldots$ solve the linear system

$$\mathbf{J}_{N;M}(\hat{\mathbf{u}}_{N;M}^{(z)};p)\;\delta\hat{\mathbf{u}}_{N;M}^{(z)}(p) = \mathbf{R}_{N;M}(\hat{\mathbf{u}}_{N;M}^{(z)};p) \tag{4.43}$$

to obtain $\delta\hat{\mathbf{u}}_{N;M}^{(z)}(p)$, and then update the solution $\hat{\mathbf{u}}_{N;M}^{(z+1)}(p) := \hat{\mathbf{u}}_{N;M}^{(z)}(p) + \delta\hat{\mathbf{u}}_{N;M}^{(z)}(p)$. The residual $\mathbf{R}_N(p) \in \mathbb{R}^N$ for the Newton's scheme must be calculated at every Newton iteration according to

$$\mathbf{R}_{N;M\,i}(\hat{\mathbf{u}}_{N;M};p) = \mathbf{F}_{N\,i}(p) - \sum_{j=1}^{N}\sum_{m=1}^{M} \mathbf{D}_{i\,m}^{j(N;M)}(\hat{\mathbf{u}}_{N;M};p)\;\psi_1(\hat{u}_{N;M}(\hat{x}_m^M;p);p)\hat{\mathbf{u}}_{N;M\,j}(p). \tag{4.44}$$

Taking the derivative of (4.42) with respect to the components $\mathbf{u}_{N;M\,j}(p)$, $1 \le j \le N$, we derive the formula for the Jacobian matrix

$$\mathbf{J}_{N;M}(\hat{\mathbf{u}}_{N;M};p) := \mathbf{A}_{N;M}(\hat{\mathbf{u}}_{N;M};p) + \mathbf{E}_{N;M}(\hat{\mathbf{u}}_{N;M};p); \tag{4.45}$$

where $\mathbf{A}_{N;M}(\hat{\mathbf{u}}_{N;M};p) \in \mathbb{R}^{N\times N}$, $(\mathbf{A}_{N;M}(\hat{\mathbf{u}}_{N;M};p))_{ij} = a_M^1[\hat{u}_{N;M}(p)](\zeta_j,\zeta_i;p)$ and $\mathbf{E}_{N;M}(\hat{\mathbf{u}}_{N;M};p) \in \mathbb{R}^{N\times N}$ with

$$(\mathbf{E}_{N;M}(\hat{\mathbf{u}}_{N;M};p))_{ij} = \sum_{s=1}^{N}\hat{\mathbf{u}}_{N;M\,s}(p)\sum_{m=1}^{M}\mathbf{D}_{i\,m}^{s(N;M)}(\hat{\mathbf{u}}_{N;M};p)\frac{\partial}{\partial\mathbf{u}_{N;M\,j}}\psi_1(\hat{u}_{N;M}(\hat{x}_m^M;p);p); \tag{4.46}$$

where $1 \quad i; j \quad N$ and

$$\frac{@}{@\mathbf{u}_{N;M\ j}}\ {}_1(\hat{u}_{N;M}(\hat{x}_m^M; p); p) = \frac{g_m^j(p)\ {}_1^{0}(\hat{u}_{N;M}(\hat{x}_m^M; p); p)}{\mathrm{j}J_{\mathrm{T}}{}^T(\hat{x}_m^M; p)\,\mathrm{r}\,\hat{u}_{N;M}(\hat{x}_m^M; p)\mathrm{j}}; \tag{4.47}$$
$$g_m^j(p) = [J_{\mathrm{T}}{}^T(\hat{x}_m^M; p)\,\mathrm{r}\,\hat{u}_{N;M}(\hat{x}_m^M; p)] \quad [J_{\mathrm{T}}{}^T(\hat{x}_m^M; p)\,\mathrm{r}\ {}_j(\hat{x}_m^M)];$$

for $1 \quad m \quad M$.

The parameter separability of reduced nonlinear stiffness matrix $\mathbf{A}_{N;M}(\hat{\mathbf{u}}_{N;M}; p)$ and reduced load vector $\mathbf{F}_N(p)$ follows from (4.29) and (4.31), correspondingly

$$\mathbf{A}_{N;M}(\hat{\mathbf{u}}_{N;M}^{(z)}; p) = \sum_{m=1}^{M}\sum_{d=1}^{\mathrm{N}}\sum_{i;j=1}^{} {}'^{(z)}_m(p)\Phi^{i;j}_{d;L_1}(p)\mathbf{A}^{i;j}_{N;m;d}; \quad \mathbf{F}_N(p) = \sum_{q=1}^{Q_f} \Phi^f_q(p)\mathbf{F}_{N;q}; \tag{4.48}$$

where ${}'^{(z)}_m(p); 1 \quad m \quad M$ represent EIM coefficients of z-th Newton iteration and

$$\mathbf{A}^{i;j}_{N;m;d} = \mathbf{V}_N^T\mathbf{A}^{i;j}_{\mathrm{N};m;d}\mathbf{V}_N; \quad \mathbf{F}_{N;q} = \mathbf{V}_N^T\mathbf{F}_{\mathrm{N};q}; \tag{4.49}$$

where $(\mathbf{A}^{i;j}_{\mathrm{N};m;d})_{s_1 s_2} = a^{i;j}_{m;d}(\ {}_{s_2};\ {}_{s_1}); 1 \quad s1; s2 \quad \mathrm{N}$, $\mathbf{F}_{\mathrm{N};q} = f_q(\ {}_i); 1 \quad i \quad \mathrm{N}$ and $\mathbf{V}_N \in \mathrm{R}^{\mathrm{N}\ N}$ denotes the projection matrix, whose columns contain the coefficients of the RB basis functions ${}_n; 1 \quad n \quad N$, that is $(\mathbf{V}_N)_{in} = \hat{\mathbf{u}}_{\mathrm{N}\ i}(\bar{p}_n)$. Based on (4.30), we also have the following parameter separable matrices

$$\mathbf{C}_{N;m}(\hat{\mathbf{u}}_{N;M}; p) := \sum_{d=1}^{\mathrm{N}}\sum_{i;j=1}^{} \Phi^{i;j}_{d;L_1}(p)\mathbf{A}^{i;j}_{N;m;d}; \quad 1 \quad m \quad M. \tag{4.50}$$

We construct $\mathbf{C}^{j(N;M)}(\hat{\mathbf{u}}_{N;M}; p)$ out of the rows of (4.50) , hence $\mathbf{C}^{j(N;M)}(\hat{\mathbf{u}}_{N;M}; p)$ is parameter separable. Although (4.46) looks quite involved, it possesses an affine decomposition and allows efficient assembling in the online phase. Indeed, the matrix $\mathbf{D}^{j(N;M)}(\hat{\mathbf{u}}_{N;M}; p)$ is parameter separable, since the matrix $\mathbf{C}^{j(N;M)}(\hat{\mathbf{u}}_{N;M}; p)$ is parameter separable and the evaluation of $g^j \in \mathrm{R}^M$ in (4.47) requires the evaluation of the reduced-basis functions only on the set of interpolation points T_M. Therefore, these quantities can be computed and stored in the offline phase and can be assembled in the online phase independently of N and we have

$$\mathbf{J}_{N;M}(\hat{\mathbf{u}}_{N;M}; p) = \sum_{q=1}^{Q_J} {}^J_q(p)\mathbf{J}^q_{N;M}; \quad \mathbf{R}_{N;M}(\hat{\mathbf{u}}_{N;M}; p) = \sum_{q=1}^{Q_R} {}^R_q(p)\mathbf{R}^q_{N;M}; \tag{4.51}$$

where ${}^J_q(p) : \mathrm{D} \to \mathrm{R}$ and ${}^R_q(p) : \mathrm{D} \to \mathrm{R}$ are parameter-dependent functions, $\mathbf{J}^q_{N;M} \in \mathrm{R}^{N\ N}$ and $\mathbf{R}^q_{N;M} \in \mathrm{R}^N$ are parameter-independent matrices and vectors. We summarize the offline-online decomposition of Newton's method in the Algorithm 5. The operation count associated with each Newton's update is then as follows: the assembling of the residual $R_N(p)$ in (4.44) is achieved at cost $\mathrm{O}(4ML_1N^2 + N^2 + Q_fN)$ $\mathrm{O}(MN^2)$ together with the EIM system solve at cost $\mathrm{O}(M^2)$. The Jacobian $\mathbf{J}_{N;M}(\hat{\mathbf{u}}_{N;M}; p)$ in (4.45) is assembled at cost $\mathrm{O}(MN^3)$, i.e. it is the cost for the assembling of $\mathbf{E}_{N;M}(\hat{\mathbf{u}}_{N;M}; p)$. It is then inverted at cost $\mathrm{O}(N^3)$. The operation count in the online phase is thus $\mathrm{O}(MN^3)$ per Newton iteration. However, we observe in our numerical experiment that it is sufficient to use $\mathbf{A}_{N;M}(\hat{\mathbf{u}}_{N;M}; p)$ and drop $\mathbf{E}_{N;M}(\hat{\mathbf{u}}_{N;M}; p)$ term in (4.45) to perform well, which results in $\mathrm{O}(MN^2 + N^3)$ operations per Newton iteration.

Next we address the computation of the a-posteriori error bound (4.35). It requires the computation

Algorithm 5: RB Newton's method: Offline-Online decomposition

1 Offline phase:

Input: finite element mesh, projection matrix $\mathbf{V}_N$, interpolation space W_M.

Output: All parameter-independent quantities, saved in *Storage*.

1: Assemble $\mathbf{A}^{i;j}_{\mathrm{N};m;d}$ for $m = 1;:::;M;\ d = 1;:::;L_1;\ i;j = 1;2$:
2: Assemble $\mathbf{F}_{\mathrm{N};q}$ for $q = 1;:::;Q_f$:
3: Compute $\mathbf{A}^{i;j}_{N;m;d}$ for $m = 1;:::;M;\ d = 1;:::;L_1;\ i;j = 1;2$ and save to *Storage*.
4: Compute $\mathbf{F}_{N;q}$ for $q = 1;:::;Q_f$ and save to *Storage*.

2 Online phase:

Input: *Storage*, tolerance $"^{NM}_{tol} > 0$, interpolation matrix $\mathbf{B}^M$, interpolation points T_M, initial value $\hat{\mathbf{u}}^{(0)}_{N;M}$, parameter $p \in \mathrm{D}$.

Output: Reduced-basis solution $\hat{\mathbf{u}}_{N;M}(p)$.

1: Compute EIM coefficients $'^{(0)}_M(p) = \mathrm{f}'^{(0)}_{M\,k}(p)\mathrm{g}^M_{k=1}$
2: Assemble Jacobian $\mathbf{J}_{N;M}(\hat{\mathbf{u}}^{(0)}_{N;M};p)$ and residual $\mathbf{R}_{N;M}(\hat{\mathbf{u}}^{(0)}_{N;M};p)$
3: Compute $_{NM} := \mathrm{k}\mathbf{R}_{N;M}(\hat{\mathbf{u}}^{(0)}_{N;M};p)\mathrm{k}$
4: **while** $_{NM} > "^{NM}_{tol}$ **do**
5: Solve the linear system $\mathbf{J}_{N;M}(\hat{\mathbf{u}}^{(z)}_{N;M};p)\ \hat{\mathbf{u}}^{(z)}_{N;M}(p) = \mathbf{R}_{N;M}(\hat{\mathbf{u}}^{(z)}_{N;M};p)$
6: Update $\hat{\mathbf{u}}^{(z+1)}_{N;M}(p) := \hat{\mathbf{u}}^{(z)}_{N;M}(p) + \ \hat{\mathbf{u}}^{(z)}_{N;M}(p)$
7: Update EIM coefficients $'^{(z+1)}_M(p) = \mathrm{f}'^{(z+1)}_{M\,k}(p)\mathrm{g}^M_{k=1}$
8: Update Jacobian $\mathbf{J}_{N;M}(\hat{\mathbf{u}}^{(z+1)}_{N;M};p)$ and residual $\mathbf{R}^{(z+1)}_{N;M}(p)$
9: Compute $_{NM} := \mathrm{k}\mathbf{R}_{N;M}(\hat{\mathbf{u}}^{(z+1)}_{N;M};p)\mathrm{k}$
10: $z := z + 1$
11: **end while**
12: $\hat{\mathbf{u}}_{N;M}(p) := \hat{\mathbf{u}}^{(z)}_{N;M}(p)$

of the dual norm of the residual (4.34). Since the right-hand side $f(\,;p)$ and $a_M[\,](\,;\,;p)$ are parameter-separable, the residual $r_M(\,;p)$ is also parameter-separable and admits an affine decomposition together with its Riesz-representative $\hat{v}_r(p) \in \hat{V}_N$ according to

$$r_M(\hat{v}_N;p) = \sum_{q=1}^{Q_r} \Phi_q^r(p) r_{M\,q}(\hat{v}_N); \quad \hat{v}_r(p) = \sum_{q=1}^{Q_r} \Phi_q^r(\,)\hat{v}_{r\,q}; \tag{4.52}$$

where $r_M(\hat{v};p) = (\hat{v}_r(p);\hat{v}_N)_{\hat{V}}$ for all $\hat{v}_N \in \hat{V}_N$ and $Q_r = Q_f + N(M + 4ML_1 + 4L_2)$. Since the dual norm of the residual is equal to the norm of its Riesz representer, we have

$$\|r_M(\,;p)\|_{\hat{V}_N'} = \|\hat{v}_r(p)\|_{\hat{V}} = (\quad^r(p)^T \mathbf{G}_r \quad^r(p))^{1/2}; \tag{4.53}$$

where $\quad^r(p) = \{\Phi_q^r(p)\}_{q=1}^{Q_r} \in \mathbb{R}^{Q_r}$ and $\mathbf{G}_r \in \mathbb{R}^{Q_r \times Q_r}$ with $(\mathbf{G}_r)_{ij} = (\hat{v}_{r\,i};\hat{v}_{r\,j})_{\hat{V}}$ and the dual norm (4.53) is then computed at cost $O(Q_r^2)$. The evaluation of the norm $\|\hat{u}_{N;M}(p)\|_{\hat{V}}$ is at cost $O(N^2)$. Once $\quad_{LB}$ is available, the constants $C_1(p)$ and $C_2(p)$ in (4.35) are computed directly.

The EIM approximation error (4.36) is computed on the discretized domain $\hat{\Omega}_h \subset \hat{\Omega}$: the nonlinearity depends on the gradient and it is evaluated on the triangle barycenters $\hat{x}_{b_j}$, $1 \le j \le N_T$, where N_T is the total number of triangles in the iron material region for a given finite-element triangulation. The EIM procedure results in the set of triangle barycenter points $T_M = \{\hat{x}_{b_1}^M;\ldots;\hat{x}_{b_M}^M\}$, where $M << N_T$. In the offline phase we evaluate the gradients $\{\nabla_n\}_{n=1}^N$ for each basis element $\{\quad_n\}_{n=1}^N$ of the reduced-basis space $\hat{W}_N^u$ on the interpolation barycenters T_M. We thus store offline $\{\nabla_n|_{T_M}(\hat{x}_{b_j}^M)\}_{j=1}^M \in \mathbb{R}^{M^2}$ for $1 \le n \le N$ and then efficiently evaluate the nonlinearity on T_M with the ansatz $\nabla\hat{u}_{N;M}(p)_{T_M} = \sum_{j=1}^N \hat{u}_{N;M\,j}(p)\,\nabla_{j\,T_M}$ online. The operation count for the EIM approximation $\quad_1^M(\hat{u}_{N;M}(\hat{x};p);p)$ is then $O(M^2 + N_T M)$, and the evaluation of $\quad_1$ at M points. We note that (4.36) requires the knowledge of $\quad_1(\hat{u}_{N;M}(\hat{x};p);p)$ and thus one full evaluation of the nonlinearity.

Remark 19. *Given an approximation $\quad_1^M(\,;p)$, for $M \le M_{max} - 1$ we define*

$$\hat{\quad}_M(p) = |\quad_1(|J_T^T(\hat{x}_{M+1}^M;p)\nabla\hat{u}_{N;M}(\hat{x}_{M+1}^M;p)|) - \quad_1^M(|J_T^T(\hat{x}_{M+1}^M;p)\nabla\hat{u}_{N;M}(\hat{x}_{M+1}^M;p)|)|.$$

If $\quad_1(\,;p) < W_{M+1}$, we only have that $\quad_M(p) \le \hat{\quad}_M(p)$ for $p \in D$. However, if the effectivity $\frac{\hat{\quad}_M(p)}{\quad_M(p)}$ tends to 1 quickly with growing M, then $\hat{\quad}_M(p)$ can be used as a cheap one-point estimator for $\quad_M(p)$, which requires only one additional evaluation of $\quad_1(\,;p)$ at the $(M+1)$-th magic point [20]. In our case the nonlinearity is of the exponential type and the effectivity of the bound is of the order 10^2 in practice. However, we can think of using $\hat{\quad}_M(p)$ in other contexts, such as an adaptive optimization with surrogate models (see, e.g. [2]), where only the local parametric complexity of the nonlinearity around the certain parameter value $\bar{p}$ matters.

4.3 Numerical results

First we introduce a parameter set $D = [18;19] \times [4;5] \times [7;8]$. The nonlinear reluctivity function $\quad_1(p)$ is reconstructed from the real B – H measurements using cubic spline interpolation, see section 2.1.2. Finite element simulations are based on a mesh composed of 121012 triangles and 60285 nodes (excluding Dirichlet boundary nodes). Piecewise linear, continuous finite element functions are chosen for the finite element approximation. We solve the finite element problem with Newton's method. We

iterate unless the norm of the residual is less than the tolerance level, which we set to 10^{-4}. The tolerance level $\varepsilon_{tol}^{NM} = 10^{-5}$ is used for the RB Newton's method.

We generate the RB-EIM model as follows: we start from $\mathcal{D}_{train}^{EIM(1)} \subset \mathcal{D}$ (a regular $6 \times 6 \times 6$ grid over $\mathcal{D}$ of size 216) and compute finite element solutions for each parameter in $\mathcal{D}_{train}^{EIM(1)}$ to approximate the nonlinearity with the EIM within the prescribed tolerance $\varepsilon_{EIM} = 5 \cdot 10^{-1}$. Since the norm $\|\hat{u}_{N;M}(p)\|_{\hat{Y}}$ is of the order 10^{-2}, we hope to further balance the contributions of the reduced-basis and EI nonlinearity approximation in the estimator on the test set. Next we run the RB-Greedy procedure with the prescribed tolerance $\varepsilon_{RB} = 10^{-2}$ for the estimator (4.35) on $\mathcal{D}_{train} \subset \mathcal{D}$, where $\mathcal{D}_{train}$ is a regular $10 \times 10 \times 10$ grid over $\mathcal{D}$ of size 1000. We set $\varepsilon_{LB} = 110$, since

$$\varepsilon_{LB} \min_{\hat{x} \in \hat{\Omega}} \nu_1(|J_T^T(\hat{x}; p)\, r\hat{u}_{N;M}(\hat{x}; p)|) \approx 110 \tag{4.54}$$

for all $p \in \mathcal{D}_{train}$ in our setting. This is a robust heuristic procedure, since for small N, the reduced-basis solution $\hat{u}_{N;M}(\hat{x}; p)$ is a good approximation to $\hat{u}(\hat{x}; p)$ in the regions with low magnetic flux density $|r\hat{u}(\,\cdot\,; p)|$. The size of the magnet (change in the parameter p) influences only the high values of the magnetic flux density $|r\hat{u}_{N;M}(\,\cdot\,; p)|$ in the magnetic circuit and does not have an impact on the minimum of the reluctivity function. We note that the evaluation of $\nu_M(p)$ (4.36) requires one full evaluation of the nonlinearity, thus it is available for the computation in (4.54) for the a-posteriori error estimation.

Once the reduced-basis model is constructed ($N_{max} = 12; M_{max} = 50$), we use it to improve the quality of the nonlinearity approximation: we generate the reduced-basis solutions over $\mathcal{D}_{train}^{EIM(2)} := \mathcal{D}_{train}$ and use them to construct the improved EIM approximation space W_M of dimension $M_{max} = 50$. With the new approximation of the nonlinearity, we run the RB-Greedy procedure over $\mathcal{D}_{train}$ again with the prescribed tolerance $\varepsilon_{RB} = 10^{-2}$, which results in the reduced-basis space $\hat{W}_N^u$ of dimension $N_{max} = 10$.

Next we introduce a parameter test sample $\mathcal{D}_{test} \subset \mathcal{D}$ of size 343 ($7 \times 7 \times 7$ grid with uniformly random sampling on each interval) and verify the convergence with N of $\max \Delta_{N;M} = \max_{p \in \mathcal{D}_{test}} \Delta_{N;M}(p)$ for different values of M (see Fig.4.2(a)). We see that with $N = 8$ and $M = 50$ the estimator is below the prescribed tolerance $\varepsilon_{RB} = 10^{-2}$ on the test set. One observes that there is an increase in the estimator for $N \geq 8$ and for $M < 50$ due to the poor quality of the EIM approximation. Moreover, we can naturally split the estimator into two parts: the reduced-basis and the nonlinearity approximation error estimation contributions

$$\Delta_{N;M}^{RB}(p) := \frac{\|r_M(\,\cdot\,; p)\|_{\hat{Y}_N'}}{\varepsilon_{LB}\, C_1(p)}; \quad \Delta_{N;M}^{EI}(p) := \frac{C_2(p)\, \varepsilon_M(p)}{\varepsilon_{LB}\, C_1(p)} \|\hat{u}_{N;M}(p)\|_{\hat{Y}}. \tag{4.55}$$

We then set

$$\Delta_{N;M}^{RB} := \max_{p \in \mathcal{D}_{test}} \Delta_{N;M}^{RB}(p); \quad \Delta_{N;M}^{EI} := \max_{p \in \mathcal{D}_{test}} \Delta_{N;M}^{EI}(p). \tag{4.56}$$

The strategy is to balance two contributions in (4.56) for the specified tolerance level ε_{RB}, e.g. by choosing $N = 8$ and $M = 50$, see Fig.4.2(b). In Fig. 4.2(b) we can also see the improvement from the described above additional EIM step.

N	M	$\max \Delta_{N,M}$	$\bar{\Delta}_{N,M}(\mu)$	$\bar{\eta}_{N,M}$	$\max \eta_{N,M}$
4	30	1.24 E-01	4.74 E-02	7.41 E02	1.46 E03
6	40	4.59 E-02	2.37 E-02	3.98 E02	7.18 E02
8	45	9.30 E-03	5.10 E-03	2.46 E02	6.24 E02
8	50	8.90 E-03	5.51 E-03	2.49 E02	6.32 E02
10	50	8.90 E-03	5.30 E-03	8.48 E02	4.65 E03

Table 4.1: Performance of RB-EIM model on the test set

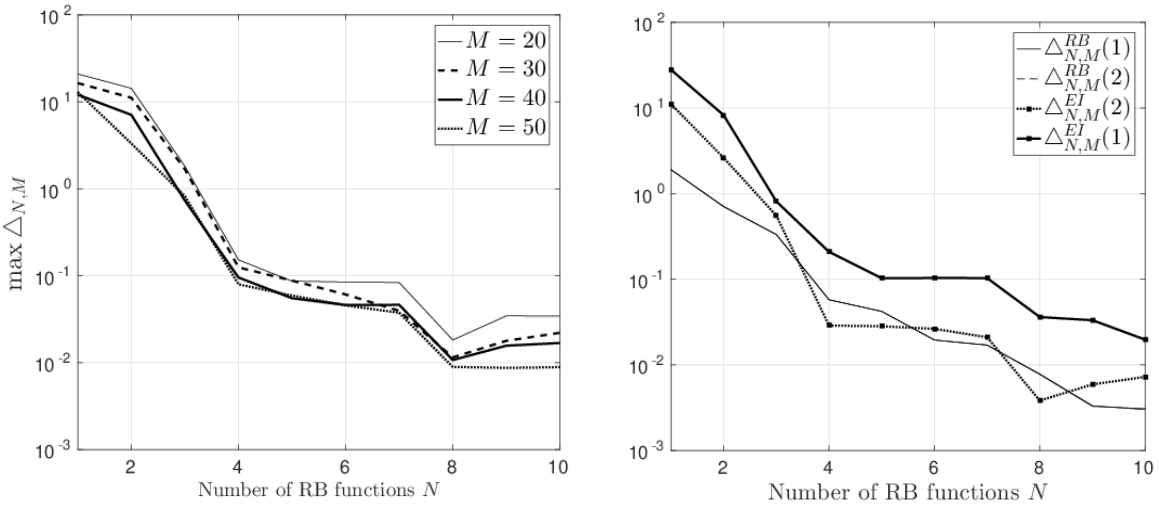

(a) (b)

Figure 4.2: Convergence with N of $\max \Delta_{N,M}$ for different values of M on the test set (a). Convergence with N of $\Delta^{RB}_{N,M}$ and $\Delta^{EI}_{N,M}$ contributions for $M = 50$ on the test set. The number in the label bracket indicates the EIM step (b).

In Table 4.1 we present, as a function of N and M, the maximum error bound $\max_{p \in \mathcal{D}_{test}} \Delta_{N,M}(p)$ as well as the mean $\bar{\eta}_{N,M}$ and max $\eta_{N,M}$ of the effectivity $\eta_{N,M}(p) := \frac{\Delta_{N,M}(p)}{\|e_{N,M}\|_{\hat{Y}}}$. The effectivities require the knowledge of "truth" solution, therefore we compute the finite element solutions for all the parameters in the test set. We observe that the values of $\bar{\eta}_{N,M}$ and max $\eta_{N,M}$ are quite large, which partially can be explained by the estimate (4.39) for the effectivity $\eta_N(p)$ of the reduced-basis approximation. In our example we have

$$\max_{\hat{x} \in \hat{\Omega}} \nu_1 (|J_T^T(\hat{x}; p) - \hat{u}_{N,M}(\hat{x}; p)|) \qquad \nu_0$$

on $\mathcal{D}_{test}$, where $\nu_0 \quad 7{:}95 \quad 10^5$ is the reluctivity of air. Therefore the upper-bound constant for $\eta_N(p)$ is of order 10^3 in practice.

In Fig. 4.3 we plot the reduced-basis solutions, i.e. the magnetic equipotential lines for several parameters in Fig. 4.3(a) and Fig. 4.3(b) and the corresponding reluctivity functions, evaluated fully with splines and with EIM in Fig 4.3(c) and Fig. 4.3(d). In Fig. 4.3(e) and Fig. 4.3(f) we zoom the reluctivity functions at some parts to see the inaccuracies of our EIM approximation. Next we compare the average CPU time required for both the finite element method, which takes 150 sec to obtain the

solution, and the RB method ($N_{max} = 10; M_{max} = 50$), which takes 0:27=0:95 sec without/with the error bound evaluation and results in the speedup factors of 555 and 158, respectively [1]. The computation of the error bound significantly increases the total CPU time, since the complexity of the error bound evaluation scales quadratically with Q_r, where Q_r is large and requires one full evaluation of the nonlinearity. The offline phase requires the knowledge of the "truth" finite-element solutions for the first EIM approximation step. Since 216 finite-element solutions were generated in the consecutive order, it takes 9 hours, but it can be done in parallel to reduced the computational time. The Greedy algorithm execution takes 4 hours and since we run it twice, it takes 8 hours for our implementation. We note that our implementation may not be optimal, therefore the offline time is only a rough estimate.

Remark 20. *We note that in the presented numerical example the relatively small parameter domain* D *was chosen. In the authors opinion, it is possible to enlarge the parameter domain with the increasing cost of the nonlinearity approximation by combining few additional EIM steps as described above and exploiting divide-and-conquer principles and hp-adaptivity in the Greedy procedure (see, e.g. [10, 47]).*

[1] All the computations are performed in MATLAB on Intel Xeon(R) CPU E5-1650 v3, 3.5 GHz x 12 cores, 64 GB RAM

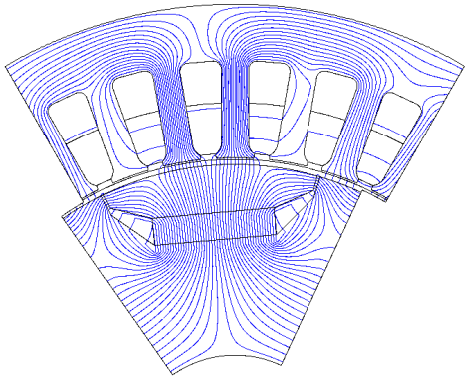

(a)

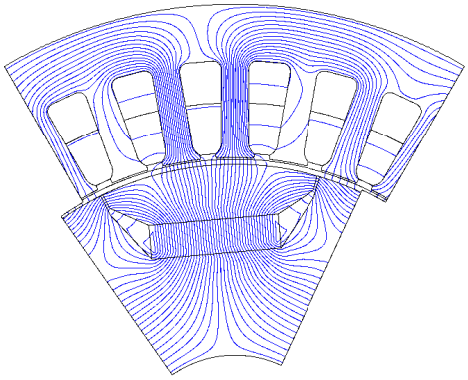

(b)

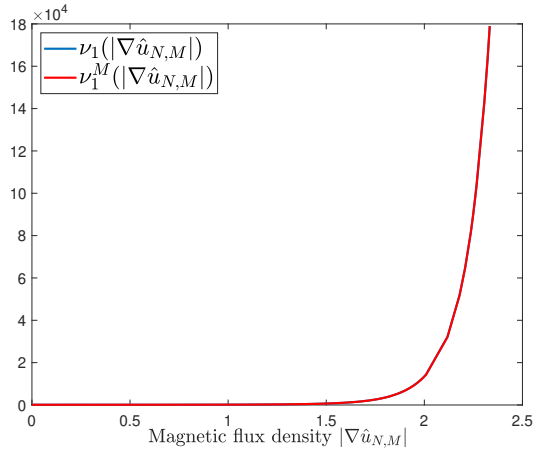

(c)

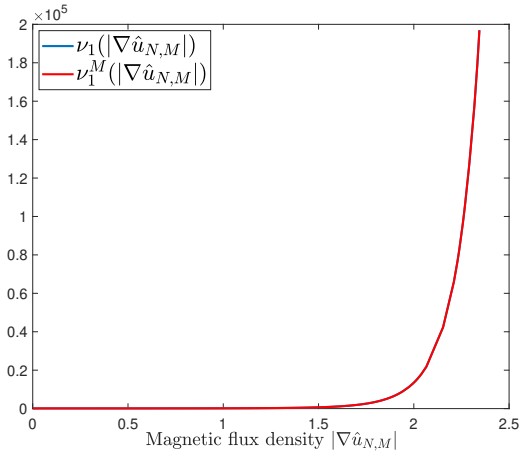

(d)

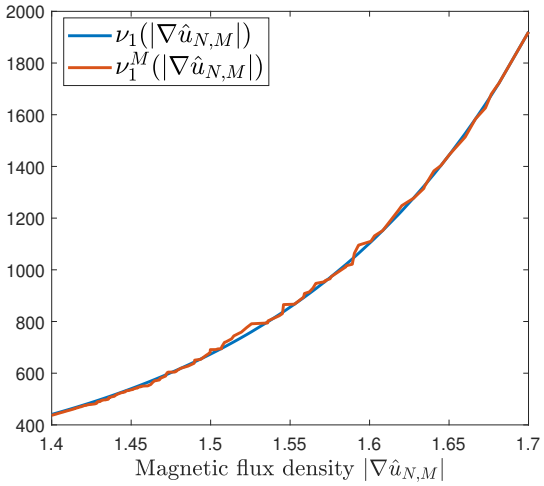

(e)

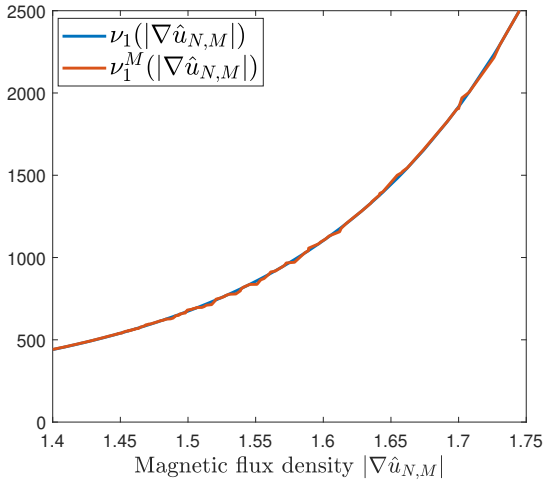

(f)

Figure 4.3: Magnetic equipotential lines, computed with reduced basis method (10 RB functions, 50 EIM basis functions) for parameter value (a) $p = (18; 4; 7)$, (b) $p = (19; 5; 8)$. Reluctivity function $_1(p)$, computed with full spline approximation and its EIM counterpart $^M_1(p)$ for parameter value (c) $p = (18; 4; 7)$, (d) $p = (19; 5; 8)$. Zoom of reluctivity functions at some parts for the parameter (e) $p = (18; 4; 7)$, (f) $p = (19; 5; 8)$.

Chapter 5

Reduced basis method for quasilinear parabolic PDEs and applications to magnetoquasistatics equation

In this chapter, we propose a certified reduced basis (RB) method for quasilinear parabolic problems. The method is based on a space-time variational formulation. We provide a residual-based a-posteriori error bound for a space-time formulation and the corresponding efficiently computable estimator for the certification of the method. We use the Empirical Interpolation method (EIM) to guarantee the efficient offline-online computational procedure. The error of the EIM method is then rigorously incorporated into the certification procedure. The Petrov-Galerkin finite element discretization allows to benefit from the Crank-Nicolson interpretation of the discrete problem and to use a POD-Greedy approach to construct the reduced-basis spaces of small dimensions. It computes the reduced basis solution in a time-marching framework while the RB approximation error in a space-time norm is controlled by the estimator. Therefore we combine a POD-Greedy approximation with a space-time Galerkin method.

5.1 Space-Time Truth Solution

In this section we consider a space-time variational formulation of quasilinear parabolic partial differential equations, which we denote as the *exact problem*. The corresponding discrete Petrov-Galerkin approximation is called the *truth* problem, as it is common in the RB setting. We assume that the solution to the exact problem can be approximated arbitrarily well by the discrete solution of the truth problem. We then neglect the corresponding approximation error.

5.1.1 Space-Time formulation

Let $\Omega \subset \mathbb{R}^d$ be the spatial domain and $\mu \in \mathcal{D} \subset \mathbb{R}^p$, where $\mathcal{D}$ is a compact parameter set. Let $V \subset H^1(\Omega)$ be a separable Hilbert space and $H := L^2(\Omega)$. We denote by $(\cdot,\cdot)_V$, $(\cdot,\cdot)_H$ and $\|\cdot\|_V$, $\|\cdot\|_H$ corresponding inner products and induced norms, respectively. To V and H we associate the Gelfand triple $V \hookrightarrow H \hookrightarrow V'$ with duality pairing $\langle\cdot,\cdot\rangle_{V'V}$. The norm of $l \in V'$ is defined by $\|l\|_{V'} := \sup_{v \in V, \|v\|_V \neq 0} \langle l, v\rangle_{V'V} / \|v\|_V$. We consider a parametrized quasilinear, bounded differential operator $A : V \times \mathcal{D} \to V'$ with induced

quasilinear form

$$\hbar A(u;\ );v\mathrm{i}_{V^0V} := a[u](u;v;\ ) = \int_\Omega (u(x);\ )\,\mathrm{r}\,u\quad \mathrm{r}\,v\,dx; \tag{5.1}$$

where the nonlinearity satisfies $(\ ;\ ) \in C^1(\mathrm{R})$. We assume that the forms (5.1) are strongly monotone on V with monotonicity constants $m_a(\ ) > 0$, i.e.

$$a[v](v;v\quad w;\ )\quad a[w](w;v\quad w;\ )\quad m_a(\ )\mathrm{k}v\quad w\mathrm{k}_V^2\quad \forall\, v;w \in V; \tag{5.2}$$

and Lipschitz continuous on V with Lipschitz constants $L_a(\ ) > 0$, i.e.

$$\mathrm{j}a[u](u;v;\ )\quad a[w](w;v;\ )\mathrm{j}\quad L_a(\ )\mathrm{k}u\quad w\mathrm{k}_V\mathrm{k}v\mathrm{k}_V\quad \forall\, u;w;v \in V. \tag{5.3}$$

In addition, we assume that these conditions hold uniformly:

$$m_a := \inf_{2\mathrm{D}} m_a(\ ) > 0;\quad L_a := \sup_{2\mathrm{D}} L_a(\ ) < 1: \tag{5.4}$$

For given $(g(\ ;\ );u_o) \in L^2(I;V^0)\quad H$ we consider the quasilinear parabolic initial value problem of finding $u(t) := u(t;\ ) \in V; t \in I$ a.e. on the time interval $I = (0;T]$, such that

$$\dot{u}(t) + A(u(t);\ ) = g(t) \text{ in } V^0;\ u(0) = u_o \text{ in } H; \tag{5.5}$$

where $\dot{u} := \frac{\partial u}{\partial t}$ is understood in the generalized sense. We now define a space-time variational formulation of (5.5). We use the trial space

$$\mathrm{X} := W(0;T) = L^2(I;V) \setminus H^1(I;V^0) = \{v \in L^2(I;V) : v;\dot{v} \in L^2(I;V^0)\}$$

with the norm $\mathrm{k}w\mathrm{k}_{\mathrm{X}}^2 := \mathrm{k}w\mathrm{k}_{L^2(I;V^0)}^2 + \mathrm{k}w\mathrm{k}_{L^2(I;V)}^2$, and the test space $\mathrm{Y} := L^2(I;V)\quad H$ with the norm $\mathrm{k}v\mathrm{k}_{\mathrm{Y}}^2 := \mathrm{k}v^{(1)}\mathrm{k}_{L^2(I;V)}^2 + \mathrm{k}v^{(2)}\mathrm{k}_H^2$ for $v := (v^{(1)};v^{(2)})$. The weak formulation of problem (5.5) reads: find $u := u(\ ) \in \mathrm{X}$ such that

$$B[u](u;v;\ ) = F(v;\ );\quad \forall\, v \in \mathrm{Y}; \tag{5.6}$$

where

$$B[u](u;v;\ ) := \int_I \hbar\dot{u};v^{(1)}\mathrm{i}_{V^0V} + a[u](u;v^{(1)};\ )dt + \hbar u(0);v^{(2)}\mathrm{i}_H;\ \text{and} \tag{5.7}$$

$$F(v;\ ) := \int_I \hbar g(\ );v^{(1)}\mathrm{i}_{V^0V}dt + \hbar u_o;v^{(2)}\mathrm{i}_H: \tag{5.8}$$

Since $\mathrm{X}\ ,!\ C(I;H)$, the initial value $u(0)$ is well-defined in H (see Proposition 2.2.1). We note that (5.2) implies coercivity of the quasilinear form $a[\ ](\ ;\ ;\ )$ and (5.3) implies hemicontinuity, i.e. the continuity of the mapping $s\ !\ \hbar A(u+sw;\ );v\mathrm{i}_{V^0V}$ for $s \in [0;1]$ and all $u;w;v \in V$. All together, the well-posedness of problem (5.6) follows, so that (5.6) admits a unique solution $u \in \mathrm{X}$, see Theorem 9.

5.1.2 Petrov-Galerkin Truth Approximation

From here onwards we omit the dependence on μ wherever appropriate. For the temporal discretization of (5.6) we use the time grid $0 = t^0 < t^1 < \ldots < t^K = T$ and set $I^k = (t^{k-1}; t^k]$ for $k = 1; \ldots; K$. We set $\Delta t^k = t^k - t^{k-1}$ and define $\Delta t := \max_{1 \le k \le K} \Delta t^k$. For the spatial discretization we set $V_h = \text{span}\{\zeta_1; \ldots; \zeta_{N_h}\} \subset V$, where $\dim V_h = N_h$ and h denotes the spatial discretization parameter. The functions ζ_i will be defined in the numerical examples. With $\Delta := (\Delta t; h)$ we introduce the discrete trial space

$$X_\Delta := \{u \in C^0(I; V);\ u|_{I^k} \in P_1(I^k; V_h);\ k = 1; \ldots; K\} \subset X$$

and the discrete test space

$$Y_\Delta := \{v \in L^2(I; V);\ v|_{I^k} \in P_0(I^k; V_h);\ k = 1; \ldots; K\} \quad V_h \subset Y:$$

With these choices of spaces the truth approximation problem reads: find $u_\Delta := u_\Delta(\cdot) \in X_\Delta$, such that $u_\Delta^0 := u_\Delta(0) = P_H^h u_o$ and

$$B[u_\Delta(\cdot)](u_\Delta; v; \cdot) = F(v; \cdot) \quad \forall v \in Y_\Delta; \tag{5.9}$$

where $P_H^h : H \to V_h$ denotes the H-orthogonal projection onto V_h. It follows as for (5.6) that problem (5.9) admits a unique solution $u_\Delta \in X_\Delta$.

The Petrov-Galerkin space-time discrete formulation (5.9) is approximated by the Crank-Nicolson time-stepping scheme. Indeed, since the test space Y_Δ consists of piecewise constant polynomials in time, the problem can be solved via the following procedure for $k = 1; \ldots; K$:

$$\int_{I^k} (\dot{u}_\Delta; v_h)_{V' V} + a[u_\Delta(\cdot)](u_\Delta; v_h; \cdot)\, dt = \int_{I^k} (g(\cdot); v_h)_{V' V}\, dt \quad \forall v_h \in V_h: \tag{5.10}$$

Since the trial space X_Δ consists of piecewise linear and continuous polynomials in time with the values $\hat{u}^k := u_\Delta(t^k)$ and $\hat{u}^{k-1} := u_\Delta(t^{k-1})$, we can represent u_Δ on I^k as the linear function

$$u_\Delta(t) = \frac{1}{\Delta t^k}\{(t^k - t)\hat{u}^{k-1} + (t - t^{k-1})\hat{u}^k\};\ t \in I^k: \tag{5.11}$$

We use the representation (5.11) in (5.10), test (5.10) against the basis functions $\zeta_i \in V_h$ $(i = 1; \ldots; N_h)$ and use the trapezoidal quadrature rule for the approximation of the appearing integrals. In this way we obtain the Crank-Nicolson time-stepping scheme, which for $k = 1; \ldots; K$ reads

$$\begin{aligned} &(u^k - u^{k-1}; \zeta_i)_H + \frac{\Delta t^k}{2}\{a[u^k](u^k; \zeta_i; \cdot) + a[u^{k-1}](u^{k-1}; \zeta_i; \cdot)\} = \\ &= \frac{\Delta t^k}{2}\{(g(t^k; \cdot); \zeta_i)_{V' V} + (g(t^{k-1}; \cdot); \zeta_i)_{V' V}\}; \quad 1 \le i \le N_h; \end{aligned} \tag{5.12}$$

where we consider u^k as our approximation of $\hat{u}^k$. Here we recall that the initial condition u^0 is obtained as an H-orthogonal projection of u_o onto V_h. Given the ansatz $u^k = \sum_{i=1}^{N_h} u_i^k \zeta_i$ and defining $\mathbf{u}^k := \{u_i^k\}_{i=1}^{N_h} \in \mathbb{R}^{N_h}$, the resulting nonlinear algebraic equations are then solved by applying Newton's method for finding

the root $\mathbf{u}^k$ of

$$\mathbf{G}_h(\mathbf{u}^k;\ ) := \frac{1}{\mathrm{M}\ t^k}\mathbf{M}_h(\mathbf{u}^k \quad \mathbf{u}^{k\ 1}) \quad \frac{1}{2}[\mathbf{g}_h^k(\ ) + \mathbf{g}_h^{k\ 1}(\ )] + \frac{1}{2}[\mathbf{A}_h(\mathbf{u}^k;\ )\mathbf{u}^k + \mathbf{A}_h(\mathbf{u}^{k\ 1};\ )\mathbf{u}^{k\ 1}]; \tag{5.13}$$

where $\mathbf{M}_h := \mathrm{f}h\ _i;\ _j\mathrm{i}_H\mathrm{g}_{i;j=1}^{N_h}$; $\mathbf{A}_h(\mathbf{u}^k;\ ) := \mathrm{f}a[u^k](\ _i;\ _j;\ )\mathrm{g}_{i;j=1}^{N_h}$ 2 $\mathrm{R}^{N_h\ N_h}$ and $\mathbf{g}_h^k(\ ) := \mathrm{f}hg(t^k;\ );\ _i\mathrm{i}_{V^0V}\mathrm{g}_{i=1}^{N_h}$ 2 R^{N_h}. The initial condition for (5.13) is given by $\mathbf{u}^0 := \mathrm{f}hu_o;\ _i\mathrm{i}_H\mathrm{g}_{i=1}^{N_h}$ 2 R^{N_h}. The strong monotonicity of the quasilinear form (5.2) guarantees that the equation (5.13) admits a unique root $\mathbf{u}^k$ for every parameter 2 D.

The Newton's iteration for finding a root of (5.13) reads: starting with $\mathbf{u}^{k;(0)}$, for $z = 0; 1; :::$ solve the linear system

$$\mathbf{J}_h(\mathbf{u}^{k;(z)};\ )\ \mathbf{u}^{k;(z)} = \ \mathbf{G}_h(\mathbf{u}^{k;(z)};\ ) \tag{5.14}$$

to obtain $\mathbf{u}^{k;(z)}$, and then update the solution $\mathbf{u}^{k;(z+1)} := \mathbf{u}^{k;(z)} + \mathbf{u}^{k;(z)}$. The system Jacobian matrix is given by

$$\mathbf{J}_h(\mathbf{u}^k;\ ) = \frac{1}{\mathrm{M}\ t^k}\mathbf{M}_h + \frac{1}{2}\mathbf{A}_h^0(\mathbf{u}^k;\ ); \tag{5.15}$$

where $\mathbf{A}_h^0(\mathbf{u}^k;\ ) := \mathrm{f}da[u^k](\ _i;\ _j;\ )\mathrm{g}_{i;j=1}^{N_h}$ 2 $\mathrm{R}^{N_h\ N_h}$. Here we assume the existence of the Fréchet derivative $A^0(u;\ ) : V \quad \mathsf{D} \ ! \ V^0$ of the nonlinear operator $A(u;\ )$ for every parameter 2 D, which induces the corresponding bilinear form $\mathrm{h}A^0(u;\ )v; w\mathrm{i}_{V^0V} = da[u](v; w;\ )$. We will specify it later for our examples. We note that $\mathbf{A}_h^0(\mathbf{u}^k;\ )$ is positive definite, since $da[u](\ ;\ ;\ )$ is coercive due to the strong monotonicity of A; therefore, the system (5.14) admits a unique solution.

5.2 The Reduced Basis method

In this section we introduce the reduced basis model and its numerical realization. Then we introduce our a-posteriori error estimate and discuss its efficient evaluation.

5.2.1 Empirical interpolation of the nonlinearity

We use the Empirical Interpolation Method (EIM) [5] to ensure the availability of an affine decomposition for the quasilinear form $a[u^k](\ ;\ ;\ )$ for every parameter 2 D. We then need to find a parameter-separable (affine) counterpart $_M(\ ;\ )$ of the nonlinear non-affine function $(\ ;\ )$. For EIM nonlinearity approximation, we treat time as an additional parameter in the problem, thus we set $\mathsf{I} := \mathrm{f}1; :::; K\mathrm{g}$ as our discrete time set. Given an EIM tolerance $_{EIM} > 0$ and a fine sample D_{train}^{EIM} D of size n_{train}^{EIM}, we construct with the Algorithm 6 the nested sample sets S_M D_{train}^{EIM} and I_M I, where $S_M := \mathrm{f}_1$ 2 $\mathsf{D}_{train}^{EIM}; :::;\ _M$ 2 $\mathsf{D}_{train}^{EIM}\mathrm{g}$ and $\mathsf{I}_M := \mathrm{f}k_1^M$ 2 $\mathsf{I}; :::; k_M^M$ 2 $\mathsf{I}\mathrm{g}$, and associated approximation spaces $W_M := \mathrm{span}\mathrm{f}\ (u^{k_m^M}(\ ;\ _m);\ _m); 1 \quad m \quad M\mathrm{g} = \mathrm{span}\mathrm{f}q_1; :::; q_M\mathrm{g}$. Algorithm 6 also provides the nested sets of interpolation points $T_M = \mathrm{f}x_1^M; :::; x_M^M\mathrm{g}$; $1 \quad M \quad M_{\max}$. We build an affine approximation $_M(u^k(x);\ )$

of $(u^k(x);\ )$ for our time-marching scheme according to

$$\begin{aligned} \mathcal{I}_M(u^k(x);\ ) &:= \sum_{m=1}^{M} \vartheta_m^k(\ )q_m(x) \\ &= \sum_{m=1}^{M} (\mathbf{B}_M^{-1}\ ^k)_m q_m(x) = \mathcal{I}(u^k(x);\ ) + \ ^k_M(x;\ ); \end{aligned} \tag{5.16}$$

where $^k_M(\ ;\ )$ is the EIM approximation error: it holds $\varepsilon_M(\ ) := \max_k \|\ ^k_M(\ ;\ )\|_{L^1(\Omega)} < \varepsilon_{EIM}$ for all $k \in \mathcal{I}$, $\in \mathcal{D}^{EIM}_{train}$. In (5.16) we also have $^k := \{\mathcal{I}(u^k(x_m^M);\ )\}_{m=1}^M \in \mathbb{R}^M$ and $\mathbf{B}_M \in \mathbb{R}^{M\ M}$ is the lower triangular interpolation matrix $(\mathbf{B}_M)_{ij} = q_j(x_i)$ with $(\mathbf{B}_M)_{ii} = 1$ $(i = 1, \ldots, M)$ by construction.

Algorithm 6: : EIM algorithm

Input: Tolerance ε_{EIM}, max. number of iterations $M_{\max}$, parameter set $\mathcal{D}^{EIM}_{train}$.

Output: Nested approximation spaces $\{W_m\}_{m=1}^M$, nested interpolation points $\{T_m\}_{m=1}^M$.

$(\ _1; k_1^M) := \underset{(\ ;k)\in\mathcal{D}^{EIM}_{train}\ \mathcal{I}}{\arg\max}\ \|\mathcal{I}(u^k(\ );\ )\|_{L^1(\Omega)}$
$S_1 \quad \mathcal{I}_1 := \{\ _1\} \quad \{k_1^M\}$
$r_1(x) := \mathcal{I}(u^{k_m^M}(x;\ _m);\ _m)$
$x_1^M := \arg\max_{x\in\Omega} |r_1(x)|; \quad q_1 := r_1 / r_1(x_1^M)$
$T_1 := \{x_1^M\}; \quad Q_1 := \{q_1\}; \quad W_1 := \mathrm{span}(Q_1)$
while $2 \quad m \quad M_{\max}$ and $\varepsilon_m^{max} > \varepsilon_{EIM}$ **do**
  $(\ _m; k_m^M) := \underset{(\ ;k)\in\mathcal{D}^{EIM}_{train}\ \mathcal{I}}{\arg\max}\ \|\mathcal{I}(u^k(\ );\ ) \quad \mathcal{I}_m(u^k(\ );\ )\|_{L^1(\Omega)}$
  $\varepsilon_m^{max} := \underset{(\ ;k)\in\mathcal{D}^{EIM}_{train}\ \mathcal{I}}{\max}\ \|\mathcal{I}(u^k(\ );\ ) \quad \mathcal{I}_m(u^k(\ );\ )\|_{L^1(\Omega)}$
  $S_m := S_{m\ 1} \cup \{\ _m\}; \quad \mathcal{I}_m := \mathcal{I}_{m\ 1} \cup \{k_m^M\}$
  $r_m(x) := \mathcal{I}(u^{k_m^M}(x;\ _m);\ _m) \quad \mathcal{I}_m(u^{k_m^M}(x;\ _m);\ _m)$
  $x_m^M := \arg\max_{x\in\Omega} |r_m(x)|; \quad q_m := r_m / r_m(x_m^M)$
  $T_m := T_{m\ 1} \cup \{x_m^M\}; \quad Q_m := Q_{m\ 1} \cup \{q_m\}; \quad W_m := \mathrm{span}(Q_m)$
  $m \quad m+1$
end while

We then have the EIM approximation $\tilde{a}[\ ](\ ;\ ;\ )$ of the quasilinear form $a[\ ](\ ;\ ;\ )$, which admits the affine decomposition

$$\tilde{a}[u^k](u^k; v;\ ) = \sum_{m=1}^{M} \vartheta_m^k(\ )\tilde{a}_m(u^k; v), \quad \tilde{a}_m(u^k; v) = \int_\Omega q_m\, \mathrm{r}\, u^k \quad \mathrm{r}\, v\, dx. \tag{5.17}$$

For mathematical convenience, we assume that the EIM approximation $\tilde{a}[\ ](\ ;\ ;\ )$ is sufficiently accurate in the sense that the form $\tilde{a}[\ ](\ ;\ ;\ )$ is strongly monotone on V_h with monotonicity constant $\tilde{m}_a(\ ) := m_a(\ ) \quad _a > 0$, i.e., for all $v_h; w_h \in V_h$ it holds

$$\tilde{a}[v_h](v_h; v_h \quad w_h;\ ) \quad \tilde{a}[w_h](w_h; v_h \quad w_h;\ ) \quad \tilde{m}_a(\ )\|v_h \quad w_h\|_V^2; \tag{5.18}$$

and Lipschitz continuous on V_h with Lipschitz constants $\tilde{L}_a(\ ) := L_a(\ ) \quad _a > 0$, i.e., for all $u_h; w_h; v_h \in$

V_h it holds

$$|\tilde{a}[u_h](u_h, v_h; \mu) - \tilde{a}[w_h](w_h, v_h; \mu)| \leq \tilde{L}_a(\mu)\|u_h - w_h\|_V \|v_h\|_V, \tag{5.19}$$

where $\varepsilon_a \in \mathbb{R}_+$ is small enough and is related to the EIM approximation error. However, in the EIM practice we can guarantee that conditions (5.18) and (5.19) hold uniformly together with $\varepsilon_a < \varepsilon_{EIM}$ only on $\mathcal{D}_{train}^{EIM}$. It is difficult to check these properties a-priori for $\mu \in \mathcal{D} \cap \mathcal{D}_{train}^{EIM}$, so that arguing the well-posedness of the upcoming discrete systems (5.23) and (5.24) in general is not possible.

We also assume the affine decomposition

$$\langle g(t^k; \mu), v\rangle_{V' V} = \sum_{q=1}^{Q_g} \theta_{g,q}^k(\mu) \langle g_q, v\rangle_{V' V} \tag{5.20}$$

for the right-hand side, where $\theta_{g,q}^k : \mathcal{D} \to \mathbb{R}$ are parameter-dependent functions and parameter-independent forms $g_q : V \to \mathbb{R}$, $k = 1, \ldots, K$, $q = 1, \ldots, Q_g$. If (5.20) is not available, the EIM procedure can be similarly applied.

5.2.2 Reduced basis approximation with the POD-Greedy method

The idea of the reduced-basis approximation consists in replacing the "truth" (high-dimensional) space V_h in the definition of $\mathcal{X}$ and $\mathcal{Y}$ by a low-dimensional subspace $V_N \subset V_h$. With V_N available we introduce the corresponding reduced trial space

$$\mathcal{X}_{4t,N} := \{u_N \in C^0(I; V);\ u_N|_{I^k} \in \mathbb{P}_1(I^k; V_N),\ k = 1, \ldots, K\}$$

and the reduced test space

$$\mathcal{Y}_{4t,N} := \{v_N \in L^2(I; V);\ v_N|_{I^k} \in \mathbb{P}_0(I^k; V_N),\ k = 1, \ldots, K\} \subset V_N.$$

We construct $V_N := \text{span}\{\zeta_1, \ldots, \zeta_N\} \subset V_h$ by the POD-Greedy procedure in Algorithm 3, compare e.g. [22]. We denote by $\mathcal{D}_{train} \subset \mathcal{D}$ a fine sample of size n_{train}. In our setting, the POD-Greedy alogorithm constructs iteratively nested spaces V_n, $1 \leq n \leq N$ using an a-posteriori error estimator $\Delta(Y; \mu)$ (see the next section for details on a-posteriori error analysis), which predicts the expected approximation error for a given parameter $\mu \in \mathcal{D}_{train}$ in the space $Y := \mathcal{Y}_{4t,n}$. We want the expected approximation error to be less than the prescribed tolerance $\varepsilon_{RB} > 0$. We initiate the algorithm with the choice of the initial basis vector $\zeta_1 := u^0/\|u^0\|_V$; this choice is motivated by the assumption in Proposition 5.2.1. The snapshots $u^k(\mu)$ for the procedure are provided by the Crank-Nicolson scheme (5.12).

The reduced-basis approximation of problem (5.9) reads: find $u_N := u_N(\mu) \in \mathcal{X}_{4t,N}$, such that $u_N^0 := u_N(0) = P_H^N u_o$ and

$$\tilde{B}[u_N](u_N, v_N; \mu) = \tilde{F}(v_N; \mu) \quad \forall v_N \in \mathcal{Y}_{4t,N}, \tag{5.21}$$

where

$$\tilde{B}[u_N](u_N; v_N; \quad) = \int_I \langle \dot{u}_N; v_N^{(1)} \rangle_{V^0 V} + \tilde{a}[u_N](u_N; v_N^{(1)}; \quad) dt + \langle P_H^N u_o; v_N^{(2)} \rangle_H;$$
$$\tilde{F}(v_N; \quad) := \int_I \langle g(\quad); v_N^{(1)} \rangle_{V^0 V} dt + \langle u^0; v_N^{(2)} \rangle_H;$$

and $P_H^N : V_h \to V_N$ denotes the H-orthogonal projection onto V_N. It follows as for (5.6) from our assumptions (5.18) and (5.19) that the problem (5.21) admits a unique solution $u_N(\quad) \in X_{4t;N}$ for all $\in D$.

The problem (5.21) is approximated by the reduced-basis Crank-Nicolson time-marching scheme with the EIM approximation of the nonlinearity, i.e.

$$\langle u_N^k \quad u_N^{k-1}; v_N^{(1)} \rangle_H + \frac{\Delta t^k}{2} \{ \tilde{a}[u_N^k](u_N^k; v_N^{(1)}; \quad) + \tilde{a}[u_N^{k-1}](u_N^{k-1}; v_N^{(1)}; \quad) \} \tag{5.22}$$
$$= \frac{\Delta t^k}{2} \{ \langle g(t^k; \quad); v_N^{(1)} \rangle_{V^0 V} + \langle g(t^{k-1}; \quad); v_N^{(1)} \rangle_{V^0 V} \};$$

where the initial condition u_N^0 is obtained as an H-projection of u^0 onto V_N. Given the ansatz $u_N^k = \sum_{i=1}^N u_{N;i}^k \, \zeta_i$ and defining $\mathbf{u}_N^k := \{u_{N;i}^k\}_{i=1}^N \in \mathbb{R}^N$, the resulting nonlinear algebraic equations are then solved with the RB counterpart of Newton's method by finding the root of

$$\mathbf{G}_{N;M}(\mathbf{u}_N^k; \quad) = \frac{1}{\Delta t^k} \mathbf{M}_N (\mathbf{u}_N^k \quad \mathbf{u}_N^{k-1}) \quad \frac{1}{2} [\mathbf{g}_N^k(\quad) + \mathbf{g}_N^{k-1}(\quad)] \tag{5.23}$$
$$+ \frac{1}{2} [\mathbf{A}_{N;M}(\mathbf{u}_N^k; \quad) \mathbf{u}_N^k + \mathbf{A}_{N;M}(\mathbf{u}_N^{k-1}; \quad) \mathbf{u}_N^{k-1}];$$

where $\mathbf{M}_N := \{\langle \zeta_i; \zeta_j \rangle_H\}_{i;j=1}^N$; $\mathbf{A}_{N;M}(\mathbf{u}_N^k; \quad) := \{\tilde{a}[u_N^k](\zeta_i; \zeta_j; \quad)\}_{i;j=1}^N \in \mathbb{R}^{N \times N}$ and $\mathbf{g}_N^k(\quad) := \{\langle g(t^k; \quad); \zeta_i \rangle_{V^0 V}\}_{i=1}^N \in \mathbb{R}^N$. The initial condition is given by $\mathbf{u}_N^0 := \{\langle u^0; \zeta_i \rangle_H\}_{i=1}^N \in \mathbb{R}^N$. The strong monotonicity (5.18) of the quasilinear form (5.17) guarantees that the equation (5.23) admits a unique root $\mathbf{u}_N^k$ for every parameter $\in D$. We remind that the strong monotonicity property (5.18) is based on the assumption about the accuracy of EIM.

The Newton's iteration for finding a root of (5.23) reads: starting with $\mathbf{u}_N^{k;(0)}$, for $z = 0; 1; \ldots$ solve the linear system

$$\mathbf{J}_{N;M}(\mathbf{u}_N^{k;(z)}; \quad) \quad \mathbf{u}_N^{k;(z)} = \quad \mathbf{G}_{N;M}(\mathbf{u}_N^{k;(z)}; \quad) \tag{5.24}$$

to obtain $\mathbf{u}_N^{k;(z)}$, and then update the solution $\mathbf{u}_N^{k;(z+1)} := \mathbf{u}_N^{k;(z)} + \mathbf{u}_N^{k;(z)}$. The system Jacobian matrix is given by

$$\mathbf{J}_{N;M}(\mathbf{u}_N^k; \quad) = \frac{1}{\Delta t^k} \mathbf{M}_N + \frac{1}{2} \mathbf{A}'_{N;M}(\mathbf{u}_N^k; \quad). \tag{5.25}$$

If the mapping $\mapsto \mathbf{A}'_{N;M}(\,;\,)$ is bounded in $\in D$, then for $\Delta t^k \quad C(D)$, where $C(D) > 0$ is some constant, the Jacobian matrix (5.25) is invertible. We will comment on the computation of the reduced basis counterpart $\mathbf{A}'_{N;M}(\mathbf{u}_N^k; \quad) := \{d\tilde{a}[u_N^k](\zeta_i; \zeta_j; \quad)\}_{i;j=1}^N \in \mathbb{R}^{N \times N}$ of $\mathbf{A}'_h(\mathbf{u}^k; \quad)$ in (5.25). We have

$$\tilde{a}[u_N^k](u_N; \zeta_i; \quad) = \sum_{j=1}^{M} \sum_{m=1}^{M} \theta_m^k(\quad) \tilde{a}_m(\zeta_j; \zeta_i) u_{N;j}^k; \quad 1 \quad i \quad N: \tag{5.26}$$

With the EIM approximation of the nonlinearity it follows that

$$\sum_{s=1}^{M} (\mathbf{B}_M)_{m;s}\, \varphi^k_s(\mu) = (u^k_N(x^M_m;\mu);\mu); \quad 1 \le m \le M \tag{5.27}$$
$$= \Big(\sum_{n=1}^{M} u^k_{N;n}\, \psi_n(x^M_m);\mu\Big); \quad 1 \le m \le M.$$

Plugging (5.27) into (5.26) results in

$$\tilde{a}[u^k_N](u_N, \psi_i;\mu) = \sum_{j=1}^{N}\sum_{m=1}^{M} \mathbf{D}^{N;M}_{i;m}(\mathbf{u}^k_N;\mu)\Big(\sum_{n=1}^{M} u^k_{N;n}\,\psi_n(x^M_m);\mu\Big) u^k_{N;j} \tag{5.28}$$

with $\mathbf{D}^{N;M}(\mathbf{u}^k_N;\mu) = \mathbf{A}_{N;M}(\mathbf{u}^k_N;\mu)(\mathbf{B}_M)^{-1} \in \mathbb{R}^{N\times M}$. Taking the derivative of (5.28) with respect to the components $u^k_{N;j}(\mu)$, $1 \le j \le N$, we derive the formula for $\mathbf{A}^0_{N;M}(\mathbf{u}^k_N;\mu) = \mathbf{A}_{N;M}(\mathbf{u}^k_N;\mu) + \mathbf{E}_{N;M}(\mathbf{u}^k_N;\mu)$, where

$$(\mathbf{E}_{N;M}(\mathbf{u}^k_N;\mu))_{ij} = \sum_{s=1}^{N} u^k_{N;s} \sum_{m=1}^{M} \mathbf{D}^{N;M}_{i;m}(\mu)\frac{\partial}{\partial u^k_{N;j}}(u^k_N(x^M_m);\mu) \tag{5.29}$$

We will give the exact form of $\frac{\partial}{\partial u^k_{N;j}}(u^k_N(x^M_m);\mu)$ in the upcoming examples. We note that a more complicated formula for (5.29) can be obtained in the presence of geometry parametrisation, see section 4.2.3.

The parameter separability of reduced nonlinear stiffness matrix $\mathbf{A}_{N;M}(\mathbf{u}^k_N;\mu)$ and reduced load vector $\mathbf{g}^k_N(\mu)$ follows from (5.17) and (5.20), correspondingly

$$\mathbf{A}_{N;M}(\mathbf{u}^{k;(z)}_N;\mu) = \sum_{m=1}^{M} \varphi^{k;(z)}_m(\mu)\mathbf{A}^m_{N;M}; \quad \mathbf{g}^k_N(\mu) = \sum_{q=1}^{Q_g} \theta^k_{g;q}(\mu)\mathbf{g}^q_N. \tag{5.30}$$

where $\varphi^{k;(z)}_m(\mu); 1 \le m \le M$ represent EIM coefficients of z-th Newton iteration and

$$\mathbf{A}^m_{N;M} = \mathbf{V}^T_N \mathbf{A}^m_h \mathbf{V}_N; \quad \mathbf{g}^q_N = \mathbf{V}^T_N \mathbf{g}^q_h; \tag{5.31}$$

where $\mathbf{A}^m_h := \{\tilde{a}_m(\psi_j, \psi_i)\}^{\mathcal{N}_h}_{i;j=1} \in \mathbb{R}^{\mathcal{N}_h\times\mathcal{N}_h}$, $\mathbf{g}^q_h := \{h_q; \psi_i\}_{V'V}\}^{\mathcal{N}_h}_{i=1} \in \mathbb{R}^{\mathcal{N}_h}$ and $\mathbf{V}_N \in \mathbb{R}^{\mathcal{N}_h\times N}$ denotes the projection matrix, whose columns contain the coefficients $\{\xi^n_i\}^{\mathcal{N}_h}_{i=1}$ of the RB basis functions $\psi_n = \sum_{i=1}^{\mathcal{N}_h} \xi^n_i \psi_i; 1 \le n \le N$, that is $(\mathbf{V}_N)_{in} = \xi^n_i$. The formula (5.29) possesses an affine decomposition and allows efficient assembling in the online phase: indeed, the matrix $\mathbf{D}^{N;M}(\mu)$ is parameter separable, since $\mathbf{A}_{N;M}(\mathbf{u}^k_N;\mu)$ is parameter separable and the evaluation of nonlinearity in (5.29) requires the evaluation of the reduced-basis functions only on the set of interpolation points T_M. Therefore, these quantities can be computed and stored in the offline phase and can be assembled in the online phase independently of $\mathcal{N}_h$ and we have

$$\mathbf{J}_{N;M}(\mathbf{u}_N;\mu) = \sum_{q=1}^{Q_J} \theta^J_q(\mu)\mathbf{J}^q_{N;M}; \quad \mathbf{G}_{N;M}(\mathbf{u}_N;\mu) = \sum_{q=1}^{Q_G} \theta^G_q(\mu)\mathbf{G}^q_{N;M}; \tag{5.32}$$

where $\theta^J_q(\mu) : \mathcal{D} \to \mathbb{R}$ and $\theta^G_q(\mu) : \mathcal{D} \to \mathbb{R}$ are parameter-dependent functions, $\mathbf{J}^q_{N;M} \in \mathbb{R}^{N\times N}$ and $\mathbf{G}^q_{N;M} \in \mathbb{R}^N$ are parameter-independent matrices and vectors. The proposed reduced numerical scheme

(see also Algorithm 7) contains parameter separable matrices and thus allows offline-online decomposition. The offline phase (model construction) depends on expensive high-dimensional finite element simulations and thus on N, but should be performed only once. However, the assembling of all the high-dimensional parameter-dependent quantities is computationally simplified due to the affine dependence on the parameters (5.30). In the online phase (RB model simulation) the computational complexity scales polynomially in N and M, independently of N_h and thus is inexpensive. The operation count associated

Algorithm 7: Reduced-basis Crank-Nicolson scheme for nonlinear problem: Offline-Online decomposition

1 Offline phase:

Input: finite element mesh, projection matrix $\mathbf{V}_N$, interpolation space W_M.
Output: All parameter-independent quantities, saved in *Storage*.

1: Assemble $\mathbf{A}_h^m$ for $m = 1, \ldots, M$:
2: Assemble $\mathbf{g}_h^q$ for $q = 1, \ldots, Q_g$:
3: Compute $\mathbf{A}_{N;M}^m$ for $m = 1, \ldots, M$ and save to *Storage*.
4: Compute $\mathbf{g}_N^q$ for $q = 1, \ldots, Q_g$ and save to *Storage*.

2 Online phase:

Input: *Storage*, tolerance $\varepsilon_{tol}^{NM} > 0$, interpolation matrix $\mathbf{B}_M$, interpolation points T_M, initial value $\mathbf{u}_N^0$, parameter $\mu \in \mathcal{D}$.
Output: Reduced-basis solution $\hat{\mathbf{u}}_{N;M}(\mu)$.

1: Set $k = 1$
2: **while** $k \le K$ **do**
3: Choose $\mathbf{u}_N^{k;(0)} = \mathbf{u}_N^{k-1}$.
4: Compute EIM coefficients $\psi_M^{k;(0)}(\mu) = \left(\psi_m^{k;(0)}(\mu)\right)_{m=1}^M$.
5: Assemble Jacobian $\mathbf{J}_{N;M}(\mathbf{u}_N^{k;(0)}; \mu)$ and residual $\mathbf{G}_{N;M}(\mathbf{u}_N^{k;(0)}; \mu)$.
6: Compute $\varepsilon_{NM} := \|\mathbf{G}_{N;M}(\mathbf{u}_N^{k;(0)}; \mu)\|$
7: **while** $\varepsilon_{NM} > \varepsilon_{tol}^{NM}$ **do**
8: Solve the linear system $\mathbf{J}_{N;M}(\mathbf{u}_N^{k;(z)}; \mu)\, \delta\mathbf{u}_N^{k;(z)} = -\mathbf{G}_{N;M}(\mathbf{u}_N^{k;(z)}; \mu)$
9: Update $\mathbf{u}_N^{k;(z+1)} := \mathbf{u}_N^{k;(z)} + \delta\mathbf{u}_N^{k;(z)}$
10: Update EIM coefficients $\psi_M^{k;(z+1)}(\mu) = \left(\psi_m^{k;(z+1)}(\mu)\right)_{m=1}^M$.
11: Update Jacobian $\mathbf{J}_{N;M}(\mathbf{u}_N^{k;(z+1)}; \mu)$ and residual $\mathbf{G}_{N;M}(\mathbf{u}_N^{k;(z+1)}; \mu)$.
12: Compute $\varepsilon_{NM} := \|\mathbf{G}_{N;M}(\mathbf{u}_N^{k;(z+1)}; \mu)\|$
13: $z := z + 1$
14: **end while**
15: $\mathbf{u}_N^k := \mathbf{u}_N^{k;(z)}$
16: **end while**

with each Newton update of the residual $\mathbf{G}_{N;M}(\mathbf{u}_N^{k;(z)})$ in the online phase is $O(N^2M + N^2 + M^2 + NQ_{f_o})$ and the Jacobian $\mathbf{J}_{N;M}(\mathbf{u}_{N;M}^{k;(z)}; \mu)$ is assembled at cost $O(MN^3)$ with the dominant cost of assembling $\mathbf{E}_{N;M}(\mathbf{u}_N^k; \mu)$, and then inverted at cost $O(N^3)$.

5.2.3 Reduced basis certification

An important ingredient of the reduced basis methodology is the verification of the error (certification of the reduced basis method). In the present work we provide a residual-based a-posteriori error estimate.

We denote by $R(\,;\,) \in Y'$ the residual of the problem, defined naturally as:

$$R(v\,;\,) := F(v\,;\,) \quad \tilde{B}[u_N](u_N; v\,;\,) = \int_I \langle r(t;\,); v \rangle_{V'V} dt \quad \forall v \in Y : \tag{5.33}$$

We have the following

Proposition 5.2.1 (A-posteriori Error Estimate)**.** *Let $m_a(\,) > 0$ be a monotonicity constant from* (5.2) *and assume that $u^0 \in V_N$. Then the error $e(\,) = u(\,) - u_N(\,)$ of the reduced basis approximation is bounded by*

$$\|e(\,)\|_Y \leq \frac{1}{m_a(\,)} (\|R(\,;\,)\|_{Y'} + \varepsilon_M(\,)\|u_N(\,)\|_{L^2(I;V)}) =: \Delta^c_{N;M}(\,); \tag{5.34}$$

where

$$\varepsilon_M(\,) = \sup_{t \in I} \sup_{x \in \Omega} |\,\rho_M(u_N(x;t);\,) \quad (u_N(x;t);\,)| \tag{5.35}$$

denotes the approximation error of the nonlinearity.

Proof. Since in the case $e = 0$ there is nothing to show, we assume that $e \neq 0$. We have $u^0 \in V_N$ and $P^N_{H\ V_N} = Id$, therefore $u^0_N := P^N_H u^0 = u^0$. It implies that $\|e(0)\|_H = 0$, $\|e\|_Y = \|e\|_{L^2(I;V)}$ and $\|R(\,;\,)\|_{Y'} = \|R(\,;\,)\|_{L^2(I;V'_h)}$. First we obtain the following estimate by applying Cauchy-Schwartz inequality:

$$\begin{aligned} \tilde{a}[u_N](u_N; e;\,) \quad a[u_N](u_N; e;\,) &= \int_\Omega [\,\rho_M(u_N;\,) \quad (u_N;\,)]\, \nabla u_N \quad \nabla e\, dx \\ &\leq \sup_{x \in \Omega} |\,\rho_M(u_N(x;\,);\,) \quad (u_N(x;\,);\,)|\, \|u_N\|_V \|e\|_V : \end{aligned} \tag{5.36}$$

Integrating (5.36) in t and applying the Cauchy-Schwartz inequality to the corresponding integral we get:

$$\int_I \tilde{a}[u_N](u_N; e;\,) \quad a[u_N](u_N; e;\,) dt \leq \varepsilon_M(\,)\|u_N\|_{L^2(I;V)} \|e\|_Y :$$

We then use the identity

$$\int_I \langle \dot{e}; e \rangle_{V'V} dt = \frac{1}{2}\|e(T)\|^2_H \quad \frac{1}{2}\|e(0)\|^2_H \tag{5.37}$$

together with the strong monotonicity condition (5.2) and the estimate above to derive the bound:

$$\begin{aligned} m_a(\,)\|e\|^2_Y &\leq \int_I a[u\,](u\,; e;\,) \quad a[u_N](u_N; e;\,) dt + \frac{1}{2}\|e(T)\|^2_H \\ &= \int_I \langle \dot{e}; e \rangle_{V'V} dt + \int_I a[u\,](u\,; e;\,) \quad a[u_N](u_N; e;\,) dt + \frac{1}{2}\|e(0)\|^2_H \\ &= \int_I \langle \dot{e}; e \rangle_{V'V} dt + \int_I a[u\,](u\,; e;\,) \quad \tilde{a}[u_N](u_N; e;\,) dt + \|e(0)\|^2_H \\ &\quad + \int_I \tilde{a}[u_N](u_N; e;\,) \quad a[u_N](u_N; e;\,) dt \\ &\leq \|R(\,;\,)\|_{Y'}\|e\|_Y + \varepsilon_M(\,)\|u_N\|_{L^2(I;V)}\|e\|_Y ; \end{aligned}$$

where we added and subtracted $\tilde{a}[u_N](u_N; e;\,)$ to get the definition of the residual (5.33). Dividing both sides by $\|e\|_Y$ yields the result.

The computation of $\|R(\cdot\,;\,\cdot)\|_{Y'}$ requires the knowledge of its Riesz representer $v_{\cdot;R}(\cdot) \in Y$. Thanks to the Riesz representation theorem, it can be obtained from the equation

$$(v_{\cdot;R}(\cdot), v)_Y = R(v;\,\cdot) \quad \forall v \in Y. \tag{5.38}$$

Since the test space Y consists of piecewise constant polynomials in time, the problem (5.38) can be solved via the time-marching procedure for $k = 1, \ldots, K$ as follows:

$$\int_{I^k} \langle v_{\cdot;R}(t;\,\cdot), v_h\rangle_V dt = \int_{I^k} \langle r(t;\,\cdot), v_h\rangle_{V'V} dt \quad \forall v_h \in V_h. \tag{5.39}$$

We note that $\hat{v}_R^k(\cdot) := v_{\cdot;R}(\cdot)|_{I^k}$ is constant in time, hence the integration on the left-hand side of (5.39) is exact. For the right-hand side of (5.39) we represent $u_N(\cdot) \in X_{4t;N}$ as the linear function (5.11) on I^k and use it as an input for the residual (5.33). We then apply the trapezoidal quadrature rule for the approximate evaluation of the integral. The quadrature rule is chosen such that the quadrature error is of the size of the error of the truth Crank-Nicolson solution. We thus need to solve the following problems:

$$\langle v_R^k(\cdot), v_h\rangle_V = R^k(v_h;\,\cdot) \quad \forall v_h \in V_h \ (k = 1, \ldots, K); \tag{5.40}$$

where $v_R^k(\cdot)$ is our approximation of $\hat{v}_R^k(\cdot)$ and the right-hand side is given by

$$\begin{aligned} R^k(v_h;\,\cdot) = \frac{1}{2}[&\langle g(t^k;\,\cdot) + g(t^{k-1};\,\cdot), v_h\rangle_{V'V} \quad a[u_N^k](u_N^k; v_h;\,\cdot) \\ &a[u_N^{k-1}](u_N^{k-1}; v_h;\,\cdot)] \quad \frac{1}{4t^k}\langle u_N^k \quad u_N^{k-1}, v_h\rangle_H. \end{aligned} \tag{5.41}$$

Therefore the computation of the Riesz representer leads to a sequence of K uncoupled spatial problems in V_h. The parameter separability structure of the residual

$$R^k(v_h;\,\cdot) = \sum_{q=1}^{Q_R} \Theta_{R;q}^k(\cdot) R_q(v_h)$$

is transferred by the linearity of the Riesz isomorphism to the parameter separability of its Riesz representer $v_R^k(\cdot)$ together with the parameter dependent functions $\Theta_{R;q}^k : D \to \mathbb{R}$. Therefore, for $1 \quad q \quad Q_R$ we have

$$v_R^k(\cdot) = \sum_{q=1}^{Q_R} \Theta_{R;q}^k(\cdot) v_{R;q} \text{ with } (v_{R;q}, v_h)_V = R_q(v_h) \quad \forall v_h \in V_h. \tag{5.42}$$

Finally, we state the formulas for the residual norm as well as the spatio-temporal norm of u_N. Since $v_{\cdot;R}(\cdot)|_{I^k}$ is constant in time, the integration on I^k is exact and we can compute the spatio-temporal norm of $v_{\cdot;R}(\cdot)$ as follows:

$$\|v_{\cdot;R}(\cdot)\|_Y^2 = \sum_{k=1}^{K} 4t^k \|\hat{v}_R^k(\cdot)\|_V^2 \qquad \sum_{k=1}^{K} 4t^k \Theta_R^k(\cdot)^T \mathbf{G}_R \Theta_R^k(\cdot);$$

where $\mathbf{G}_R := \{\langle v_{R;q}, v_{R;q'}\rangle\}_{q,q'=1}^{Q_R} \in \mathbb{R}^{Q_R \quad Q_R}$ and $\Theta_R^k(\cdot) := \{\Theta_{R;q}^k(\cdot)\}_{q=1}^{Q_R} \in \mathbb{R}^{Q_R}$. The isometry of the Riesz isomorphism implies that $\|R(\cdot\,;\,\cdot)\|_{Y'} = \|v_{\cdot;R}(\cdot)\|_Y$. Since $u_N(\cdot)|_{I^k}$ is a linear function in time,

the trapezoidal quadrature rule on I^k is exact. We then can compute the spatio-temporal norm $\|u_N\|_Y$ of $u_N \in X_{4t;N}$ according to

$$\begin{aligned}\|u_N\|_Y^2 &= \sum_{k=1}^{K} \frac{\Delta t^k}{2}(\|u_N^k\|_V^2 + \|u_N^{k-1}\|_V^2) + \|u_N^0\|_H^2 \\ &= \sum_{k=1}^{K} \frac{\Delta t^k}{2}[\mathbf{u}_N^{k\,T}\mathbf{K}_N\mathbf{u}_N^k + \mathbf{u}_N^{k-1\,T}\mathbf{K}_N\mathbf{u}_N^{k-1}] + \mathbf{u}_N^{0\,T}\mathbf{M}_N\mathbf{u}_N^0;\end{aligned} \tag{5.43}$$

where $\mathbf{K}_N := (\zeta_i, \zeta_j)_V)_{i,j=1}^N \in \mathbb{R}^{N\times N}$. Since in our case the reduced basis is orthonormal in V, $\mathbf{K}_N$ is the identity matrix. Despite of our quadrature rule exactness, the right-hand side of (5.43) serves as our approximation of $\|u_N\|_Y^2$, since we use the solution of problem (5.22) in computing the norm of the reduced-basis problem (5.21). The operation count in the online phase, associated with computation of the residual norm and the spatio-temporal norm on Y is correspondingly $O(Q_R^2 K)$ and $O(NK + N^2)$.

We note that our a-posteriori error estimate takes into account the error of the nonlinearity approximation (5.35). In our discrete time setting, it is approximated by a computable quantity

$$\varepsilon_M(\cdot) \quad \max_{k\in K}\max_{x\in\Omega} |\,(g_M(u_N^k(x);\cdot) \quad (u_N^k(x);\cdot)|. \tag{5.44}$$

Since the EIM approximation $g_M(\cdot;\cdot)$ is constructed out of truth solutions, we assume that N is chosen in such a way that $g_M(u_N^k(x);\cdot) \quad g_M(u^k(x);\cdot)$. We note that (5.44) requires the knowledge of $(u_N^k(\cdot);x;\cdot)$ and thus one full evaluation of the nonlinearity for all K time steps on our finite-element mesh. Therefore the certification procedure is not fully mesh-independent in the online phase and requires our mesh storage.

We note that we performed the series of numerical approximations in order to provide a computable bound for the right-hand side of (5.34). In particular, the residual (5.33) coincides with the residual (5.41) for the Crank-Nicolson time-marching scheme (5.12) after application of the trapezoidal quadrature rule. However, in order to invoke the definition of the residual (5.33), u must be the solution to our reference problem (5.9). We also replace $\varepsilon_M(\cdot)$ by its computable surrogate (5.44). This finally gives

$$\Delta_{N;M}(\cdot) \quad \Delta^c_{N;M}(\cdot); \tag{5.45}$$

where $\Delta_{N;M}(\cdot)$ is the computable. However, the bound in general is not rigorous, since we can not guarantee that $\Delta^c_{N;M}(\cdot) \quad \Delta_{N;M}(\cdot)$ holds.

Remark 21. *In [18] authors follow the approach "First discretize, then estimate and reduce" to treat nonlinear parabolic problems. They consider the semi-discrete (the Implicit Euler) in time weak form of the nonlinear parabolic PDE*

$$(u^k(\cdot) \quad u^{k-1}(\cdot);v)_H + \Delta t a(u^k(\cdot);v) + \int_\Omega g(u^k(\cdot);x;\cdot)v\,dx = \Delta t(f(t^k);v)_{V'V};\ \forall v \in V, \tag{5.46}$$

where $k \in I$, $a(w;v) = \int_\Omega \nabla w \quad \nabla v\,dx$ and initial condition is given by $u^0 = u_o$. Here $g(w;x;\cdot) : \mathbb{R} \quad \Omega \quad D \to \mathbb{R}$ is a nonlinear, non-affine function, continuous in its arguments, increasing it its first argument and satisfies $sg(s;x;\cdot) \quad 0\ \forall s \in \mathbb{R};\forall x \in \Omega;\forall \mu \in D$. The error bound for the semi-discrete

scheme (5.46) *is then proposed with respect to the "spatio-temporal" energy norm*

$$|||v^k|||^2 := \langle v^k; v^k \rangle_H + \sum_{k'=1}^{k} a(v^k; v^k)\Delta t; \quad \forall k \in I:$$

In this approach time is treated as the parameter and it allows to prove the proper error bound for problem (5.46)*. However, problem* (5.46) *has a different structure of the nonlinearity and we think that the techniques of [18] are not directly applicable to the class of problems we consider. In our problem setting we use the approach "First estimate, then discretize and reduce", where the corresponding error estimate* $\Delta^c_{N;M}(\mu)$ *is proved with respect to the natural Bochner norm* $\|\cdot\|_Y$ *and requires relatively mild assumptions for its computable counterpart* $\Delta_{N;M}(\mu)$*.*

5.3 Examples and numerical results

In this section we consider examples of quasilinear parabolic PDEs with strongly monotone differential operators and apply the proposed reduced-basis techniques to these problems.

5.3.1 1-D magnetoquasistatic problem: analysis

For the first numerical example we choose a 1-D magnetoquasistatic approximation of Maxwell's equations (see, e.g. [4, 46]). Let $d = 1$, $\Omega = (0; 1)$ and $V := H^1_0(\Omega) \hookrightarrow L^2(\Omega) =: H$. The norm on V is $\|u\|^2_V := \langle u'; u' \rangle_{L^2}$, which is indeed a norm due to Poincare-Friedrichs inequality. We use the time interval $I = (0; 0{:}2]$ and the parameter set $\mathcal{D} := [1; 5{:}5] \subset \mathbb{R}$. For a parameter $\mu \in \mathcal{D}$, we want to find $u := u(\mu)$ which solves

$$\begin{aligned} \dot{u} - (\nu(|u'|; \mu)u')' &= g \quad \text{on } I \times \Omega; \\ u(t; x) &= 0 \quad \forall (t; x) \in I \times \partial\Omega; \\ u_0(x) &= 0 \quad \forall x \in \Omega: \end{aligned} \tag{5.47}$$

We here used $g(x; t) := 12 \sin(2\mu x) \sin(2\mu t)$ and define $\nu(s; \mu) = \exp(-\mu s^2) + 1$ as the reluctivity function.

We consider the quasilinear form for the weak formulation (5.6), which here is given by

$$a[u](u; v; \mu) = \int_\Omega \nu(|u'|; \mu) u' v' dx: \tag{5.48}$$

If the function $\nu(\cdot; \mu) : \mathbb{R}^+_0 \to \mathbb{R}^+_0$ is strongly monotone, i.e. if

$$(\nu(s_2; \mu)s_2 - \nu(s_1; \mu)s_1)(s_2 - s_1) \geq m_a(\mu)(s_2 - s_1); \quad \forall s_2; s_1 \in \mathbb{R}^+_0 \tag{5.49}$$

holds, then (5.48) satisfies the strong monotonicity condition (5.2). Indeed, we set $s_1 = w'; s_2 = v'$ and integrating we get

$$\begin{aligned} a[v](v; v - w) - a[w](w; v - w) &= \int_\Omega (\nu(v'; \mu)v' - \nu(w'; \mu)v')(v' - w')dx \\ &\geq m_a(\mu) \int_\Omega (v' - w')^2 dx = m_a(\mu)|v - w|^2_V: \end{aligned}$$

It is clear that the reluctivity function $\nu(s; \mu)$ in our example satisfies (5.49). Furthermore, the monotonicity constant can be taken as $m_a = \inf_{\mu \in \mathcal{D}} \inf_{s \in \mathbb{R}_+} \nu(s; \mu)$, hence we have $m_a = 2$ for our problem and

the constant is parameter-independent. We also note that continuity of $(\,;\,)$ implies hemicontinuity of (5.48) for every parameter $\in \mathsf{D}$. Thus the weak formulation (5.6) of the PDE (5.47) admits a unique solution.

We specify the bilinear form $\hbar A^0(u;\,)v, w i_{V^0 V} = da[u](v, w;\,)$ induced by the Fréchet derivative $A^0(u;\,) : V \quad \mathsf{D} \;!\; V^0$ of the nonlinear operator $A(u;\,)$. It is then used to compute the Jacobian matrix (5.15) for Newton method. In the present example we have

$$da[u](v, w;\,) = \int_\Omega 2 \quad {}^0(\mathrm{j}u^0\mathrm{j};\,)u^0 + \quad (\mathrm{j}u^0\mathrm{j};\,)\; v^0 w^0 \, dx:$$

The derivative for the reduced-basis scheme in the formula (5.29), thanks to the chain rule, is given by

$$\frac{@}{@u^k_{N;j}} \; (\mathrm{j}u^{0k}_N(x^M_m)\mathrm{j};\,) = 2 \quad {}^0(\mathrm{j}u^{0k}_N(x^M_m)\mathrm{j};\,)u^{0k}_N(x^M_m) \;\; {}^0_j(x^M_m);$$

where all the indices are according to (5.29). In our numerical experiments we drop the term $\mathbf{E}_{N;M}(\mathbf{u}^k_N;\,)$ in $\mathbf{A}^0_{N;M}(\mathbf{u}^k_N;\,)$. This then corresponds to an inexact Newton-like method, which we use in our numerical experiments and which performed well.

5.3.2 1-D magnetoquasistatic problem: numerical results

The truth approximation is performed by the Petrov-Galerkin scheme, which is introduced in section 5.1, where V_h is the finite element space, composed of piecewise linear and continuous functions, defined on the partition of $\bar{\Omega}$ into 100 equal subintervals and $\mathsf{N}_h = 98$ nodes (excluding Dirichlet boundary nodes). For the time discretization we divide the interval I into $K = 200$ subintervals of length $4t = 10^{-3}$. We solve the problem with the Crank-Nicolson scheme (5.12), while applying Newton's method, described in section 5.1.2 on each time step for the numerical computation of the time snapshots. We iterate the Newton's method unless the norm of the residual (5.13) is less than the tolerance level, which we set to 10^{-8}.

We generate the RB-EIM model as follows: we start from $\mathsf{D}^{EIM}_{train} \quad \mathsf{D}$ (a uniform grid of size 200) and compute truth solutions for each parameter in D^{EIM}_{train} to approximate the nonlinearity with its EIM counterpart $_M$. We set $M_{max} = 8$ as the maximal dimension of the EIM approximation space. Next we run the POD-Greedy procedure with $M = M_{\max}$ and obtain $N_{\max} = 5$ for $"_{RB} = 10^{-5}$, where D_{train} is a uniform grid over D of size 400. For the POD-Greedy procedure and method certification we use the computable bound $4_{N;M}$ (5.45) for our error estimate $4^c_{N;M}$ (5.34). We solve the problem with the reduced Crank-Nicolson scheme (5.22), while applying RB Newton's method, described in section 5.2.2 on each time step for the numerical computation of the time snapshots. We iterate the Newton's method unless the norm of the residual (5.23) is less than the tolerance level, which we set to 10^{-8}.

Next we introduce a test sample $\mathsf{D}_{test} \quad \mathsf{D}$ of size 200 (uniformly random sample from D) and the maximum of the estimator $\max 4_{N;M} := \max_{2\mathsf{D}_{test}} 4_{N;M}(\,)$. We also introduce the following approximation of the "truth norm" error

$$"^{true}_{N;M}(\,) := \left(\sum_{k=1}^{K} \frac{\mathsf{M}\, t^k}{2} (\mathrm{k}u^k(\,) \quad u^k_N(\,)\mathrm{k}^2_V + \mathrm{k}u^{k\ 1}(\,) \quad u^{k\ 1}_N(\,)\mathrm{k}^2_V) \right)^{1=2}; \tag{5.50}$$

and its maximum over the test sample $\max "^{true}_{N;M} := \max_{2\mathsf{D}_{test}} "^{true}_{N;M}(\,)$, where we use the Crank-Nicolson

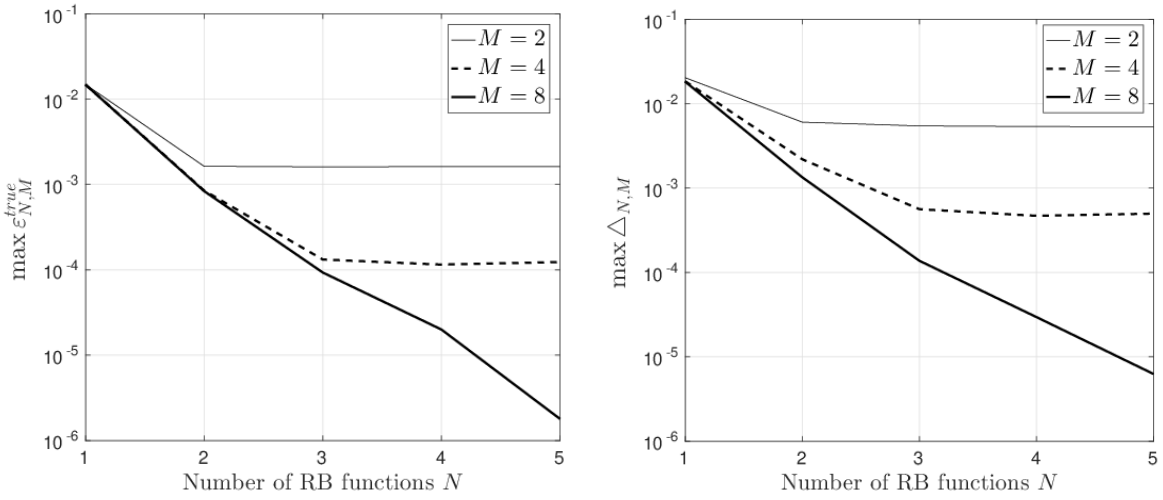

(a) (b)

Figure 5.1: (a): Convergence with N of $\max \varepsilon_{N;M}^{true}$ for different values of M on the test set, 1-D example. (b): Convergence with N of $\max \Delta_{N;M}$ for different values of M on the test set, 1-D example.

solutions $u^k(\ )$ and $u_N^k(\ )$ to compute (5.50). Hence $\varepsilon_{N;M}^{true}(\ )$ is only an estimate for $\|e(\ )\|_Y$ in (5.34), where the solution $u(\ )$ of (5.9) and $u_N(\ )$ of (5.21) enters. Once the reduced-basis model is constructed ($N_{\max} = 7; M_{\max} = 8$), we verify the convergence with N of $\max \Delta_{N;M}$ and $\max \varepsilon_{N;M}^{true}$ on a test sample $\mathcal{D}_{test}$ and plot in Fig.5.1 the N-M convergence curves for different values of M. We can see that the estimator in Fig.5.1(b) reaches the desired tolerance level $\varepsilon_{RB} = 10^{-5}$ for $(N_{\max}; M_{\max}) = (5; 8)$.

Next we investigate the influence of the EIM approximation error in the estimation process. We can split the bound (5.45) into two parts: the reduced-basis and the nonlinearity approximation error estimation contributions

$$\Delta_{N;M}^{RB}(\ ) \quad \frac{1}{m_a}\|R(\ ;\ )\|_{Y'} \text{ and } \Delta_{N;M}^{EI}(\ ) \quad \frac{\gamma_M(\ )}{m_a}\|u_N(\ )\|_Y: \tag{5.51}$$

We compute these contributions as described in section 5.1.2 and note that they serve only as computable surrogates for the respective contributions in our error estimate (5.34). We then set

$$\Delta_{N;M}^{RB} := \max_{\mathcal{D}_{test}} \Delta_{N;M}^{RB}(\ ); \quad \Delta_{N;M}^{EI} := \max_{\mathcal{D}_{test}} \Delta_{N;M}^{EI}(\ ): \tag{5.52}$$

In Fig.5.2(a) we plot $\Delta_{N;M}^{RB}$ and $\Delta_{N;M}^{EI}$ for $1 \quad N \quad 5$ and $M = 4$, $M = 8$: we can see that M has nearly no influence on $\Delta_{N;M}^{RB}$, but we observe the "plateau" in $\Delta_{N;M}^{EI}$, which limits the convergence of the bound (5.45) with increasing N. The separation points, or "knees", of the N-M-convergence curves then reflect a (close-to) balanced contribution of both error terms.

In Table 5.1 we present, as a function of N and M, the values of $\max \Delta_{N;M}$, $\Delta_{N;M}^{RB}$, $\Delta_{N;M}^{EI}$, $\varepsilon_{N;M}^{true}$ and mean effectivities $\bar{\eta}_{N;M} := \frac{1}{|\mathcal{D}_{test}|} \sum_{\mathcal{D}_{test}} \eta_{N;M}(\ )$, where $\eta_{N;M}(\ ) := \Delta_{N;M}(\ )/\|u(\ ) \quad u_N(\ )\|_Y$. We note that the tabulated $(N; M)$ values correspond roughly to the "knees" of the N-M-convergence curves. We can see that the effectivities are lower bounded by 1 and are of moderate size, thus the bound (5.45) is reliable and there is no significant overestimation of our approximation of the "truth norm" error (5.50).

We then plot (see Fig. 5.2(b)) the reluctivity function $(|u_N^{0k}|; \ )$ and its EI approximation $_M(|u_N^{0k}|; \ )$ for the parameter $= 5{:}5$ at $t = 0{:}2$; we can see that there is no visible difference between the origi-

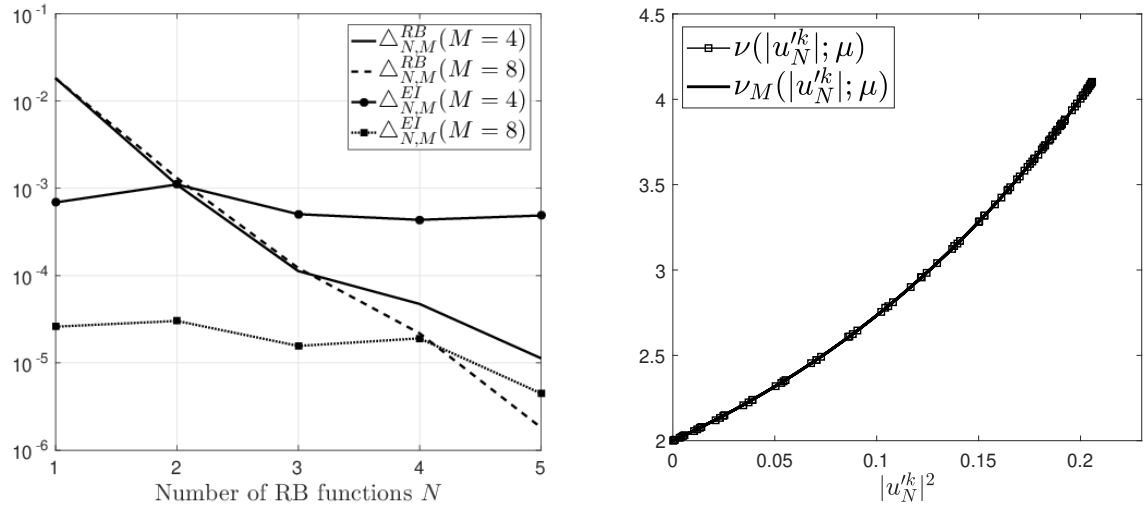

(a) (b)

Figure 5.2: (a): The dependence of $4^{RB}_{N;M}$ and $4^{EI}_{N;M}$ contributions with N for fixed values of M. (b): The reluctivity function (ju^{0k}_Nj;) and its EI-approximation ($M = 8$) $_M$(ju^{0k}_Nj;) for the parameter = 5:5 at t = 0:2 (b).

N	M	max $4_{N;M}$	$4^{RB}_{N;M}$	$4^{EI}_{N;M}$	max $"^{true}_{N;M}$	$^-_{N;M}$
2	2	6.10 E-03	5.60 E-03	7.60 E-04	1.60 E-03	4.00
3	4	5.62 E-04	5.05 E-04	1.12 E-04	1.32 E-04	5.82
5	8	6.25 E-06	4.47 E-06	1.81 E-06	1.79 E-06	4.58

Table 5.1: Performance of the 1D RB-EIM magnetoquasistatic approximation of Maxwell's equations on the test set

nal function and its EIM counterpart. Although the problem at hand is merely chosen to illustrate the methodology, we report on the average CPU time for comparison. The finite element method takes 0:47 sec to obtain the solution, and the RB method ($N_{\max}$; $M_{\max}$), which takes 0:08=0:10 sec without and with the a-posteriori certification and results in the speed-up factor of 5.87/4.70[1]. We note that our implementation in the offline phase needs a large number of high-fidelity finite element solutions for the EIM approximation and the Riesz representers in (5.42). This implies large offline computational costs. However, these computations can be done in parallel to significantly reduce the time needed for the offline phase.

5.3.3 2-D magnetoquasistatic problem: analysis

As second example we consider a 2-D magnetoquasistatic problem for modelling of eddy currents in a steel pipe[2]. Let $\bar{\Omega} = \bar{\Omega}_1 \,^{S}\, \bar{\Omega}_2$ be a circular cross-section of the steel pipe with radius r_2, where Ω_1 is the conducting domain (iron) and Ω_2 is the non-conducting domain of radius r_1. The wire is represented by the part with the radius r_0 and the complementary part is the air gap (see Fig.5.3(a)). We assume that the magnetic reluctivity function and the electric conductivity function have different structure on

[1]All the computations are performed in MATLAB on Intel Xeon(R) CPU E5-1650 v3, 3.5 GHz x 12 cores, 64 GB RAM
[2]http://www.femm.info/wiki/TubeExample

conducting and non-conducting domains, respectively, i.e.

$$(x; s) = \begin{cases} {}_1(s); & \text{for } x \in \Omega_1; \\ {}_2; & \text{for } x \in \Omega_2 \end{cases} \quad \text{and} \quad (x) = \begin{cases} {}_1 > 0; & \text{for } x \in \Omega_1; \\ > 0; & \text{for } x \in \Omega_2; \end{cases}$$

where ${}_2;\ {}_1 > 0$ denote constants. We assume that the reluctivity function satisfies

$$0 < {}_{\mathrm{LB}} \quad (x; s) \quad {}_{UB}; \quad 8x \in \Omega;\ s \in \mathbb{R}_0^+; \tag{5.53}$$

where ${}_{\mathrm{LB}}$ and ${}_{UB}$ are accessible constants. We note that the air-gap and the coils in the steel pipe are electrically non-conductive, i.e. $(x) = 0$ for $x \in \Omega_2$. However, we introduce a regularization parameter $= 10^{-8}$ as a value of for the non-conducting domain. This allows us to consider a pure parabolic problem instead of a parabolic-elliptic system with differential-algebraic structure (see, e.g. [35]). We set $:= {}_1$ and define the parameter set $\mathsf{D} = [5 \quad 10^6; 10^7]$ and the time interval $I = (0; 0{:}02]$. We thus have a parametrized quasilinear parabolic equation

$$\begin{aligned} (x; \ )\dot{u} \quad \mathrm{r} \ (\ (x; \mathrm{j}\,\mathrm{r}u\mathrm{j})\,\mathrm{r}\,u) &= g \qquad \text{on } I \quad \Omega; \\ u(t; x) &= 0 \qquad 8\,(t; x) \in I \quad @\Omega; \\ u_0(x) &= 0 \qquad 8\,x \in \Omega: \end{aligned} \tag{5.54}$$

The right-hand side is the electric-flux density

$$g(x; t) = \begin{cases} \frac{I_e(t)}{2\ r_0}; & \text{for } x \in \Omega_1; \\ 0; & \text{for } x \in \Omega_2; \end{cases}$$

where $I_e(t) = 100 \quad \sin(100\ t)$ is the electric current. We consider the quasilinear form for the weak formulation (5.6), which here is given by

$$a[u](u; v; \ ) = \int_\Omega (x; \mathrm{j}\,\mathrm{r}u\mathrm{j}; \ )\,\mathrm{r}\,u \quad \mathrm{r}\,v\,dx: \tag{5.55}$$

The nonlinear reluctivity function (see Fig 5.3(b)) in our case is reconstructed from $B \quad H$ curves, see section 2.1.2. The form (5.55) then is strongly monotone with the monotonicity constant ${}_{LB}$ and Lipschitz continuous with the Lipschitz constant $3\ {}_{UB}$ (see [24] for the corresponding proofs). Hence the weak formulation (5.6) of the PDE (5.54) admits a unique solution.

We specify the bilinear form $\hbar A^0(u; \ )v; w\mathrm{i}_{V^0V} = da[u](v; w; \ )$ induced by the Fréchet derivative $A^0(u; \ ) : V \quad \mathsf{D} \ ! \ V^0$ of the nonlinear operator $A(u; \ )$. It is then used to compute the Jacobian matrix (5.15) for Newton method. With

$$n[u] = \begin{cases} \frac{\mathrm{r}\,u}{\mathrm{j}\,\mathrm{r}u\mathrm{j}}; & \text{for } \mathrm{r}\,u \ , \ 0; \\ 0; & \text{for } \mathrm{r}\,u = 0; \end{cases}$$

we have

$$da[u](v; w; \ ) = \int_\Omega {}^0(x; \mathrm{j}\,\mathrm{r}u\mathrm{j}; \ )(n[u] \quad \mathrm{r}\,w)(\mathrm{r}\,u \quad \mathrm{r}\,v) + \ (x; \mathrm{j}\,\mathrm{r}u\mathrm{j}; \ )\,\mathrm{r}\,v \quad \mathrm{r}\,w\,dx;$$

and the derivative for the reduced-basis scheme in the formula (5.29), thanks to the chain rule, is given

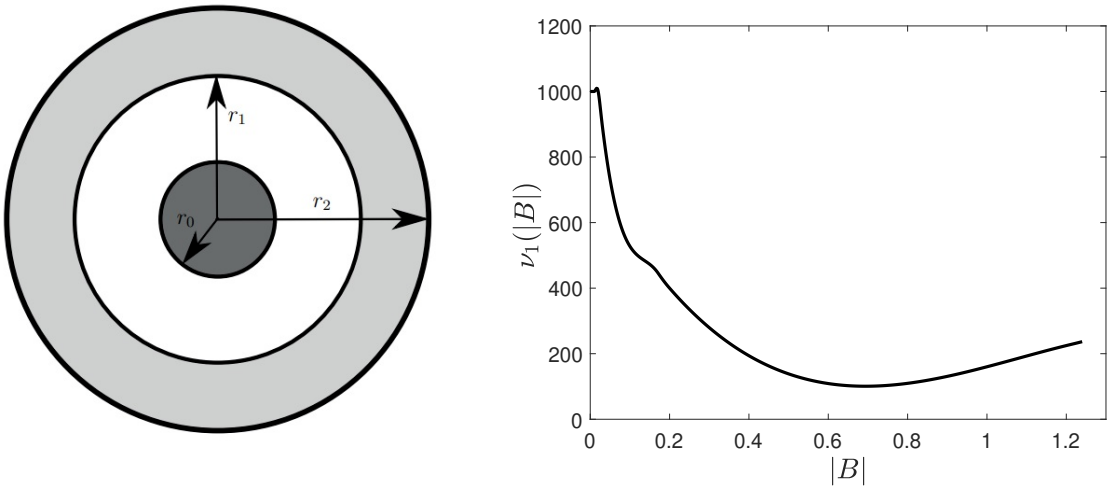

(a) (b)

Figure 5.3: (a): Geometry of the computational domain: the wire (dark grey), the air gap (white), the iron (bright grey). (b): An example of magnetic reluctivity function $_1(\mathsf{j}B\mathsf{j})$ of ferromagnetic material used in our simulations.

by

$$\frac{@}{@u^k_{N;j}}\ (x;\mathsf{j}\,\mathsf{r}\,u^k_N(x^M_m)\mathsf{j};\ \ ) := \ ^0(x;\mathsf{j}\,\mathsf{r}\,u^k_N(x^M_m)\mathsf{j};\ \ )n[u^k_N](x^M_m)\quad \mathsf{r}\ _j(x^M_m);$$

where all the indices are according to (5.29).

In this example, the monotonicity constant $m_a(\ )$ is not available analytically. As it was mentioned earlier in the discussion on $\mathsf{j}B\mathsf{j}$-$\mathsf{j}H\mathsf{j}$ curves, we can choose $_{LB} > 0$ as our monotonicity constant. However, since for each parameter $\ 2\ \mathsf{D}$ there holds

$$m_a(\ ) := \min_{k2K}\min_{x2\Omega}\ _1(\mathsf{j}\,\mathsf{r}\,u^k_N(x)\mathsf{j};\ \ )\qquad _{LB}; \tag{5.56}$$

and the computation of (5.56) only requires one full evaluation of the nonlinearity, which already has been performed to evaluate (5.44), we here use $m_a(\ )$ as our constant for the estimation.

5.3.4 2-D magnetoquasistatic problem: numerical results

The truth approximation is performed by the Petrov-Galerkin scheme, which is introduced in section 5.1, where V_h is the finite element space, composed of piecewise linear and continuous functions, defined on a triangle mesh containing 4374 triangles and $\mathsf{N}_h = 2107$ nodes (excluding Dirichlet boundary nodes). For the time discretization we divide the interval I into $K = 200$ subintervals of length $4t = 10^{\ 4}$. The nonlinear reluctivity function $_1$ is reconstructed from the real $B\quad H$ measurements using monotonicity-preserving cubic spline interpolation and $_2$ value is chosen as the reluctivity of air. We then solve the problem with the Crank-Nicolson scheme (5.12), while applying Newton's method, described in section 5.1.2, on each time step for the numerical computation of the time snapshots. We iterate the Newton's method unless the norm of the residual (5.13) is less than the tolerance level, which we set to $10^{\ 8}$.

We generate the RB-EIM model as follows: we start from $\mathsf{D}^{EIM}_{train}\quad \mathsf{D}$ (a uniform grid of size 200) and compute truth solutions for each parameter in D^{EIM}_{train} to approximate the nonlinearity $_1$ with the EIM

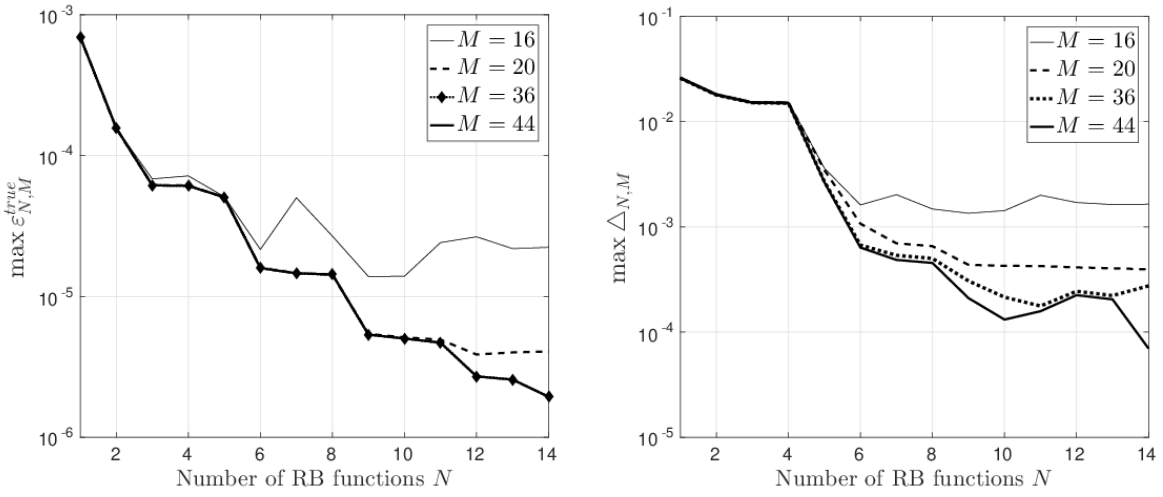

(a) (b)

Figure 5.4: (a): Convergence with N of $\max \varepsilon^{true}_{N;M}$ for different values of M on the test set, 2-D example. (b): Convergence with N of $\max \Delta_{N;M}$ for different values of M on the test set, 2-D example.

counterpart $\mathcal{I}_1^M$. We set $M_{\max} = 44$ as the maximal dimension of the EIM approximation space. Next we run the POD-Greedy procedure with $M = M_{\max}$ and obtain $N_{\max} = 14$ for $\varepsilon_{RB} = 10^{-4}$, where $\mathcal{D}_{train}$ is a uniform grid over $\mathcal{D}$ of size 400. For the POD-Greedy procedure and method certification we use the computable bound $\Delta_{N;M}$ (5.45) for our error estimate $\Delta^c_{N;M}$ (5.34). The monotonicity constant is evaluated as in (5.56). We solve the problem with the reduced Crank-Nicolson scheme (5.22), while applying RB Newton's method, described in section 5.2.2, on each time step for the numerical computation of the time snapshots. We iterate the Newton's method unless the norm of the residual (5.23) is less than the tolerance level, which we set to 10^{-8}.

Then we verify the convergence with N of $\max \varepsilon^{true}_{N;M}$ (Fig. 5.4(a)) and $\max \Delta_{N;M}$ (Fig. 5.4(b)) on a test sample $\mathcal{D}_{test}$ (a uniformly random sample of size 200) for different values of M. We can see that the estimator in Fig.5.3(b) reaches the desired tolerance level $\varepsilon_{RB} = 10^{-4}$ for $(N_{\max}; M_{\max}) = (14; 44)$. We note that the convergence is not monotone at some points due to the EIM interpolation of the non-polynomial nonlinearity behind the problem. We can also see from Fig.5.4(a) that increasing M above 20 has nearly no impact on the convergence of the approximation of the "truth norm" error (5.50), but the bound (5.45) in Fig.5.4(b) still shows a considerable decrease with increasing M. Indeed, in Fig.5.5(a) we plot $\Delta^{RB}_{N;M}$ and $\Delta^{EI}_{N;M}$ as defined in (5.52) for $1 \quad N \quad 14$ and $M = 20$, $M = 44$: we can see that M has nearly no influence on $\Delta^{RB}_{N;M}$, but we can observe the "plateau" in $\Delta^{EI}_{N;M}$, which limits the convergence of the bound (5.45) with increasing N. We also plot the values of $\Delta_{N;M}(\ )$ and $\varepsilon^{true}_{N;M}(\ )$ and the error (5.50) for $(N_{\max}; M_{\max})$ for every parameter $\quad 2 \mathcal{D}_{test}$ in Fig.5.5(b).

In Table 5.2 we present, as a function of N and M, the values of $\max \Delta_{N;M}$, $\Delta^{RB}_{N;M}$, $\Delta^{EI}_{N;M}$, $\max \varepsilon^{true}_{N;M}$ and the mean effectivities $\bar{}_{N;M}$. We note that the tabulated $(N; M)$ values correspond roughly to the "knees" of the N-M-convergence curves (see example 1 for the terminology and definitions). We can see that the effectivities are lower bounded by 1, but the values are relatively large. Based on our estimate (4.39) for the nonlinear magnetostatics problem, we conject that this is related to the structure of the nonlinearity and the effectivities are proportional to $C \quad _{UB}= \ _{LB}$, where C is some constant.

In Fig.5.6 we show the truth finite element magnetic flux density $\mathrm{j}\mathrm{r}\, u^k(x; \ )\mathrm{j}$ and the corresponding reduced magnetic flux density $\mathrm{j}\mathrm{r}\, u^k_N(x; \ )\mathrm{j}$ for $\quad = 10^7$ and $t = 0{:}01$ and $t = 0{:}02$. We observe that flux

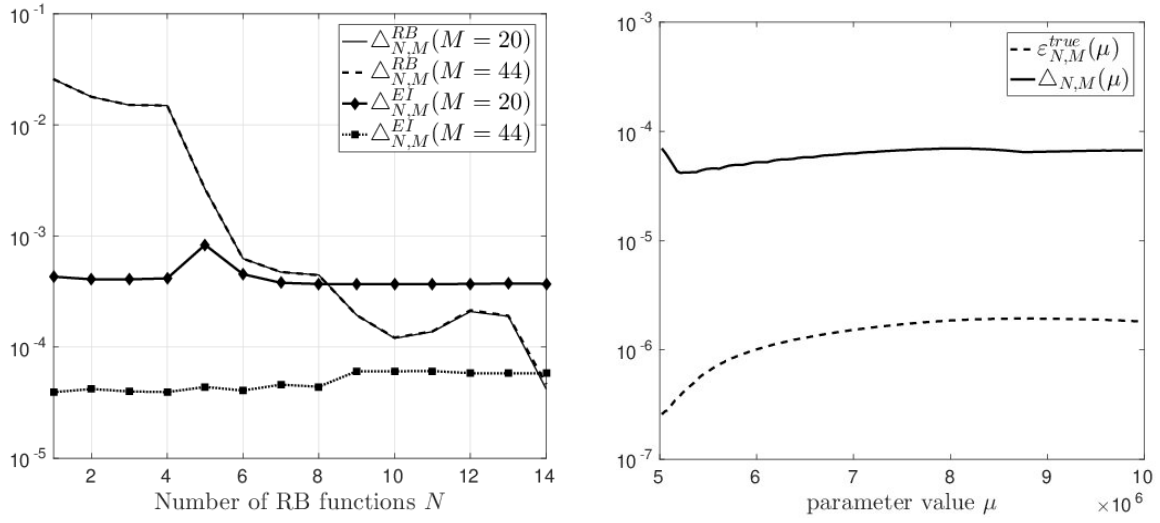

(a) (b)

Figure 5.5: (a): The dependence of $4^{RB}_{N;M}$ and $4^{EI}_{N;M}$ contributions with N for fixed values of M. (b): Values of $"^{true}_{N;M}$ and max $M_{N;M}$ for $(N_{\max}; M_{\max}) = (14; 44)$ on the test set.

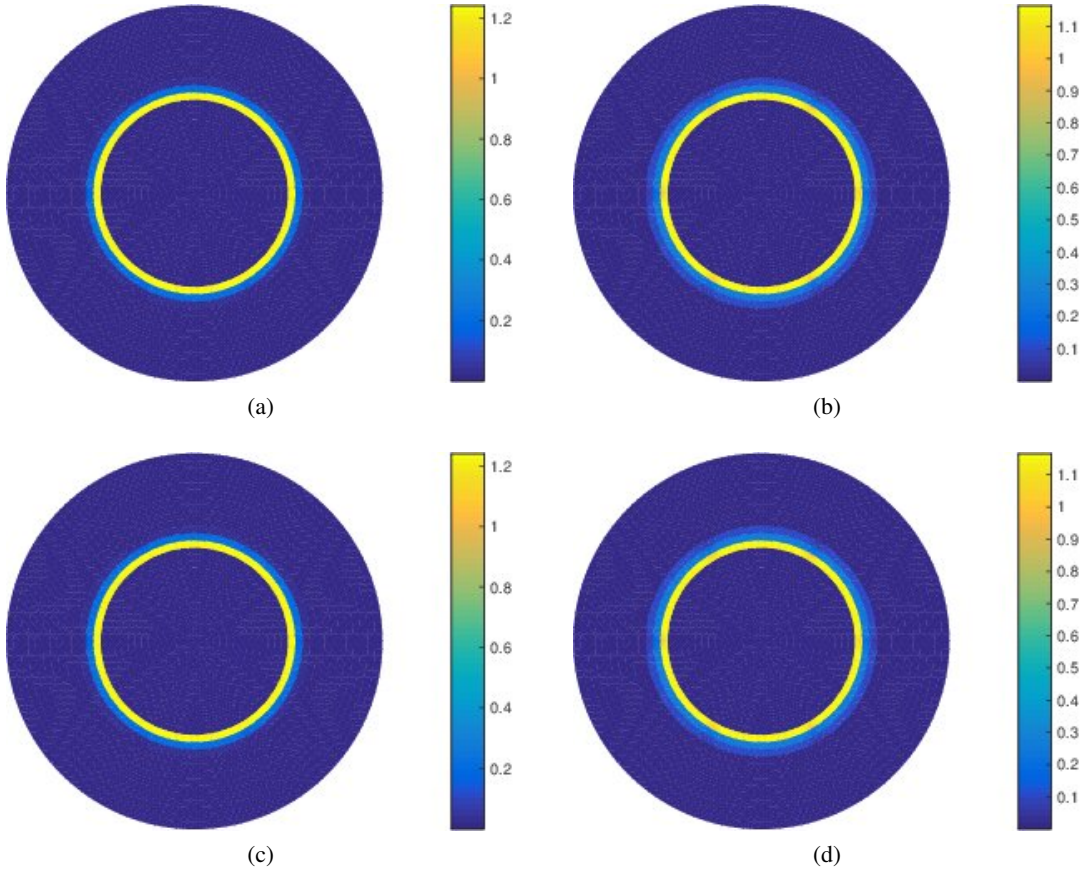

(a) (b)

(c) (d)

Figure 5.6: The truth magnetic flux density j r u^kj for $= 10^7$ at (a) $t = 0{:}01$, (b) $t = 0{:}02$. The reduced-basis magnetic flux density j r u^k_Nj for $= 10^7$ at (c) $t = 0{:}01$, (d) $t = 0{:}02$.

N	M	$\max \Delta_{N;M}$	$\Delta^{RB}_{N;M}$	$\Delta^{EI}_{N;M}$	$\max \varepsilon^{true}_{N;M}$	$\bar{\ }_{N;M}$
6	16	1.60 E-03	6.68 E-04	1.40 E-03	2.15 E-05	98.06
9	20	4.34 E-04	1.94 E-04	3.67 E-04	5.40 E-06	89.84
11	36	1.76 E-04	1.38 E-04	1.04 E-04	4.68 E-06	64.28
14	44	6.97 E-05	4.63 E-05	5.81 E-05	1.93 E-06	48.27

Table 5.2: Performance of 2-D RB-EIM model on the test set

densities look very similar. Next we compare the average CPU time required for both the finite element method, which takes 70 sec to obtain the solution, and the RB method with $(N_{\max}; M_{\max}) = (14; 44)$, which takes 1:80=2:42 without and with the a-posteriori certification and results in the speed-up factors (rounded) of 39 and 29, respectively. The offline phase requires the knowledge of the truth finite-element solutions for the EIM approximation step. Since 200 truth solutions were generated in the consecutive order, it takes 4 hours. The generation of these truth solutions could be performed in parallel, which would reduce the offline time. The POD-Greedy sampling takes 40 minutes for our implementation. We note that our implementation in the offline phase needs a large number of high-fidelity finite element solutions for the EIM approximation and the Riesz representers in (5.42). This implies large offline computational costs. However, these computations can be done in parallel to significantly reduce the time needed for the offline phase.

Chapter 6

Conclusion

In this thesis the reduced basis methods for quasilinear elliptic and parabolic PDEs with strongly monotone differential operator have been addressed and applied to the parametrized nonlinear magnetostatic and magnetoquasistatic approximations of Maxwell's equations.

The reduced basis method for quasilinear elliptic PDEs is applied to the magnetostatic problem in the context of the permanent magnet synchronous motor. The parameter dependence enters through the geometric parametrisation of the permanent magnet in the rotor part of the machine. The complex industrial setting with the geometric parametrisation, multi-physics and strong non-polynomial nonlinearity makes our reduction problem for magnetostatic equation challenging. We present the a-posteriori error bound, which appeals to the monotonicity of the differential operator and use the EIM to guarantee the offline-online decomposition of the problem. The Greedy algorithm is used to produce the reduced basis space of small dimension and the reduced basis approximation is introduced as the Galerkin projection on the reduced basis space. Then we present the reduced counterpart of Newton's method to efficiently solve the nonlinear equation for the reduced basis coefficients in the online phase. Our numerical results confirm a significant speed-up factor, compared to our finite element method, which supports the validity of the approach.

We also introduce the space-time reduced basis method for quasilinear parabolic PDEs. We think that our space-time formulation combined with the chosen Petrov-Galerkin discretization provides an elegant approach to treat these kind of problems. We present the new a-posteriori error estimate, which appeals to the strong monotonicity of the spatial differential operator, and further discretize it to obtain the computable bound. We note that our reduced basis approximation is based on the time-marching approximation of the Petrov-Galerkin problem and the reduced basis space is obtained by the POD-Greedy procedure. We also used the EIM to obtain the affine decomposition of the problem and to guarantee the Offline-Online decomposition. The developed methodology is applied to the 1-D and the 2-D magnetoquasistatic approximations of Maxwell's equations and the numerical results confirm a good speed-up factor, which supports the validity of this approach.

We believe that the reduced basis methods developed in this thesis can be extended to treat more complicated industrial problems. It will further have a significant impact on the PASIROM project[1], where the surrogate reduced-basis models are planned to be used in the optimization of electrical machines.

[1] http://www.pasirom.de/

Bibliography

[1] Assyr Abdulle, Yun Bai, and Gilles Vilmart. “Reduced basis finite element heterogeneous multiscale method for quasilinear elliptic homogenization problems”. In: *Discrete and Continuous Dynamical Systems-Series S* 8.1 (2015), pp. 91–118.

[2] Alessandro Alla et al. “A certified model reduction approach for robust parameter optimization with PDE constraints”. In: *Advances in Computational Mathematics* 45.3 (2019), pp. 1221–1250.

[3] Roman Andreev. “Space-time discretization of the heat equation”. In: *Numerical Algorithms* 67.4 (2014), pp. 713–731.

[4] Florian Bachinger, Ulrich Langer, and Joachim Schöberl. “Numerical analysis of nonlinear multiharmonic eddy current problems”. In: *Numerische Mathematik* 100.4 (2005), pp. 593–616.

[5] Maxime Barrault et al. “An ‘empirical interpolation’method: application to efficient reduced-basis discretization of partial differential equations”. In: *Comptes Rendus Mathematique* 339.9 (2004), pp. 667–672.

[6] Peter Binev et al. “Convergence rates for greedy algorithms in reduced basis methods”. In: *SIAM journal on mathematical analysis* 43.3 (2011), pp. 1457–1472.

[7] Zeger Bontinck et al. “Robust optimisation formulations for the design of an electric machine”. In: *IET Science, Measurement & Technology* 12.8 (2018), pp. 939–948.

[8] Haim Brezis. *Functional analysis, Sobolev spaces and partial di erential equations*. Springer Science & Business Media, 2010.

[9] Annalisa Buffa et al. “A priori convergence of the greedy algorithm for the parametrized reduced basis method”. In: *ESAIM: Mathematical Modelling and Numerical Analysis-Modélisation Mathématique et Analyse Numérique* 46.3 (2012), pp. 595–603.

[10] Jens L Eftang and Benjamin Stamm. “Parameter multi-domain ‘hp’empirical interpolation”. In: *International Journal for Numerical Methods in Engineering* 90.4 (2012), pp. 412–428.

[11] Lawrence C Evans. “Partial differential equations”. In: *Graduate studies in mathematics* 19.2 (1998).

[12] Jan Francu. “Monotone operators. A survey directed to applications to differential equations”. In: *Aplikace matematiky* 35.4 (1990), pp. 257–301.

[13] Frederick N Fritsch and Ralph E Carlson. “Monotone piecewise cubic interpolation”. In: *SIAM Journal on Numerical Analysis* 17.2 (1980), pp. 238–246.

[14] Peter Gangl. “Sensitivity-based topology and shape optimization with application to electrical machines/eingereicht von Dipl.-Ing. Peter Gangl, Bakk. Techn.” PhD thesis. Universität Linz, 2016.

[15] Peter Gangl, Samuel Amstutz, and Ulrich Langer. “Topology optimization of electric motor using topological derivative for nonlinear magnetostatics”. In: *IEEE Transactions on Magnetics* 52.3 (2015), pp. 1–4.

[16] Peter Gangl et al. “Shape optimization of an electric motor subject to nonlinear magnetostatics”. In: *SIAM Journal on Scientific Computing* 37.6 (2015), B1002–B1025.

[17] Silke Glas, Antonia Mayerhofer, and Karsten Urban. “Two ways to treat time in reduced basis methods”. In: *Model reduction of parametrized systems*. Springer, 2017, pp. 1–16.

[18] Martin A Grepl. “Certified reduced basis methods for nonaffine linear time-varying and nonlinear parabolic partial differential equations”. In: *Mathematical Models and Methods in Applied Sciences* 22.03 (2012), p. 1150015.

[19] Martin A Grepl and Anthony T Patera. “A posteriori error bounds for reduced-basis approximations of parametrized parabolic partial differential equations”. In: *ESAIM: Mathematical Modelling and Numerical Analysis* 39.1 (2005), pp. 157–181.

[20] Martin A Grepl et al. “Efficient reduced-basis treatment of nonaffine and nonlinear partial differential equations”. In: *ESAIM: Mathematical Modelling and Numerical Analysis* 41.3 (2007), pp. 575–605.

[21] Bernard Haasdonk. “Reduced basis methods for parametrized PDEs–a tutorial introduction for stationary and instationary problems”. In: *Model reduction and approximation: theory and algorithms* 15 (2017), p. 65.

[22] Bernard Haasdonk and Mario Ohlberger. “Reduced basis method for finite volume approximations of parametrized linear evolution equations”. In: *ESAIM: Mathematical Modelling and Numerical Analysis-Modélisation Mathématique et Analyse Numérique* 42.2 (2008), pp. 277–302.

[23] MD Rokibul Hasan et al. “Stabilized reduced-order model of a non-linear eddy current problem by a gappy-POD approach”. In: *IEEE Transactions on Magnetics* 54.12 (2018), pp. 1–8.

[24] Bodo Heise. “Analysis of a fully discrete finite element method for a nonlinear magnetic field problem”. In: *SIAM Journal on Numerical Analysis* 31.3 (1994), pp. 745–759.

[25] Jan S Hesthaven, Gianluigi Rozza, Benjamin Stamm, et al. *Certified reduced basis methods for parametrized partial di erential equations*. Vol. 590. Springer, 2016.

[26] Michael Hinze and Denis Korolev. “A space-time certified reduced basis method for quasilinear parabolic partial differential equations”. In: *Advances in Computational mathematics* 47.3 (2021).

[27] Michael Hinze and Denis Korolev. “Reduced basis methods for quasilinear elliptic PDEs with applications to permanent magnet synchronous motors”. In: *arXiv preprint arXiv:2002.04288* (2020).

[28] Michael Hinze et al. *Optimization with PDE constraints*. Vol. 23. Springer Science & Business Media, 2008.

[29] Fabian Hoppe and Ira Neitzel. “A-posteriori reduced basis error-estimates for a semi-discrete in space quasilinear parabolic PDE”. Available as INS Preprint No. 2005. 2020.

[30] Austin Hughes and Bill Drury. *Electric motors and drives: fundamentals, types and applications*. Newnes, 2019.

[31] Dinh Bao Phuong Huynh et al. “A successive constraint linear optimization method for lower bounds of parametric coercivity and inf-sup stability constants”. In: *Comptes Rendus Mathematique* 345.8 (2007), pp. 473–478.

[32] Nathan Ida and Joao PA Bastos. *Electromagnetics and calculation of fields*. Springer Science & Business Media, 2013.

[33] Ion Gabriel Ion et al. “Robust shape optimization of electric devices based on deterministic optimization methods and finite-element analysis with affine parametrization and design elements”. In: *Electrical Engineering* 100.4 (2018), pp. 2635–2647.

[34] John David Jackson. *Classical electrodynamics*. American Association of Physics Teachers, 1999.

[35] Johanna Kerler-Back and Tatjana Stykel. “Model reduction for linear and nonlinear magnetoquasistatic equations”. In: *International Journal for Numerical Methods in Engineering* 111.13 (2017), pp. 1274–1299.

[36] Denis Korolev. *Reduced basis concepts for linear parabolic equations*. Master thesis, University of Hamburg, 2018.

[37] Oliver Lass and Stefan Ulbrich. “Model order reduction techniques with a posteriori error control for nonlinear robust optimization governed by partial differential equations”. In: *SIAM Journal on Scientific Computing* 39.5 (2017), S112–S139.

[38] Yvon Maday et al. “A general multipurpose interpolation procedure: the magic points”. In: *Communications on Pure & Applied Analysis* 8.1 (2009), p. 383.

[39] Melina Merkel, Peter Gangl, and Sebastian Schops. “Shape optimization of rotating electric machines using isogeometric analysis”. In: *IEEE Transactions on Energy Conversion* (2021).

[40] Laurent Montier et al. “Robust model order reduction of an electrical machine at startup through reduction error estimation”. In: *International Journal of Numerical Modelling: Electronic Networks, Devices and Fields* 31.2 (2018), e2277.

[41] Mario Ohlberger and Stephan Rave. “Reduced basis methods: Success, limitations and future challenges”. In: *Proceedings of ALGORITMY* (2016).

[42] Clemens Pechstein. *Multigrid-Newton-methods for nonlinear magnetostatic problems*. Johannes Kepler University Linz, 2004.

[43] Alfio Quarteroni, Andrea Manzoni, and Federico Negri. *Reduced basis methods for partial di erential equations: an introduction*. Vol. 92. Springer, 2015.

[44] Ulrich Römer. *Numerical approximation of the magnetoquasistatic model with uncertainties and its application to magnet design*. Technische Universität Darmstadt, 2015.

[45] Gianluigi Rozza, Dinh Bao Phuong Huynh, and Anthony T Patera. “Reduced basis approximation and a posteriori error estimation for affinely parametrized elliptic coercive partial differential equations”. In: *Archives of Computational Methods in Engineering* 15.3 (2007), p. 1.

[46] Sheppard Joel Salon. *Finite element analysis of electrical machines*. Vol. 101. Kluwer academic publishers Boston, 1995.

[47] Sugata Sen. “Reduced-basis approximation and a posteriori error estimation for many-parameter heat conduction problems”. In: *Numerical Heat Transfer, Part B: Fundamentals* 54.5 (2008), pp. 369–389.

[48] Kristina Steih and Karsten Urban. “Space-time reduced basis methods for time-periodic partial differential equations”. In: *IFAC Proceedings Volumes* 45.2 (2012), pp. 710–715.

[49] Karsten Urban and Anthony Patera. “An improved error bound for reduced basis approximation of linear parabolic problems”. In: *Mathematics of Computation* 83.288 (2014), pp. 1599–1615.

[50] Karen Veroy et al. “A posteriori error bounds for reduced-basis approximation of parametrized noncoercive and nonlinear elliptic partial differential equations”. In: *16th AIAA Computational Fluid Dynamics Conference*. 2003, p. 3847.

[51] Stefan Volkwein. “Proper orthogonal decomposition: Theory and reduced-order modelling”. In: *Lecture Notes, University of Konstanz* 4.4 (2013).

[52] Masayuki Yano. “A space-time Petrov–Galerkin certified reduced basis method: Application to the Boussinesq equations”. In: *SIAM Journal on Scientific Computing* 36.1 (2014), A232–A266.

[53] Masayuki Yano, Anthony T Patera, and Karsten Urban. “A space-time hp-interpolation-based certified reduced basis method for Burgers’ equation”. In: *Mathematical Models and Methods in Applied Sciences* 24.09 (2014), pp. 1903–1935.

[54] Eberhard Zeidler. *Nonlinear Functional Analysis and Its Applications: I/A: Linear Monotone Operators*. Springer Science & Business Media, 2013.

[55] Eberhard Zeidler. *Nonlinear Functional Analysis and Its Applications: II/B: Nonlinear Monotone Operators*. Springer Science & Business Media, 2013.

Eidesstattliche Erklärung

Hiermit erkläre ich an Eides statt,

- dass ich die die eingereichte Dissertation selbstständig verfasst habe und alle von mir für die Arbeit benutztenHilfsmittel und Quellen in der Arbeit angegeben sowie die Anteile etwaig beteiligter Mitarbeiterinnen oderMitarbeiter sowie anderer Autorinnen oder Autoren klar gekennzeichnet habe;
- dass ich nicht die entgeltliche Hilfe von Vermittlungs- oder Beratungsdiensten (Promotionsberater oder andere Personen) in Anspruch genommen habe;
- dass ich die Dissertation nicht in gleicher oder ähnlicher Form als Prüfungsarbeit für eine staatliche oderandere wissenschaftliche Prüfung im In oder Ausland eingereicht habe;
- dass ich weder die gleiche noch eine andere Abhandlung in einem anderen Fachbereich oder einer anderenwissenschaftlichen Hochschule als Dissertation eingereicht habe;
- dass mir bewusst ist, dass ein Verstoß gegen einen der vorgenannten Punkte den Entzug des Doktortitelsbedeuten und ggf. auch weitere rechtliche Konsequenzen haben kann.

Ort, Datum Denis Korolev